

HDR luminance measurement:
Comparing real and simulated data

By

Peony Pui Yue Au

A thesis

submitted to the School of Architecture, Victoria University of Wellington,

in fulfilment of the requirements for the degree of

Master of Building Science

Victoria University of Wellington

March 2013

**No material within this thesis may be used without
permission of the copyright owner.**

Preface

This research thesis was submitted in fulfilment of the requirements for the degree of Master of Building Science at the School of Architecture and Design, Victoria University of Wellington, New Zealand.

Author:

Peony Pui Yue Au

School of Architecture

Victoria University of Wellington

Email: peony_au@hotmail.com

Contract Number: +64 27 751 4389

Research Supervisor:

Michael Donn

Director of Centre for Building Performance Research

School of Architecture

Victoria University of Wellington

Email: Michael.Donn@vuw.ac.nz

Contract Number: +64 4 463 6221 work

+64 21 611 280 mobile

Postal Address: PO Box 600 Wellington, New Zealand

Abstract

The objective of this research was to determine the adequacy of Android devices capturing High Dynamic Range (HDR) photography, and using it as a tool for daylight analysis in New Zealand's commercial building stock. This study was conducted with an Android Smartphone and later an Android Tablet, employing the use of a US\$50 magnetic fisheye lens. The overall aim of this research was to evaluate whether an inexpensive programmable data acquisition system could provide meaningful and useful luminance data.

To complete this research, the adequacy of computer simulation using HDR photography of the real horizontal and vertical skies was explored. Using the method documented in this research, the luminance distribution of the building interiors could then be mapped accurately in daylight simulations.

The BRANZ Building Energy End-Use Study (BEES) team currently have one internal lighting measurement point, which records light levels in each of more than 100 commercial buildings randomly selected to be representative of commercial buildings in New Zealand. The HOBO U12 data logger typically records the environmental data on a desktop within the main area of the monitored premises. The HOBO data loggers only provide the environmental measurement of that specific location and do not provide the researcher the daylight distribution of the whole space. Using the data collected by BEES, a thesis was developed to explore the utility of HDR imaging as a supplement to the use of a single internal light measurement in the analysis of daylight potential in New Zealand's commercial building stock.

Three buildings were randomly selected from the BEES targeted strata five database to be monitored over a one day period. Within each building, at least three rooms were studied, all facing different orientations. The pilot study and the first two buildings monitored employed the use of a Motorola Defy Smartphone to capture the low dynamic range (LDR) photographs of each scene using both the HDR Camera application available from the Android Google Play Application Store, and the built-in camera application that came with the Smartphone. The vertical (by pressing the Smartphone hard up against the window) and horizontal (from the ground) skies were also captured simultaneously as only one device was available at each monitored building and to ensure consistency in each building. These photographs were fused using an HDR software called Photosphere, into a single HDR image.

However, before the HDR images could be generated to contain accurate luminance data within the images, a camera response curve is required to be generated. A camera response curve is unique to each device and only needs to be generated once and can be generated

using Photosphere. Unfortunately, a camera response curve could not be generated for the Motorola Defy Smartphone and through various experimentations and tests in both the lighting laboratory and in-field, it was discovered that this had nothing to do with the EXIF data contained within the photographs captured as originally thought, but the JPEG image format itself. This resulted in a generic camera response curve, from Photosphere, being used for the pilot study and the first two monitored buildings. For the final building that was monitored, a Galaxy Note Tablet was used. A camera response curve for this device could be easily generated using Photosphere.

The pilot study and three monitored buildings were geometrically simulated using Google SketchUp 8 and were then exported in to Radiance Lighting Simulation and Rendering System using the `su2rad` plug-in. The files were then edited in Ecotect™ Radiance Control Panel, after which the real and simulated images were compared using HDRShop and RadDisplay.

The four comparison methods were used to compare the real and simulated data were pixel to pixel comparison; section to section pixel comparison; surface to surface comparison and visual field comparison. Of the four methods used the first two were visual based comparisons, whereas the latter two were numerical, which employ the use of a calculation method to calculate the relative error percentages. The biggest problem that arose from the visual comparisons was the geometrical misalignment due to the use of a fisheye lens and only provided the luminance difference ranging from a scale of 0 cd/m^2 to 50 cd/m^2 . The numerical comparison methods provided a 60% correlation between real and simulated data.

It was concluded that, depending on the Android device used, HDR photographs are able to provide reliable images that contain accurate luminance data when a camera response curve for the device could be generated.

Acknowledgements

I would like to thank everyone who has helped during my research study. Firstly, I would like to thank my research supervisor Michael Donn. Without your feedback and guidance throughout the past year, this research would not be made possible.

Secondly, I would like to thank the BRANZ BEES team for the Scholarship and financial funding to assist with the research and for their partial funding to attend the ANZAScA 2012 Conference in the Gold Coast.

I would also like to thank Michael Babylon from BRANZ for your assistance in finding the three strata five buildings for me to monitor, and providing feedback for my study and during the measurement periods. I would like to say a huge thank you for the building owners and business managers that agreed to allow me to take measurements at their premises.

I would also like to thank Paul Hillier, photographic technician; Peter Ramutenas, electronics and instrumentation technician; Kevin Cook, technical staff; and Eric Camplin, helpdesk technician; from Victoria University of Wellington for all your help in assisting with the equipment required to complete this study.

Finally, I would like to thank my family, friends and colleagues for your support throughout my research.

Table of Contents

Preface.....	v
Abstract.....	vii
Acknowledgements	ix
Table of Contents.....	xi
List of Figures	xv
List of Tables	xix
Abbreviations.....	xxi
Chapter 1: Introduction	1
1.1. Thesis Statement	1
1.2. Research Significance	2
1.3. Scope of Research.....	4
1.4. Aims and Objectives	5
1.5. Research Questions	5
1.6. Thesis Structure	5
Chapter 2: Literature Review.....	9
2.1. Research Methodology.....	9
2.1.1. Experimental Research	10
2.1.2. Simulation and Modelling Research	10
2.2. Daylight Measurement Error	11
2.3. HDR Photography	13
2.3.1. HDR Image File Formats.....	14
2.3.2. Exposure Value	14
2.3.3. Camera Response Curve	15
2.3.4. HDR Sky Models and Image-Based Lighting Techniques	16
2.3.5. Computer Simulations with HDR Photography	19
2.3.6. HDR Software.....	20
2.4. Computer Simulation and Modelling.....	22
2.4.1. Simulation Errors	24
2.4.2. Simulating Skies	25
2.4.3. Daylight Simulation Software	25
2.5. Physically Scaled Models	27

2.6. Mirror Box as a Sky Simulator	29
2.7. Conclusion.....	30
Chapter 3: Equipment.....	31
3.1. HDR Camera	31
3.1.1. Mobile Smartphone and Tablet	31
3.1.2. DSLR Camera	33
3.2. Luminance and Illuminance Sensors.....	35
3.3. X-Rite ColorMunki	37
3.4. Macbeth ColorChecker	38
3.5. Conclusion.....	38
Chapter 4: Pilot Study	41
4.1. The Lighting Laboratory	41
4.1.1. Camera Response Curve	42
4.1.2. Physically Scaled Model	43
4.2. The Study Room	45
4.2.1. Measurement Process	47
4.3. Simulation of Pilot Study.....	48
4.3.1. Simulating an HDR Sky	49
4.4. Comparison Between Real and Simulated Data	50
4.5. Conclusion.....	54
Chapter 5: Methodology.....	55
5.1. Measurement Process	55
5.2. Creating HDR image	56
5.3. Simulation	58
5.3.1. Potential Simulation Errors and Variations in Simulation.....	59
5.4. Creating HDR Skies.....	60
5.5. Comparison of Real and Simulated Measurements	60
5.6. Conclusion.....	61
Chapter 6: The Buildings	63
6.1. Building 1	63
6.2. Building 2	64
6.3. Building 3	66

6.4. Conclusion.....	67
Chapter 7: Results.....	69
7.1. Pixel to Pixel Comparison	69
7.1.1. Building 1	70
7.1.2. Building 2	71
7.1.3. Building 3	73
7.2. Section to Section Pixel Comparison	74
7.2.1. Building 1	75
7.2.2. Building 2	75
7.2.3. Building 3	76
7.3. Surface to Surface Comparison	76
7.3.1. Building 1	76
7.3.2. Building 2	78
7.3.3. Building 3	80
7.4. Visual Field Comparison.....	81
7.4.1. Building 1	81
7.4.2. Building 2	82
7.4.3. Building 3	82
7.5 Conclusion.....	83
Chapter 8: Conclusions	85
8.1 HDR Photography Using an Android Operated Device.....	86
8.2 Comparison of Real and Simulated Measurements	87
8.3 Accuracy of HDR Imagery as a Tool for Daylight Analysis.....	88
8.4 Future work	89
Bibliography	91
Appendix	97
Appendix A: HDR Software	99
Appendix B: Daylight Simulation Software	101
Appendix C: Equipment	103
Appendix D: Equipment Calibration Process	105
Appendix E: Lighting Laboratory Measurements	107

Appendix F: Daylight Measurements Using Photometric Illuminance Sensors in the Study Room	109
Appendix G: Generating a Camera Response Curve.....	111
Appendix H: Variation of Surface Colours in the Pilot Study	113
Appendix I: Radiance Sky Mapping Scripts	115
Appendix J: Surface Reflectances in the Monitored Buildings	119
Appendix K: Results.....	122

List of Figures

Figure 1.01: HOBO U12 data loggers from BRANZ used to record the environmental data in over 100 buildings	1
Figure 1.02: Magnetic fisheye lens attachment for the Smartphone	4
Figure 3.01: Motorola Defy with fisheye lens attachment.....	32
Figure 3.02: Samsung Galaxy Tablet with fisheye attachment.....	32
Figure 3.03: Four HDR images created from the Motorola Defy Smartphone (From left to right: -1.50 EV, +0.0 EV, +1.5 EV and +3.0 EV)	33
Figure 3.04: Three HDR images created from the Samsung Galaxy Tablet (From left to right: -1.50 EV, +0.0 EV, and +1.5 EV).....	33
Figure 3.05: Nikon DSLR camera and fisheye lens.....	34
Figure 3.06: Difference between a circular fisheye lens and a full-frame fisheye lens.....	34
Figure 3.07: AF Fisheye Nikkor lens used for this study (Nikon 2012)	35
Figure 3.08: Hagner Universal Photometer Model S2 measurement recording technique (left) and the view through the view-finder (right) (Hagner International UK Limited 1974, 6)	35
Figure 3.09: Photometric Illuminance sensors used to record the daylight measurements in the physically scaled model and the study room	36
Figure 3.10: Minolta hand-held light meter placed on desktops for illuminance measurements in the field.....	37
Figure 3.11: HOBO U12 data logger used by BRANZ to record the environmental measurements including lux measurements.....	37
Figure 3.12: X-Rite ColorMunki spectrophotometer used to capture the RGB and reflectance values of the surfaces in a scene	38
Figure 3.13: Macbeth ColorChecker colour chart used to calibrate the HDR images capture on site	38
Figure 4.01: Dimensions of the lighting laboratory at Victoria University of Wellington	42
Figure 4.02: Rotating effulger panels with glossy white or mirrored options.....	42
Figure 4.03 Camera response curve for Nikon D200.....	43
Figure 4.04: Interior and exterior photographs of the physically scaled model used for the pilot study	44
Figure 4.05: Plan view of the physically scaled model illustrating the location of the Photometric Illuminance sensors.	45
Figure 4.06: HDR photographs taken inside the physically scaled model using the Android Smartphone (From left to right: -1.50 EV, +0.0 EV, +1.5 EV and +3.0 EV).....	45

Figure 4.07: Site plan showing the location of the study room in relation to surrounding environment (Not to scale) (Image adapted from (Google 2012)).....	46
Figure 4.08: The study room used for validation of the daylight measurements recorded under the artificial sky	46
Figure 4.09: HDR photographs capturing the real horizontal (top) and vertical skies (bottom) for the pilot study (From left to right: -1.50 EV, +0.0 EV, +1.5 EV and +3.0 EV).....	46
Figure 4.10: Location of the Photometric Illuminance sensors in the study room (Not to scale)	47
Figure 4.11: Comparison between the HDR image of study room, Radiance simulation with the real horizontal and vertical HDR skies	51
Figure 4.12: Pixel to pixel comparison between real and simulated luminance data using horizontal HDR sky (left) and vertical HDR sky (right) generated in HDRShop and RadDisplay	52
Figure 4.13: Resultant images produced from HDRShop and RadDisplay of the four sections selected in the study room using the horizontal sky (top) and vertical sky (bottom).....	52
Figure 5.01: Camera response curve for the Samsung Galaxy tablet.....	58
Figure 5.02: An example from the pilot study illustrating the pixel to pixel comparison study process	61
Figure 6.01: Site plan of Building 1 (Not to scale) (image adapted from (Google 2012))	63
Figure 6.02: Floor plan illustrating level 2 in Building 1 (Not to scale)	64
Figure 6.03: Site plan of Building 2 (Not to scale) (image adapted from (Google 2012)).....	65
Figure 6.04: Floor plan illustrating level 3 in Building 2 (Not to scale)	65
Figure 6.05: Site plan of Building 3 (Not to scale) (image adapted from (Google 2012)).....	66
Figure 6.06: Floor plan illustrating level 11 in Building 3 (Not to scale)	67
Figure 7.01: Pixel to pixel comparison between real and simulated luminance data of the waiting area using horizontal left) and vertical (right) HDR sky generated in HDRShop and RadDisplay.....	70
Figure 7.02: Pixel to pixel comparison between real and simulated luminance data of the lunchroom using horizontal (left) and vertical (right) HDR sky generated in HDRShop and RadDisplay.....	70

Figure 7.03: Pixel to pixel comparison between real and simulated luminance data of the meeting room using horizontal (left) and vertical (right) HDR sky generated in HDRShop and RadDisplay	71
Figure 7.04: Pixel to pixel comparison between real and simulated luminance data of the lunchroom using horizontal (left) and vertical (right) HDR sky generated in HDRShop and RadDisplay	71
Figure 7.05: Pixel to pixel comparison between real and simulated luminance data of the large meeting room using horizontal (left) and vertical (right) HDR sky generated in HDRShop and RadDisplay	72
Figure 7.06: Pixel to pixel comparison between real and simulated luminance data of the small meeting room using horizontal (left) and vertical (right) HDR sky generated in HDRShop and RadDisplay	72
Figure 7.07: Pixel to pixel comparison between real and simulated luminance data of the corner open plan office using horizontal (left) and vertical (right) HDR sky generated in HDRShop and RadDisplay	72
Figure 7.08: Pixel to pixel comparison between real and simulated luminance data of the open plan office using horizontal (left) and vertical (right) HDR sky generated in HDRShop and RadDisplay	73
Figure 7.09: Pixel to pixel comparison between real and simulated luminance data of the large meeting room using horizontal (left) and vertical (right) HDR sky generated in HDRShop and RadDisplay	73
Figure 7.10: Pixel to pixel comparison between real and simulated luminance data of the small meeting room using horizontal HDR sky (left) and vertical HDR sky (right) generated in HDRShop and RadDisplay	74
Figure 7.11: Pixel to pixel comparison between real and simulated luminance data of the open plan office using horizontal (left) and vertical (right) HDR sky generated in HDRShop and RadDisplay	74
Figure 7.12: Comparison between sections of real and simulated images using horizontal (top) and vertical (bottom) HDR sky. From left to right; waiting room, lunchroom and meeting room.	75
Figure 7.13: Comparison between sections of real and simulated images using horizontal (top) and vertical (bottom) HDR sky. From left to right; lunchroom, large meeting room, small meeting room, corner open plan office and an open plan office.	75

Figure 7.14: Comparison between sections of real and simulated images using horizontal (top) and vertical (bottom) HDR sky. From left to right; large meeting room, small meeting room and open plan office.	76
Figure 8.01: An example from Building 1 waiting area illustrating the pixel to pixel comparison under a horizontal (left) and vertical (right) HDR sky simulations.....	87
Figure 8.02: An example from Building 1 illustrating the section to section pixel comparison between the real and simulated images under a horizontal (top) and vertical (bottom) HDR sky simulations.	87

List of Tables

Table 2.01: Table illustrating the difference between bit images and image file formats (McCollough 2008, 17).....	14
Table 2.02: Comparison table between the four HDR software, adapted from (McCollough 2008).....	21
Table 2.03: Comparison between four daylight simulation programs that are suitable for this research, adapted from (U.S Department of Energy 2011)	27
Table 2.04: “Scale choice as a function of daylighting design purpose (International Energy Agency 2000)”	28
Table 4.01: Average surface colours in the study room captured using the ColorMunki	49
Table 4.02: Relative error percentage between real and simulated data under the horizontal HDR sky	53
Table 4.03: Relative error percentage between real and simulated data under the vertical HDR sky	53
Table 6.01: The average surface RGB and reflectance values for Building 1	64
Table 6.02: The average surface RGB and reflectance values for Building 2	66
Table 6.03: The average surface RGB and reflectance values for Building 3	67
Table 7.01: Relative error percentage for the lunchroom under the horizontal (left) and vertical (right) HDR skies.....	76
Table 7.02: Relative error percentage for the lunchroom under the horizontal (left) and vertical (right) HDR skies.....	77
Table 7.03: Relative error percentage for the waiting area under the horizontal (left) and vertical (right) HDR skies.....	77
Table 7.04: Relative error percentage for the lunchroom under the horizontal (left) and vertical (right) HDR skies.....	78
Table 7.05: Relative error percentage for the small meeting room under the horizontal (left) and vertical (right) HDR skies.....	78
Table 7.06: Relative error percentage for the large meeting room under the horizontal (left) and vertical (right) HDR skies.....	79
Table 7.07: Relative error percentage for the corner open plan office under the horizontal (left) and vertical (right) HDR skies.....	79
Table 7.08: Relative error percentage for the open plan office under the horizontal (left) and vertical (right) HDR skies.....	79

Table 7.09: Relative error percentage for the large meeting room under the horizontal (left) and vertical (right) HDR skies.....	80
Table 7.10: Relative error percentage for the small meeting room under the horizontal (left) and vertical (right) HDR skies.....	80
Table 7.11: Relative error percentage for the open plan office under the horizontal (left) and vertical (right) HDR skies.....	81

Abbreviations

BEES – Building Energy End-Use Study

CIE - International Commission on Illumination

DF – Daylight Factor

DSLR - Digital single-lens reflex

EV – Exposure Value

EXIF – Exchangeable Image File Format

GUIs – Graphic User Interfaces

HDR – High Dynamic Range

HDRI – High Dynamic Range Imaging

IBL – Image Based Lighting

IBR – Image-Based Rendering

LDR – Low Dynamic Range

MDR – Medium Dynamic Range

RGB – Red Green Blue

RGBE – Red Green Blue Exponent

UDI – Useful Daylight Index

Chapter 1: Introduction

“We may like to think that the considerable technological advances in 21st century digital imaging make it possible now to accurately reproduce any scene...despite all the remarkable accomplishments, we cannot capture and reproduce the light in the world exactly”

(McCann and Rizzi 2012, 4)

1.1. Thesis Statement

The Building Research Association of New Zealand (BRANZ) Building Energy End-Use Study (BEES) team currently have at least one internal lighting measurement point recording light levels in each of more than 100 commercial buildings randomly selected to be representative of commercial buildings in New Zealand. Environmental data was monitored and recorded in the selected buildings using HOBO U12 data loggers, illustrated in figure 1.01. These loggers record the temperature, humidity and illuminance measurements every ten minutes for a period of two weeks. The HOBO data logger typically records the environmental data on a desktop within the main area of the premises and if more than one HOBO data logger was employed, they were typically placed at opposite sides of the premise. The HOBO data loggers only provided the environmental measurement of that specific location and did not provide the researcher the daylight distribution in the space.



Figure 1.01: HOBO U12 data loggers from BRANZ used to record the environmental data in over 100 buildings

The objective of this research is to further develop this measurement technique by employing the use of High Dynamic Range (HDR) photography as a supplement to the use of a single internal light measurement in the analysis of daylight potential in New Zealand's commercial building stock. The ultimate goal of this research is to use a simple programmable Android device with a fisheye lens to capture HDR images that can contain accurate and reliable

luminance distribution within a space and in the future, be able to capture and transfer the photographs wirelessly.

This research could also benefit the BEES data collection process on daylighting by improving the quantity and quality of data gathered while not increasing the level of complexity of the detailed measurement regime in commercial buildings. If this research can provide accurate results, using the process developed and the technology used, the BEES team can use this process to determine the daylight distribution within the monitored buildings.

1.2. Research Significance

The BEES team are analysing how, why, and where energy is primarily consumed within New Zealand's commercial buildings. As part of this study, they have visited a wide range of commercial buildings throughout New Zealand, of various sizes to measure the end-uses of energy, as well as measures of service delivery for a two-week period. The buildings are separated into five different strata according to the floor areas. The measures of service delivery include light level measurements at ten-minute intervals for two week periods. Simulation of building performance for other times of the year is an integral part of the analysis of this data. Documenting the potential of daylighting in commercial buildings could help reduce energy use in New Zealand's commercial buildings, as it is estimated that artificial lighting accounts for 20-30% of total energy use (Li and Tsang 2008).

With the data collected by BEES, a preliminary study was conducted in 2011 examining the adequacy of one internal lighting measurement in a commercial building in New Zealand. The study was completed in two stages; first was to compare the recommended lighting measurements required for daylight analysis and measurements the BEES team had gathered with the HOBO data loggers, illustrated in figure 1.01. A daylight simulation methodology was developed in the second stage which determined that there was some correlation between the simulated daylight model and the measured lighting levels. This comparison was done only for one building and requires a systematic validation for the BEES measurement process, not just the one case examined in the study. One of the principal issues was that both the CIE and Perez sky models provided the daylight simulation with an evenly distributed sky and cloud cover, whereas, a real sky often has an uneven distribution of clouds in the sky that currently cannot be simulated.

Daylight distribution in a building is typically measured using a light meter positioned at desk level (800 mm above floor level) at points in an evenly spaced lighting grid. A light measurement is recorded at each point of the grid and the researcher is able to graph the

isolux contours displaying daylight penetration levels within that grid. However, this method can often be a time consuming process, depending on the size of the room. Inaccuracies can also occur due to the uncontrollable climatic conditions of the surrounding environment during the measurement process.

With daylight measurement techniques developing throughout the years, digital photography has been developed immensely as a daylight analysis tool. High dynamic range (HDR) photography is a relatively new technology for daylight measurement and has been developed as a tool to discover the potential of daylight in a space through simulation. Christoph F. Reinhart and Shelby Doyle have explored the effectiveness of simulation when it comes to daylighting and HDR images have been used to discover the “full dynamic range of a scene, from direct sunlight to deep shadow” (Doyle and Reinhart 2010). HDR images are generated by fusing four or more photographs together captured under different exposures. The resultant HDR image contains the details in both under and over exposed sections a typical photograph would not be able to contain.

This thesis explores the possibilities of using an inexpensive programmable data acquisition system to provide meaningful and useful daylight data. This research explores the possibilities of using an ordinary Android device and a US\$50 magnetic fisheye lens to map the daylight distribution of a scene instead of a \$2000 DSLR camera and a \$2000 fisheye lens attachment. Producing accurate results, this thesis could allow more students to study lighting distribution of a room using HDR photography at a much lower cost. Also with more and more applications becoming readily available to download online, a simple Smartphone device can have the potential to conduct the all the daylight measurement within a space instead of having multiple measurement devices.

This study was conducted by capturing a series of HDR images of an interior space providing the researcher a whole field of view of the scene. Simultaneously, real horizontal and vertical HDR skies were captured so that it can be mapped as a light source for the daylight simulations. This process has been previously done using an expensive DSLR camera (Cheney 2008) (Inanici 2010). The internal space was then geometrically modelled in Google SketchUp 8 and exported to Radiance Lighting Simulation and Rendering System so that the model could be simulated and an HDR image of the same scene was produced. The real and simulated images were then compared and the difference between the two images was calculated using four comparison methods. This determined whether this method of measurement is able to provide adequate lighting information in determining the potential of daylight in commercial buildings in New Zealand’s commercial building stock.

1.3. Scope of Research

This thesis could immensely improve the BEES data on daylighting by significantly improving the quantity and quality of data gathered while not increasing the level of complexity of the detailed measurement regime in commercial buildings. The technique developed throughout this thesis could then be used by BRANZ to report on the potential of daylighting in New Zealand's commercial building stock. The process developed in this study will minimise the time required when it comes to daylight measurements in the field and a single image can provide the researcher lighting information with a whole field of view. Also with the cheaper Smartphone and fisheye lens option the equipment to conduct this research will become more readily available.

The BEES building database was split into five strata depending on their floor areas. Within the strata five database, only six buildings were monitored. Each building had a minimum floor area of 9,000 m² (Isaacs, et al. 2009). The three buildings were randomly selected from the monitored BEES strata five building database, had their daylight distribution studied with the use of an Android Smartphone camera and a magnetic fisheye lens, illustrated in figure 1.02. The sky images were captured from ground level as roof access was not available at the selected buildings.



Figure 1.02: Magnetic fisheye lens attachment for the Smartphone

The lighting information in the HDR images was also compared to the BEES lighting data collected by the HOBO data loggers to ensure that the two sets of data measurements collected can be reliable and accurate. A digital daylight model was simulated as accurately as possible in Radiance with an HDR sky representing the real sky instead of using a generic sky model with an evenly distributed sky conditions, as generic sky model provides the daylight simulation with unrealistic sky condition. A comparison was made between real and simulated data via HDR imaging.

Boundaries will need to be established to ensure that this research can be successfully completed within the available time frame. A pilot study was first conducted in the lighting laboratory at the School of Architecture and Design Campus, Victoria University of Wellington using a physically scaled model under an artificial sky to ensure the accuracy of the method and to develop the methodology before the daylight measurement technology using the Smartphone camera was used at the three monitored buildings.

1.4. Aims and Objectives

The objective of this research was to determine the adequacy of Smartphone based High Dynamic Range (HDR) photography as a tool for daylight analysis in New Zealand's commercial building stock. This study was conducted with an Android Smartphone and later an Android Tablet, employing the use of a US\$50 magnetic fisheye lens. The overall aim of this research was to evaluate whether an inexpensive programmable data acquisition system could provide meaningful and useful data.

1.5. Research Questions

Four research questions were developed for this research so that criteria could be set and to provide a focus for the research. The research questions developed are:

- Can capturing HDR images using (an Android) Smartphone be an adequate tool in determining the potential of daylight analysis?
- Can a suitable comparison technique be developed to compare the real and simulated luminance data?
- How accurate could using HDR photography as a daylight measurement tool be for daylight analysis?
- How can this measurement process be implemented into further research?

1.6. Thesis Structure

This thesis documents the process involved in determining the adequacy of Smartphone based HDR photography as a tool for daylight analysis in New Zealand's commercial building stock.

Chapter two documents the background information to this research, starting off with a literature review on the research methodology techniques applicable for this research, including the development of HDR photography as a tool for daylight analysis including camera response curves and computer simulations with HDR photography and the use of Image-Based Rendering (IBR) techniques to create an environment map. A comparison

between the free or inexpensive HDR software will be done. This leads into the exploration of digital simulations and modelling for daylight analysis including simulation errors and how skies are simulated in order to create an accurate daylight simulation model, as well as a comparison between the software available for daylight simulations. Lastly, this chapter will explore daylight analysis using a physically scaled model, and the complications associated with using a mirrored box as a sky simulator.

The third chapter explores the equipment required for this research. This includes a DSLR camera, an Android Smartphone, an Android Tablet, luminance and illuminance sensors, the X-Rite ColorMunki device and software, and the Macbeth ColorChecker Chart. It summarises how each item of equipment was used as well as the necessary calibration processes required to minimise errors when using them in this research. The calibration for all the equipment used in this research was conducted in the lighting laboratory under a controlled environment.

Chapter four documents the pilot study conducted in the lighting laboratory located in the basement of the School of Architecture and Design Campus at Victoria University of Wellington, using a physically scaled model of a study room. The daylight measurements collected in the scale model was compared to the real daylight measurements collected by the Photometric Illuminance sensors set up in the study room under an overcast sky to ensure that the measurements collected in the lighting laboratory are accurate and any inaccuracies could be factored in. Next low dynamic range (LDR) photographs with various exposure values of each space were captured and these images were combined into a single HDR image using an HDR software called Photosphere. Finally, a simulation of the study room was created in Radiance and a comparison between real and simulated data was conducted using HDRShop (USC Institute for Creative Technologies 2012). This was to determine the accuracy of the tool and to ensure that the equipment used will perform correctly and accurately before measurements are conducted in the three commercial buildings.

The fifth chapter documents the process and methodology developed from the pilot study. This process was used and followed for all three buildings, with additional changes made where necessary. It looks at the measurement process, followed by the process taken to create HDR images. This leads onto the discussion of the simulation process and an exploration on any possible simulation errors and variables. Lastly a discussion on the process used to compare real and simulated data.

Chapter six documents the three different building that were anonymously measured and analysed, before chapter seven goes onto a comparison between the real and simulated results using four comparison methods.

Lastly, the conclusions of this study are documented in chapter eight.

Chapter 2: Literature Review

“The range of light in the world is the product of material reflectances and scene illumination. Much of our time is spent in rooms designed to have uniform illumination and desirable spectral content. Both factors improve the colour constancy of objects.”

(McCann and Rizzi 2012, 27)

The objective of this chapter was to document the background study for this research. This begins with an exploration of the two research methodologies applicable for this research in section 2.1. This leads to a discussion on possible daylight measurement errors using traditional measurement techniques in section 2.2. Section 2.3 documents the recent work in using HDR photography as a daylight measurement tool. Section 2.4 explores the use of physically scaled models to discover the potential of daylighting in a space and section 2.5 explores the use of mirror box as a sky simulator for scaled models. Section 2.6 will explore daylight simulation and modelling including possible errors that may arise and the different daylight simulation programs available. Lastly, sections 2.7 and 2.8 explore the use of Image Based Lighting (IBL) and Physically-Based Rendering techniques for daylight simulations.

2.1. Research Methodology

The three main types of research are qualitative; quantitative; and mixed method research. It was important to select and develop a research methodology to help guide the path to answer the research questions set out at the beginning of the research project. Research methodologies “can yield either outstanding or flawed research, depending on how appropriately it is applied to a particular research question” (Groat and Wang 2001, 251).

Within each type of research, there are seven different research strategies that can be used to ensure the research questions set can be answered. For this research, two research methodology approaches were used: experimental research, and simulation and modelling research. This section will provide an outline of how each task in the research study should be completed and to determine how many times and the period of which a building will need to be monitored to ensure the accuracy of the tool and that the results produced are reliable.

2.1.1. Experimental Research

“Experimental research isolates a context and identifies variables that can be manipulated to see how they affect other variables”

(Groat and Wang 2001, 283)

The first research methodology that was explored for this research was the *experimental research* method. The five characteristics that define experimental research are; use of a treatment, independent variable; measurement of one or more outcome variable; designation of a unit of assignment; use of a comparison or control group; and a focus on causality (Groat and Wang 2001, 252-255).

This research will focus on the *environmental technological* aspect of experimental research. Groat and Wang state that the characteristics incorporated in environmental technology are:

1. *“The use of laboratory settings where relevant variables can be easily controlled;*
2. *Dependent variables that are in many instances inert, and therefore not likely to change except as a consequence of the treatment;*
3. *Explicit theories that enable researchers to specify the expected effects of a particular treatment; and*
4. *Instrument that are calibrated to measure such effects.”*

(Groat and Wang 2001, 254)

For this research, experimental research methodology was used to determine the amount of building that will need to be monitored to ensure that the technology was developed adequately and can provide reliable outcomes.

Experimental research relates to simulation and modelling research, that is why it is quite common to use both approaches when completing a research study. Both approach “isolate context and manipulate variables” (Groat and Wang 2001, 283). Sometimes the experimental research methodology “uses simulation comfortably as the primary tactic” (Groat and Wang 2001, 283).

2.1.2. Simulation and Modelling Research

The second research methodology method employed in this research was simulation and modelling research where;

“Simulation research involves controlled replications of real-world contexts or events for the purpose of studying dynamic interactions within that setting”

(Groat and Wang 2001, 278).

Computer simulations can calculate the effects of daylight in a space as well as the illuminance and luminance distribution of a space. This provides the tool for the designer to visualise the design quality of a space. Some computer software allows the designer to simulate artificial lighting including light fixtures directly from manufacture. “These kinds of programs underline the blurring between mere representation and simulation” (Groat and Wang 2001, 281).

“Simulation research comes out of a general human fascination with the replication of real-world realities” (Groat and Wang 2001, 275). Having a spatial experience by a client before the building is constructed allows the client to experience the space before it is built, even if they are in different parts of the world. Using a computer program called CAVE (Computer Assisted Virtual Environments) developed at the University of Illinois Chicago allowing both the client and the designer to “meet in a virtual space” (Groat and Wang 2001, 275). This has obvious benefits as it can provide the designer information on any “dangerous conditions without placing people in harm’s way” as well as cost savings (Groat and Wang 2001, 276).

Simulation and modelling is an important aspect in this research. This methodology approach was used from the pilot study stage and all the way through to the end of the research.

2.2. Daylight Measurement Error

There is a range of uncertainties that can occur during a daylight measurement process. However, if planned in advance, these uncertainties can be addressed and reduced early on. It is important that the daylight measurements recorded are as accurate as possible. Larger projects may demand some variety in the method of measurement taking.

Daylight distribution in a building is typically measured using a light meter positioned at desk level (800 mm) at points on an evenly spaced grid. A light measurement is recorded at each point of the grid and the researcher is able to graph the isolux contours of daylight penetration within that room. However, this method can often be a time consuming process, depending on the size of the room. Inaccuracies can also occur due to the uncontrollable climatic conditions of the surrounding environment.

“All measurement is subject to error where the overall accuracy of measurement is the total of all possible errors. The degree of accuracy is dependent upon the occurrence and magnitude of errors.”

(Hayman 2003, 101)

Most systematic and random errors can be “controlled”. Systematic errors are controlled by “standardising the assumptions made and the methodologies used”. Whereas, by checking the procedures, random errors can be controlled especially if the errors are the “misreading of data in tables” (Hayman 2003, 102). No matter how precise and thorough the measurement procedures were, “errors will always occur and there will be a degree of variation, or tolerance, about the “exact value”” (Hayman 2003, 102). Expressed as “absolute deviations”, these variations or tolerances have a \pm in-front of the measurement units, or a “percentage deviation”. And if the measurement is recorded within the variation or tolerance, the data must be within that range (Hayman 2003, 102).

To minimise the error in daylight measurements, all equipment’s are required to undergo “the same calibration requirements” (Hayman 2003, 106). This calibration process for the lighting equipment used in a research is calibrated under “laboratory conditions [...] via photometric bench tests”. If the calibrated equipment is out of sync by $\pm 10\%$, then that piece of equipment will need to be looked at by a specialist (Hayman 2003, 106).

“As a function of ever changing sky conditions, absolute values of interior illuminance will vary greatly. Although representative of a building’s performance at a single moment in time, absolute illuminance levels do not allow comparative evaluation to take place.”

(Carrier and Ubbelohde 2005, 1)

As a light meter contains “complex systems”, the elements within the device will individually contribute to “its overall accuracy”. For example the spectral response of a light meter depends on all the components that are wavelength dependent, not just the “performance of the V-lambda filter” (Hayman 2003, 102). In order to “reduce errors to very low levels in measurement systems is costly”. This result in the acceptance of “levels of accuracy in measurements” dependent on the circumstances of the measurement device used (Hayman 2003, 102).

Due to the varying internal illuminance, daylight factors (DF) are becoming more commonly used “as it represents a more constant approach to determining daylight performance”

(Carrier and Ubbelohde 2005, 1). Daylight factor is the ratio between the internal illuminance (E_i) and the external illuminance (E_o) recorded at the same time under an overcast sky. The formula to calculate the daylight factor is:

$$DF = \frac{E_i}{E_o} * 100\%$$

Both measurement methods are assumed to be under the CIE overcast sky and measurements are rarely conducted under clear sky conditions. This is because the luminance distribution varies depending on the sun position. Daylight factor is a measurement unit used to “quantify the amount of diffuse daylight in space,” but the quality of daylighting is not determined (Otis and Reinhart 2009). If daylight factor is the only daylight performance measurement recorded in a space, then problems, like glare cannot be determined. This was why this study explores the use of HDR photography as a tool for daylight analysis so that more detail regarding the daylight performance of a building can be measured.

2.3. HDR Photography

Realistically, a room contains an “enormous range of light”. Unfortunately, a single photograph from any camera cannot capture the entire range of light. This causes the photographs to be either over or underexposed. This resulted in inconsistencies with different sections of photographs being either too bright or too dark (Bloch 2007). This is why High Dynamic Range (HDR) photography was originally developed.

“Dynamic range refers to the variation in luminance from the brightest to the darkest areas of a scene. High dynamic range simply means a wide range of brightness values.”

(McCollough 2008, 9)

An HDR image is created by fusing a number of photographs of the same scene captured under different exposures. The resultant image allows the photographer to be able to capture “all the details in the shadows, as well as the highlights” (Concepcion 2011, 49). The HDR image produced, if calibrated with a camera response curve and single spot measurements, contains an accurate lighting distribution within a physical environment.

At least four photographs are required in order to create an “accurate” HDR image. All of these photographs contribute “important information about the scene”. The brighter sections of a scene are captured by the underexposed photographs whereas the darker sections of a

scene are captured by the overexposed photographs (McCollough 2008, 9). The resultant image is a “32-bit” HDR image containing the “full dynamic range of the scene”.

However, this resultant HDR image cannot be viewed properly on a computer screen. In order to accurately view an HDR image, two techniques can be used. These are “tone mapping” and “false colour rendering”. Tone mapping compresses the light values in the image so that the image can be viewed on the limited brightness range of a computer screen or printed page. “The goal of tone mapping HDR images is usually to recreate human perception as close as possible, or to show the most important range of light with as much differentiation as possible” (Cheney 2008, 16). The final tone-mapped image is an 8-bit or 16-bit image. False colour renderings use a range of colours that correspond to the luminance data contained in the underlying HDR image. The luminance data for an HDR image is recorded by a “specific file format” so that the information can be viewed either visually or numerically (Cheney 2008, 18).

2.3.1. HDR Image File Formats

DSLR cameras capture photographs in a RAW format and to save the digital files, the camera converts them to either a JPEG or TIFF file format. The JPEG image produced is an 8-bit image, and is known as a “low dynamic range (LDR)”. A “medium dynamic range (MDR)” is saved under the TIFF file image. RAW files record approximately 10 exposure value (McCollough 2008, 15). Table 2.01 illustrates the difference between the three file formats used.

Bit image	Dynamic range	Luminance value	File format
8-bit images	Low dynamic range	Luminance values of 0-255	JPEG
16-bit images	Medium dynamic range	Luminance values of 0-65,535	TIFF
32-bit images	High dynamic range	Floating point (unlimited) luminance values	RAW

Table 2.01: Table illustrating the difference between bit images and image file formats (McCollough 2008, 17)

2.3.2. Exposure Value

“HDR effectively expands the exposure value you can capture, allowing you to extend the dynamic range of your camera and properly expose different elements of a photograph.”

(Carr and Correll 2009, 9)

Exposure value (EV) controls the amount of light entering the camera. It is controlled by changing the aperture and/or shutter speed of your camera so that the resultant photograph is not over or underexposed.

Aperture is the opening size of the lens that allows light penetration through the shutter and onto the sensor and the larger the opening is, the more light that is able to penetrate (Carr and Correll 2009, 8).

Shutter speed, measured by units of time sets the speed of opening and shutting the shutter. The longer the shutter opens, the larger amount of light penetrates into the camera (Carr and Correll 2009, 8).

“An EV increment of one (1 EV) is the same as a “stop” and refers to half as much or double the amount of light. The greater the exposure value, the greater the luminance of the scene.”

(McCollough 2008, 14)

Our eyes can view exposure values of up to 20 EV, and an external scene can have an exposure value of up to 17 EV. Current technology, for example “digital cameras, monitors, and print media’s”, only allows 5-10 EV to be captured (McCollough 2008, 14).

“Therein lies the problem: How do we capture and display scenes with higher exposure values than present technology is capable of rendering?”

(McCollough 2008, 14)

2.3.3. Camera Response Curve

When the researchers require an HDR image to contain accurate lighting distribution within a scene, a camera response curve needs to be generated for the image capturing device. The camera response curve is unique for each camera, and once generated for the specific device, it does not need to be generated again.

Camera response curve is a “polynomial function that models how the camera records the lighting intensity at a pixel level” (Cheney 2008, 13). A camera response curve can be generated using a HDR software.

“Without the calibration achieved by the proper camera response function, the luminance data encompassed in an HDR photo would not be accurate.”

(Cheney 2008)

To generate a camera response curve, a HDR software is used. Software like Photosphere, the camera response curve is automatically calculated while the photographs were fused. However, using software like HDRShop, a camera response curve is generated by going to the “Create” tab. To generate an accurate camera response curve, it is recommended to capture four to five photographs of a scene with “large luminance variations with gradient changes and neutral colours” (Cheney 2008, 13). The exposure values should be as close as possible – typically in 0.5 f-stop increments; however, 1 f-stop increments will also be adequate.

“The camera response function is computationally derived through a self-calibration algorithm; and then it is used to fuse these photographs into a single HDR image, where pixel values can correspond to the physical quantity of luminance.”

(Inanici 2010, 2)

2.3.4. HDR Sky Models and Image-Based Lighting Techniques

Shooting photographs of the sky is made possible with HDR photography and has advanced dramatically in terms of digital photography. Mehlika Inanici, of University of Washington conducted a study to evaluate HDR imaging using sky models in lighting simulations. The study, conducted in 2010, had a goal to “develop advance lighting simulation techniques to empower researchers and practitioners with better predictive capabilities” (Inanici 2010, 2).

“The specific objectives include

- I. development and utilisation of high resolution data acquisition techniques to collect image based sky luminance information;*
- II. demonstration of utilisation of the image based sky models in lighting simulations; and*
- III. evaluation of image based sky models.”*

(Inanici 2010, 2)

Even though lighting simulations have advanced through the years and are becoming more accurate, a “faithful representation of sky luminance distributions” at “specific location and time” continues to be problematic (Inanici 2010, 1). Sky luminance distribution varies depending on the weather conditions, geographical location, and time of day. With 15 generic sky models developed by CIE, ranging from overcast to “cloudless” skies, none of these sky models represent the “actual sky conditions” causing uncertainties in simulations (Inanici 2010, 1).

Researchers have recently “utilised photography to derive empirical sky models” and captured the “sky through a single photograph using a calibrated camera” (Inanici 2010, 1). The calibration process can only be done manually and can be tedious. The accuracy of the calibration is camera dependent as well. The use of a single image limits the “dynamic range of luminance values” and the “acquired photograph is used to derive a customised mathematic model, and is not used as a direct simulation input” (Inanici 2010, 1).

However, with the use of HDR imaging and Image Based Lighting (IBL), also known as Image-Based Rendering (IBR), is a recent development in the Computer Graphics field. The use of HDR imaging as a light source or an environment map consists of capturing photographs with a variety of exposures within the scene allowing the “wide luminance variation” to be captured. Through various laboratory and field studies, this technique has been validated for “lighting measurement purposes” and has been discovered that the “pixel values in the HDR photographs can correspond to the physical quantity of luminance with reasonable precision and repeatability (within $\pm 10\%$ error margin)” (Inanici 2010, 3).

“Reflective surfaces have to be treated as a light source a reflection of the sun or any other light sources will dramatically increase the contrast. Some reflections can be ignored, but large reflections need to be considered.”

(McCollough 2008, 98)

This study uses a 180° sky dome captured using HDR photography and a fisheye lens instead of using generic CIE sky models. This technique allows the researcher to capture the “actual sky conditions at a place and time”. Using IBL techniques, the HDR photograph is used to light the simulated environment while the luminance information is stored as pixel values of the HDR image.

IBL is an “analytical tool for studying daylighting effects in a design space” as it provides “accurate visual aids and light level data to accelerate and improve the design process” (Cheney 2008, 11). The four simple steps in creating an IBL are as follows:

1. Create either a 180° or 360° luminance map by taking HDR photographs of the environment.
2. Create the digital model of the space studied – including “geometry, materials, synthetic light sources, and camera viewpoints” (Cheney 2008, 29).
3. The hemisphere or spherical luminance map is used as the sky model for the digital model.
4. The rendered image is then produced with an HDR image as the luminance map.

IBL is one of the most accurate processes when it comes to daylight simulation. Using IBL techniques, the simulation can produce visually and numerically accurate results and can help with design options. However, it is not a very common simulation technique as it is a “script based technique” and the lack of “designer-friendly graphic user interfaces (GUIs) hampers the wide adoption of IBL among architectural professionals” (Cheney 2008, 33). However, the geometrical form of the building can be created in a more user friendly interface like Autodesk Ecotect™ or Google SketchUp and later exported.

Instead of using a standard sky, IBL techniques simulate a real sky based upon the luminance map captured in an HDR image of the sky. Currently, it is not known whether a horizontal (ground level or rooftop) or a vertical (at the window) HDR sky is more accurate for daylight simulation. Therefore, for this research both types of skies would be explored.

It is recommended that the HDR images created should be calibrated using a “single measurement” measured using a luminance meter. A luminance meter is pointed towards a grey surface and daylight measurements are recorded in cd/m^2 . The measured value is calibrated against the pixel value in the HDR image in an HDR software like Photosphere. A different method is required to calibrate HDR sky images. An illuminance meter is placed at camera level, and the measurements are recorded during the image capturing process.

“Illuminance can be derived from the over luminance values in hemispherical fisheye images. Hemispherical fisheye projection is a half sphere projected such that each differential area corresponds to the original area multiplied by the cosine of the polar angle. [...] value illuminance can be derived from luminance values in a hemispherical fisheye projection.”

(Inanici 2010, 6)

The study determined that “image based sky models can provide an accurate and efficient method for defining the sky luminance distributions” (Inanici 2010, 19). For un-built buildings, it is recommended that the sky model is captured on ground level. Whereas, for “existing structures, vertical fisheye images that capture the sky as well as the surrounding are recommended for best results”. Capturing the sky image at roof level can provide the researcher with an “unobstructed view”, however, the surrounding environment would not be included (Inanici 2010, 19).

Orientation is one of the main issues that are rarely addressed when it comes to IBL. Additional attention is required regarding the orientation of the digital model and the HDR sky so that the two elements are orientated in the same direction. This could be simplified if

when capturing HDR sky photographs in the scene, by making the top of the photograph north. To transform a 2-D image to a 3-D image in Radiance Lighting Simulation and Rendering System, a script is required to be written. Generally, in a plan view of a digital model, north is assumed to be “up” or the “+y direction” (Cheney 2008, 38).

2.3.5. Computer Simulations with HDR Photography

HDR images can contain the entire range of lighting information required for daylight simulations including the light sources and light reflections from the surrounding environment as well as the entire range of light levels available to the human eye. HDR imaging is also known as “an environment map, a radiance map, or a luminance map” (Cheney 2008, 7). This technique of using HDR imaging to achieve “luminance mappings” is a recent development in the “lighting research community” (Borisuit, Scartezzini and Thanachareonkit 2010, 360).

Comparisons between luminance measurements in an HDR image and “point-to-point luminance meter” was conducted to “determine the accuracy and reliability” of this recently developed technique (Borisuit, Scartezzini and Thanachareonkit 2010, 360). Errors of up to 20% were identified using this technique and though various studies, it was discovered that this technique “provides very reasonable accuracy for a wide range of luminance” when comparing real and simulated measurements (Borisuit, Scartezzini and Thanachareonkit 2010, 360).

Christoph F. Reinhart and Jan Wienold, (Reinhart and Wienold 2011) have explored the effectiveness of simulation when it comes to daylighting and HDR images have been used to discover the “full dynamic range of a scene, from direct sunlight to deep shadow”. HDR images are currently used to “derive empirical sky models” (Inanici 2010, 26). An HDR image can capture the lighting data of a physical scene accurately and can “match human perception” of a scene (Cheney 2008, 19). The accuracy of this tool can provide HDR images to be used for daylight analysis within a space.

Greg Ward created the Radiance RGBE (.hdr) file format in 1989. The large data file format uses “real world luminance values to light computer generated objects” (McCollough 2008, 16). In the decade following the development of the new file format, the .hdr extension was becoming the “leading method for lighting computer generated images in the world of major motion pictures” (McCollough 2008, 16). The other commonly used file format to save HDR images is the OpenEXR (.exr) format. After the photographs are fused as a single HDR image, .exr format opens the image as a 48-bit image. After processing, the image is reduced to a 32-bit image. Both file formats “are lossless; saving and reopening the files does not cause any

data loss” and are “able to express luminance over much wider range than other file formats” (McCollough 2008, 17).

2.3.6. HDR Software

There are many HDR programs available to calibrate generate HDR images. The programs that were explored for this research were either free or could be purchased at a low cost. These all have various advantages and disadvantages and various user complexities. The HDR software that was selected for this research must be able to create camera response curve. Next, a 32-bit HDR image is generated by fusing photographs containing multiple exposures together and be able to provide a calibration process to ensure that the lighting measurements within the image are as accurate as possible.

The last step for this research is a comparison study between the pixel values of a real and simulated HDR image. Table 2.02 illustrates the comparison between four HDR programs and further information for each software is available in *Appendix A: HDR Software*.

	hdrscope	HDRShop	Photomatix	Photosphere
Platform	Windows	Windows	Apple Windows	Apple
Price	Free	V1 free V2 \$400	Free Pro \$99	Free
HDR formats	Radiance (.hdr and .pic)	Radiance, PFM, TIFF Float (Pro: OpenEXR, TIFF LogLuv)	Radiance, EXR, TIFF Float	Radiance, EXR, PFM, TIFF Float, TIFF LogLuv, HDR- JPEG
Align source images	Rotation, flip	No	Translation, rotation, manual control-points	Translation and rotation
Create HDRI directly from RAW images	No	Pro only	Yes	Yes
Ghost removal	No	No	Automatic	Automatic
Batch processing	No	Yes	Yes	No
Panoramic transformations	No	Remaps all standard projection	Unwrap mirror ball	Rudimentary panorama stitching
Global tone- mapping operators	Reinhard photographic, Ward histogram	Via Plugins	Photoreceptor	Permanently tone-mapped display: histogram adjustment
Create camera response curve	No	Yes	Yes	Yes
Calibration	Luminance, illuminance	No	No	Luminance
Comparison study – pixel subtraction	Yes	Yes	No	No
Usability	2/3	1/3	3/3	2/3

Table 2.02: Comparison table between the four HDR software, adapted from (McCollough 2008)

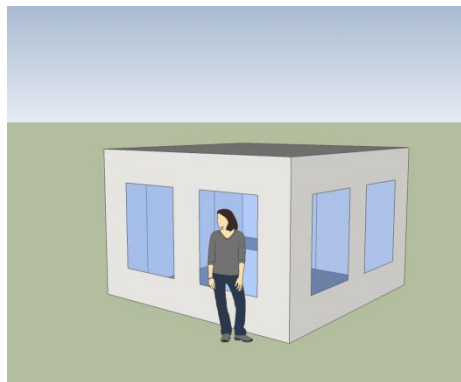
For this research, it was decided that Photosphere was used to fuse the photographs as it has been validated by previous studies and was determined that it is one of the most accurate HDR software currently available.

Only two HDR software were suitable to conduct the comparison study. Both software produces a resultant image with the difference between two images blacked out. HDRShop accepts more image file formats than hdrscope and allows easier editing and scaling of images. Therefore, HDRShop was selected for this study. RadDisplay will also be used to supplement the visual aspects of this research as it can provide false colour renderings with a scale present on the left-hand side of the image.

2.4. Computer Simulation and Modelling

Simulated data has been proven to be a “realistic measure” of daylight prediction in a space and therefore can be used for a “real world analysis”, but it is very important for the input data to be properly measured for the simulation to be accurate (Cheney 2008, 22). With the development of digital modelling in the architectural profession, architects and clients are expecting that the results from computer simulations are more realistic and reliable for real world analysis.

Digital modelling in the architectural profession currently has three different methods to simulate the built environment, and each one has its disadvantages. These are:



- Digital modelling in an empty environment providing no visualisation of the site context;



- Inserting a photograph as the background to the digital model providing an unrealistic representation of the site; and



- Rendering the digital model with a digitally modelled built environment, increasing the simulation and rendering time.

Generally lighting simulation uses light sources made up by the software users according to their own “rules” and “prescribed number of light-bounces off materials” (Cheney 2008, 1). However, this process cannot always be accurate and can be misleading when used as a basis for design decisions.

“Digital modelling programs tend to provide a multitude of lighting options, many of which affect the lighting in unrealistic ways. The complexity and availability of unrealistic options can easily confuse the user and result in a poorly lit digital environment that does not accurately predict the final appearance of a design.”

(Cheney 2008, 1)

Most rendered images from lighting simulations cannot be an “exact match of the physical environment”. Digital modelling cannot create the “inter-reflections and light diffusion caused by surrounding buildings, vegetation, [and] sky variability” (Cheney 2008, 10). Daylight systems that simulate “light reflections from the sky [...] and direct sunlight” and “standardised sky models” are possible in some simulation software. However, this cannot always be accurate (Cheney 2008, 10). The biggest problem when it comes to “digital modelling and rendering” is the knowledge the users are required to have on the “effects of lighting in a physical environment in order to mimic these effects accurately” (Cheney 2008, 10). Different lighting software requires different techniques to create a simulation that is realistic; therefore it is very difficult to master the skills required to create a “photorealistic rendering” within a limited timeframe. Creating an accurate lighting environment in a physically-based renderer is very difficult and requires a “steep learning curve and unavoidable approximations” (Cheney 2008, 10).

When simulating a particular room within a building using computer software for analysis, both the room and the surrounding environment will also be simulated. This is because the

level of daylight reflected from the surrounding environment will affect the room being analysed. There are two common outputs for daylight simulations. These are “luminance distributions” and “various daylight metrics” (Reinhart, Landry and Breton 2008). Even though the accuracy of daylight simulation has been questioned, it has also been said to prove “realistic measures” (Nabil and Mardaljevic July 2004).

“Hourly [...] predictions of daylight illuminance under variable sky and sun conditions can provide a realistic measure of the true daylighting performance of an internal space.”

(Nabil and Mardaljevic July 2004)

2.4.1. Simulation Errors

It is essential when simulating a building that all the material properties entered, are as accurate as possible. It is also essential that any assumptions made in simulating the building are listed in a document so that any possible “errors” that may arise can be found easily. Simulations can take a long period of time to ensure that each step in the creation of the model is simulated correctly. After the model is built in a daylight simulation software, a thorough “inspection” of the model is recommended to ensure that all properties are entered in correctly and the building is simulated correctly.

Both internal and external environment factors must be taken into consideration when building a computer simulated model. The internal factors include window sizes, the geometry of the room and the surface colours. The external environment factors include street light reflectances and surrounding façade. Another aspect the external environment will play is the effect of daylight penetration into the building. So it is important to ensure that they are included in the simulation as the surrounding surfaces will reflect light into the building.

Visible transmittance, also known as the visible light transmittance, is the amount of natural light that penetrates the glazing material into the building. The higher the transmittance values, the more natural light is available to penetrate into the building. This information is not always available as it required the original design specifications to be kept by the building owners, however, it could be measured using a light meter, but uncertainties will need to be taken into consideration.

Daylight design guides recommend that surfaces should have a high reflectance value so that light levels at the “rear of the space” are higher and will provide an even distribution of natural light (eCubed Building Workshop Limited 2008). Surface reflectances are crucially

important. In 2011, an experiment conducted at Victoria University of Wellington by Michael Donn and Jack Osborne showed for a 3% change in reflectances for all surfaces in the model, predicted internal illuminances increased by between 1 and 14%, depending on the measurement point. On average for a 3% higher reflectivity, the space was predicted to be 6% brighter (Osborne and Donn 2011).

2.4.2. Simulating Skies

Climatic conditions play an important aspect when it comes to daylight simulations as it affects the amount of daylight available to penetrate into the building. *Chapter 2.3.4: HDR Sky Models and Image-Based Lighting Techniques*, discussed the use of IBL to map the HDR image as the environment map and use the image as a light source.

Before the use of HDR environment maps, Perez and CIE sky models were used for daylight simulation. There are 15 generic sky models identified by CIE ranging from clear sky, overcast sky, and intermediate sky. Unfortunately neither Perez nor CIE skies can provide realistic cloud coverage of a real sky as the amount of daylight available and the distribution of sky luminance “vary spatially and temporally depending on geography, weather, and other local conditions” (Inanici 2010, 1). Therefore it is important to determine how precise sky models are.

“It is to be noted that all sky patterns except the absolutely overcast are permanently changing their orientation with the gradual movement of the sun, thus the sky patterns follow the sun path also in its daily and annual tracks.”

(Kittler 2007, 96)

2.4.3. Daylight Simulation Software

There are various daylight simulation programs available. Different programs requires different inputs, presents results in different methods, and different levels of complexity. This section explores the possible daylight simulation programs available for this research and the advantage and disadvantage of each.

Table 2.03 summaries the four possible programs that could be used in this research adapted from the U.S. Department of Energy. Each software is further explained in *Appendix B: Daylight Simulation Software*.

	Autodesk 3ds Max Design	DAYSIM	DIVA plugin	Radiance
Keywords	<ul style="list-style-type: none"> • Electric lighting; • Daylighting; • Rendering 	<ul style="list-style-type: none"> • Annual daylight simulations; • Electric lighting energy use; • Lighting controls 	<ul style="list-style-type: none"> • Annual glare maps; • Electric lighting 	<ul style="list-style-type: none"> • Lighting; • Daylighting; • Rendering
Strength	Provides annual and daily lighting performance from CIE sky	<ul style="list-style-type: none"> • Provides reliable predictions of lighting energy use in offices; • Accurate annual daylight availability predictions and energy saving potential. 	<ul style="list-style-type: none"> • Annual lighting performance from weather data; • Provide the overall performance of the daylight solution and help identify any potential savings. 	<ul style="list-style-type: none"> • Physical accuracy in a graphics rendering package; • Reliability and source code availability; • Arbitrary surface geometry and reflectance properties
Weaknesses	Can get confusing with all the different types of simulations available.	Complexity of the software as it is based on Radiance.	Has to go through Rhino or Grasshopper so have to learn either software before this plugin can be used.	Lacks graphical user interface, documentation and models.
Input	<ul style="list-style-type: none"> • EnergyPlus weather data; • Models from Google SketchUp 	<ul style="list-style-type: none"> • Radiance building scene files; • Radiance sensor point grid file; • EnergyPlus weather data. 	<ul style="list-style-type: none"> • Rhinoceros models; • EnergyPlus weather data; • Radiance materials. 	Geometry and materials of design space including surface reflectance characteristics
Output	<ul style="list-style-type: none"> • Renders; • CSV file with annual luminance measurements at light meter grid. 	<ul style="list-style-type: none"> • Annual illuminance/ luminance profile due to daylight at invested sensor points • Daylight autonomy distribution • Daylight factor distribution • Annual electric lighting energy use for different lighting control systems 	<ul style="list-style-type: none"> • Useful Daylight Index(UDI); • Daylight; • CSV files with hourly or monthly data. 	<ul style="list-style-type: none"> • Luminance and illuminance values; • Plots and contours; • Visual comfort levels; • Photograph-quality images; • Video animations.

Expertise required	Have background in CAD, but easy to pick up.	Ideal to have experience using Radiance.	Easier modelling software to use compared to the other.	High level of computer literacy with a minimum of four days training.
---------------------------	--	--	---	---

Table 2.03: Comparison between four daylight simulation programs that are suitable for this research, adapted from (U.S Department of Energy 2011)

The selected daylight simulation software used for this research is Radiance Lighting Simulation and Rendering System. It is a physically-based rendering program that has been validated for daylight analysis “with physically-based modelling of material and sky conditions” (Cheney 2008:10). Radiance is a script-based program comprising of 50 individual programs and is a script-based program with text files. The models geometrical form cannot be generated visually and only a resultant image is produced of the camera view. Therefore, Google SketchUp 8 was used to simulate the geometric model so that it can be visually viewed and later exported, by layers, to Radiance for further editing.

2.5. Physically Scaled Models

A physically scaled model can be used to accurately “portray the distribution of daylight within the model exactly as it would in a full-size room” (Bodart, et al. 2007, 1). Physical models can also provide information on daylighting that can provide lessons for computer modelling. This research utilises the tool of physically scaled model in the pilot study. The physically scaled model of a study room will be placed in the lighting laboratory under the artificial sky to experiment and test the equipment used for this research to minimise inaccuracy in-field.

“When properly constructed, scale models portray the distribution of daylight within the model exactly as in a full size room. Comparison studies of simple models have shown that daylighting studies carried out under sky and sun simulators can give very accurate results.”

(Bodart, et al. 2007, 1)

To build accurate scale models, there are rules that should be followed. A study was conducted by Magali Bodart in 2007 to outline these rules when conducting a daylight study under an artificial sky. The first aspect when it comes to constructing a physically scaled model is the scale. The scale of the model will depend on the researcher’s objectives and what they want to achieve from the scale model. Table 2.04 illustrates the table provided by the International Energy Agency detailing the scale of which the daylight model should be in order to fulfil the objectives of the research.

Scale	Objectives
1/200 to 1/500	For preliminary design and concept development To provide a gross sense of the massing of the project To study the shadows generated by the future building or from a neighbouring building
1/200 to 1/50	To study direct sunlight penetration into a building To study diffuse daylight in a very big space
1/100 to 1/10	To consider detailed refinements of spatial components To have highly detailed inside views To study accurately diffuse and direct daylight penetration
1/10 to 1/1	To integrate critical industrial components To consider daylighting devices that cannot be reduced in scale To proceed to final evaluation of advanced daylighting systems through monitoring and user assessment

Table 2.04: “Scale choice as a function of daylighting design purpose (International Energy Agency 2000)”

If internal photographs are required of the scale model for daylight study, it is suggested that a *macro* lens is used. In order to conduct a comparison study between a full size room and a scaled model, it is recommended to construct the building in a 1/20 scale or higher so that the lens could be placed at eye height; which is between 1500 mm and 1700 mm (Bodart, et al. 2007, 33).

Another aspect of the daylight monitoring process that should be considered when constructing the scale model is the illuminance meters in terms of the size of the sensors and where they should be placed. If the scale model is at 1/20, then with a sensor height of 150 mm, the measurements would have been recorded at “work plane height of 0.8 m [800 mm]” (Bodart, et al. 2007, 33). Interior access to the scale model is required to insert the illuminance meters. An opening, either via a window or through a removable wall, is required, but the possibility of light leakage must be considered.

“Light leaks are a key source of inaccuracy, especially in poorly daylit rooms. For scale model made of foam core, joints can be made following the technique [...] and covered by black tape.”

(Bodart, et al. 2007, 34)

Another aspect that will affect the accuracy of the scale model is materiality and geometry of the analysed room. Almost all materiality can be used to construct the scale model, however, if the “material property” relates to light, it “should be as close to those of real building materials as possible” (Bodart, et al. 2007, 35). It is important that the surface reflectivity is not “over valued” as this can lead to errors.

“For example, if a vertical wall has a reflectance of 50% and the scale model has white walls of 86% reflectance, the measurements made in the scale model can over predict the results by about 150 to 200% for a point located at the far end of the room [...] for a quantitative daylighting study, it is preferable to select a material with a reflectance very close to that of the full-scale material.”

(Bodart, et al. 2007, 35)

Windows are one of the most important aspects when it comes to model construction as this limits the amount of daylight penetration. Window sizes need to be modelled correctly and the window sill detail needs to be included. If glazing is able to be inserted into the daylight model, i.e. a 3 mm to 6 mm thick glass with “the same optical properties as the real glazing”. If glazing material is not available daylight measurements can be recorded without glazing, but a “reduction factor” needs to be introduced so that the results are accurate (Bodart, et al. 2007, 35).

Furniture and internal walls play a vital part due to reflectivity of the surfaces. However, constructing the furniture for the scale model can be very time consuming causing modelling costs to increase. Furniture modelling is not required for preliminary studies (Bodart, et al. 2007, 33). The surrounding environment will need to be considered as this will also reflect daylight into the building. The external material of the building has minimal influence with regard to internal light levels.

2.6. Mirror Box as a Sky Simulator

For physically scaled models, a mirror box sky simulator is typically used to provide an artificial sky for physically scaled models. It provides the model with a similar sky distribution to the CIE overcast sky and the daylight potential of a full-scaled building can be determined using this technique. However, this does depend on the accuracy of the scaled model.

“Mirror-box artificial skies can reproduce reasonable approximations to the standard overcast sky luminance pattern. They provide a controlled luminous environment for daylight factor measurement in scale models.”

(Mardaljevic 2002, 2)

Mirror boxes, also known as artificial skies, are usually square or rectangular. They are used to “simulate the overcast sky” and “have luminous ceiling and walls made of mirrors” (Matusiak and Arnesen 2005, 315). The daylight model is placed on a desktop, where the mirror and brown card intercept, at the centre of the mirror box. Both illuminance and photograph

measurements can be recorded in this space. Artificial light tubes, in this case, fluorescent lights are the light source and the *light rays* are reflected from the mirrors.

The distribution of luminance in the mirror box depends on five factors. They are:

1. **Ceiling luminance** - should be consistent with “equal artificial light sources” (Matusiak and Arnesen 2005, 319);
2. **Mirror box shape in plan** - if the mirror box is in a square shape, then the “luminance distribution” will be more symmetrical when compared to a rectangular box (Matusiak and Arnesen 2005, 319);
3. **Height-width ratio and reflection factor of the mirrors** – a mirror box with a height/width ratio of 2/3 “works well in approximating the CIE standard overcast sky” (Matusiak and Arnesen 2005, 319);
4. **Inclination of the mirrors** will affect the “angle of inclination” (Matusiak and Arnesen 2005, 319); and
5. **Mirror reflectance pattern.**

2.7. Conclusion

This chapter provided the background study for this study. The aim was to provide information regarding why HDR photograph is suitable and reliable as a daylight measurement tool and how this technique has been used in previous studies.

HDR photography is a huge topic to cover. This research only explored what has been done in terms of using HDR image as an environment map to light a daylight simulation and the important aspects in HDR photography that will affect the accuracy of the results. It is only recently that researchers have started to explore the possibility of using Smartphones as a daylight measurement device.

Another important aspect of this chapter is computer software in both generating HDR images and daylight simulations. There are numerous programs available that are suitable for both tasks, but only some of these have been validated to provide accurate results. For this research, Google SketchUp 8 was used to create the geometric form of the models and be exported into Radiance Lighting Simulation and Rendering Systems via a plugin. Photosphere was used to generate the HDR images and HDRShop was used to compare the real and simulated data along with the help of RadDisplay.

Chapter 3: Equipment

The objective of this chapter was to document the equipment that was used for this research. Section 3.1 outlines the three image capturing devices employed for this research – an Android operated Smartphone, an Android operated Tablet, and a DSLR camera. Section 3.2 documents the luminance and illuminance sensors used in the lighting laboratory, the study room, and in the field to calibrate the photographs captured. This was followed by the X-Rite ColorMunki device and software to calibrate the material surfaces in the buildings studied in section 3.3. Lastly in section 3.4, the Macbeth ColorChecker chart was explored. The colour chart was placed in all the photographs captured to help calibrate the photographs. Each of the equipment used in this research were calibrated in the lighting laboratory.

3.1. HDR Camera

The precedents for HDR photography as a daylight analysis tool have typically used a high quality DSLR camera (costing NZ\$1500-2000) in association with a fisheye lens (an additional NZ\$1000-2000) to capture the full field of view in a scene. This research is focused on the application of Smartphone and Tablet technology for the same purpose. The basic rationale for this was not just cost, though a much reduced cost will ensure HDR image based lighting assessment was available to all. The rational was that the highly detailed, high resolution HDR photograph from an expensive DSLR camera contains far too many pixels than are needed plot the light distribution in a scene.

Therefore, this study will primarily focus on using an Android Smartphone. However, due to some complications that arose from the pilot study and the first two buildings monitored, an Android operated tablet was introduced for the final monitored building. However, before heading out into the three buildings monitored, a Nikon D200 DSLR camera with a fisheye lens was used to calibrate and compare the image capturing devices. This calibration process was conducted in the lighting laboratory in the lighting laboratory at Victoria University of Wellington.

3.1.1. Mobile Smartphone and Tablet

The mobile Smartphone used in this research was a Motorola Defy with an Android 2.3.7 operating system, illustrated in figure 3.01. The tablet used in the third building monitored for this study was a Samsung Galaxy Note 10.1 Tablet with an Android 4.1 operating system, illustrated in figure 3.02. Both devices have a five megapixel camera with flash and a magnetic fisheye lens, which can be attached to the camera lens via a magnetic ring. The magnetic ring

was attached to the device with adhesive tape. The fisheye lens attachment was purchased online for US\$50. During the monitoring process, both devices were mounted on a solid surface to ensure that any movement between the HDR photographs captured was minimised.



Figure 3.01: Motorola Defy with fisheye lens attachment



Figure 3.02: Samsung Galaxy Tablet with fisheye attachment

To ensure that the HDR photographs were taken quickly and without having to change the settings, the HDR Camera 2.20 application (Google Play 2012) was downloaded. This application is available for all Android devices with an Android 2.2 operating system or above, at no additional costs. This application captures three to four photographs under various exposures depending on the type of device used. Using the Motorola Defy, four photographs are captured with exposure values of -1.50, +0.00, +1.50, and +3.00, illustrated in figure 3.03. Whereas the Samsung Galaxy Note Tablet captures three photographs with exposure values of -2.00, +0.00, and +2.00, illustrated in figure 3.04. The HDR camera application will fuse all of the photographs into a single tone-mapped HDR image when all the LDR images were captured. However, this research requires all four original frames to be kept and saved otherwise some lighting information may be lost through tone-mapping. The photographs were then calibrated and fused manually using a HDR software like Photosphere (Ward Larson, Anywhere Software).



Figure 3.03: Four HDR images created from the Motorola Defy Smartphone (From left to right: -1.50 EV, +0.0 EV, +1.5 EV and +3.0 EV)



Figure 3.04: Three HDR images created from the Samsung Galaxy Tablet (From left to right: -1.50 EV, +0.0 EV, and +1.5 EV)

The built-in camera application available for the two Android devices was used as well for comparison and to collect the exchangeable image file format (EXIF) data as the photographs captured using the HDR Camera application does not provide an EXIF file. The EXIF files contain the image data for that particular photograph and are required to fuse the images together. Therefore, the photographs captured using the built-in application were used to provide the EXIF data required to fuse the photographs captured using the HDR Camera application into single HDR images.

3.1.2. DSLR Camera

The DSLR camera used was a Nikon D200 DSLR camera with an AF Fisheye Nikkor 10.5 mm lens, illustrated in figure 3.05. The camera was set to capture the scene in five different exposures; -2.0, -1.0, +0.0, +1.0, and +2.0. The photographs can then be fused manually using an HDR software. To ensure the HDR image created achieve optimum accuracy, five or more exposures are recommended as this allows the “HDR algorithm to better approximate how your camera translate light into digital value (digital sensors response curve) – creating a more even tonal distribution” (Cambridge in Colour). The DSLR camera must be mounted on a tripod during the image capturing process to reduce camera movement and “ghosting”. If any movement was evident in the resultant image, the five photographs captured can be aligned in one of the HDR analysis software.



Figure 3.05: Nikon DSLR camera and fisheye lens

3.1.2.1. Fisheye Lens

Fisheye lenses were first introduced into the photography industry in the 1960s by Nikon. “It was a device built to enable meteorologists to take images of the full sky dome in one shot” (Bloch 2007, 261). This allows the photographer the opportunity to capture a maximum of 180° of its surrounding, depending on the type of fisheye lens used.

There are two main types of fisheye lens, circular fisheye lenses and full-frame fisheye lenses and these are further differentiated by the circular image size. The difference between the two types of fisheye lenses is illustrated in figure 3.6.

“Circular fisheye lenses cover 180 degrees in all directions, but have black edges.

Full-frame fisheye lenses cover 180 degrees along the diagonal only, producing a less wide-angle rectangular photo without the black borders.”

(Photography Mad n.d.)

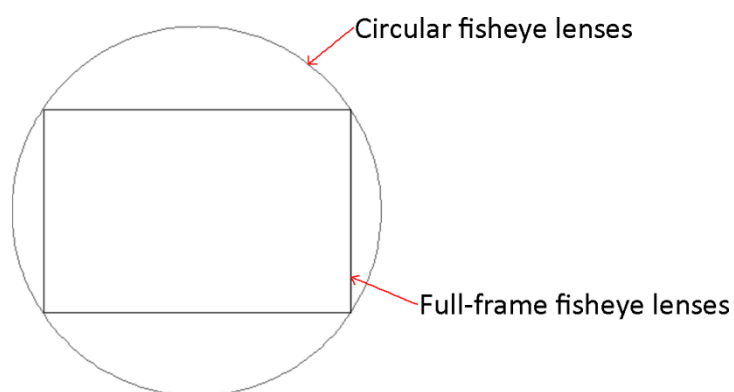


Figure 3.06: Difference between a circular fisheye lens and a full-frame fisheye lens

The AF Fisheye Nikkor lens, illustrated in figure 3.07, used for the pilot study of this research was a full frame fisheye lens suitable for a selected few Nikon digital cameras, it is also known as a *rectangular fisheye*. The angle of view of the fisheye lens is 180° (diagonally) (Nikon 2012). This will allow a wider view of the room to be captured and analysed.



Figure 3.07: AF Fisheye Nikkor lens used for this study (Nikon 2012)

3.2. Luminance and Illuminance Sensors

Three different luminance and illuminance sensors were used throughout this study as well as a HOBO U12 data logger that was used during the BEES study. Each light measurement device was previously calibrated by the manufacturers in the past couple of years. The documentation of the spectral response curve for the light meters used for this research could be found in *Appendix C: Equipment*. However, all of the luminance and illuminance sensors were taken to the lighting laboratory under the artificial sky to calibrate them against each other to ensure the accuracy of the measurement when out in the field. The calibration process and results were documented in *Appendix D: Equipment Calibration Process*.

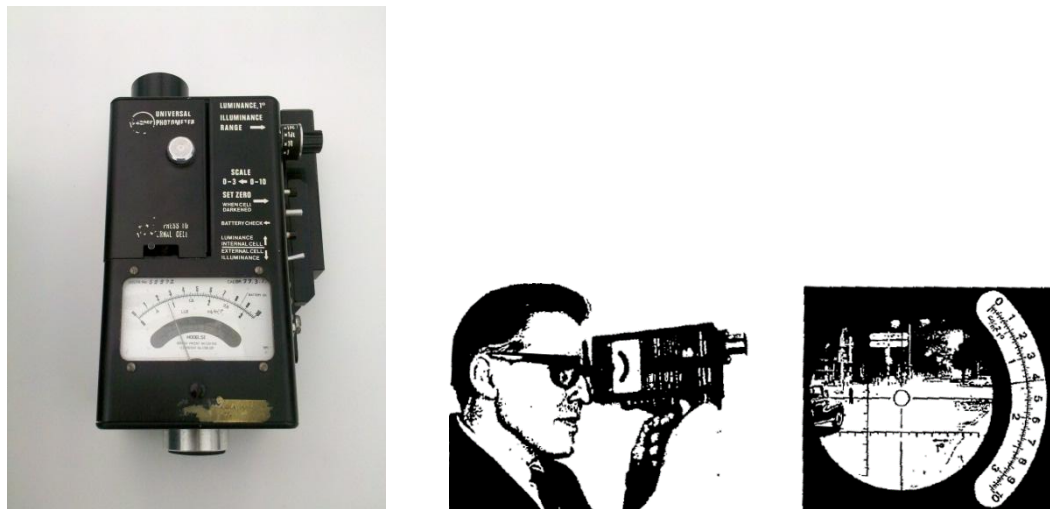


Figure 3.08: Hagner Universal Photometer Model S2 measurement recording technique (left) and the view through the view-finder (right) (Hagner International UK Limited 1974, 6)

The luminance meter used was a Hagner Universal Photometer Model S2. The Hagner Photometer was able to capture both luminance and illuminance measurements, but for the purpose of this study, only the luminance measurements were recorded using this device. This was used to calibrate the HDR sky images produced. By pointing the device towards the measured surface, the user can then look through the view-finder showing the measurement

scale. The “range-finder (range)” could be adjusted so that the luminance measurements could be recorded (Hagner International UK Limited 1974). Figure 3.08 illustrates how the measurements are read and what can be seen through the view-finder.

Photometric Illuminance sensors, illustrated in figure 3.09, are used for daylight measurements where the human eye is the “primary receiver”, for example and indoor environment (LI COR Environmental Division 2012). It measures the illuminance in lux and can be “mounted at any angle” with a calibration uncertainty of $\pm 5\%$.



Figure 3.09: Photometric Illuminance sensors used to record the daylight measurements in the physically scaled model and the study room

Five LI-Cor LI210A Photometric Illuminance sensors were connected to a laptop and were taken into the lighting laboratory prior to being used in the pilot study. The five sensors were placed in a line and light measurements were recorded every minute for an hour to ensure that the readings on each were calibrated against each other and against an external, calibrated lighting standard. The five sensors were used throughout the pilot study record the illuminance in both the physically scaled model and the study room

The other illuminance meter used was a standard Minolta Illuminance Meter T-1H, illustrated in figure 3.10. This was placed on the desktop in the photographed scene to capture the illuminance meter in the space so that the resultant HDR image can be calibrated in an HDR software. This was placed on desktops in the three monitored buildings.



Figure 3.10: Minolta hand-held light meter placed on desktops for illuminance measurements in the field

The BRANZ measurement device, the HOBO U12 data logger, illustrated in figure 3.11, was an environmental data logger that records light levels, temperature and humidity levels in the space. The data loggers are placed in the “main areas of the building,” for example; offices and meeting rooms and a reading from this equipment was set to record measurements every ten minutes for a period of two weeks. Within the premise monitored, the HOBO data loggers are typically placed at opposite ends of the building, and approximately 3000 mm away from external windows on all façades. These “small battery-powered loggers” were positioned away from “heat sources, draughts and direct daylight” and artificial lighting. They are placed between 400 mm to 2000 mm high as that is the typical height range in which occupants are in (Isaacs, et al. 2009, 59).



Figure 3.11: HOBO U12 data logger used by BRANZ to record the environmental measurements including lux measurements

3.3. X-Rite ColorMunki

The X-Rite ColorMunki spectrophotometer, illustrated in figure 3.12, is a colour measurement device that records the RGB (Red Green Blue) values and reflectances of a surface in a scene. By downloading an additional plug-in, the ColorMunki software can load the pallet of colours

captured in a scene directly into Autodesk 3ds Max Design through a .cxf file. To capture the colours in a scene, the ColorMunki was plugged into a laptop (both Mac and Windows can be used) via a USB cable and spot measurements of the surfaces can be taken. A library of colours can be created in 3ds Max Design so that the exact values of the surface colours of the tested area can be modelled. In each monitored building the surface reflectance of each material was recorded with this device five times and the average was used for simulation.



Figure 3.12: X-Rite ColorMunki spectrophotometer used to capture the RGB and reflectance values of the surfaces in a scene

3.4. Macbeth ColorChecker

The Macbeth ColorChecker, illustrated in figure 3.13, is a colour chart containing 24 standardised colours which can assist in the calibration of photographs to ensure the accuracy of the images taken on site. The Macbeth ColorChecker chart was inserted into the real scene when the photographs were captured so that they could be calibrated using the published colour coordinates for each colour on the chart.

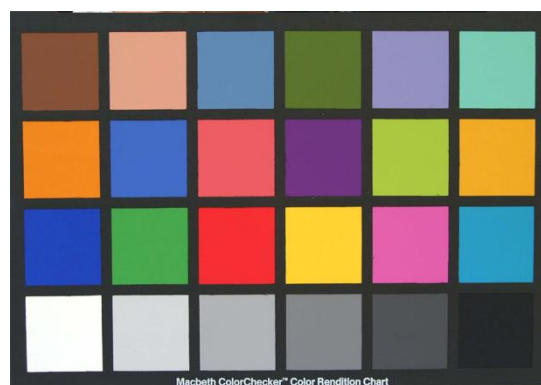


Figure 3.13: Macbeth ColorChecker colour chart used to calibrate the HDR images capture on site

3.5. Conclusion

This chapter explored the equipment used to conduct this research ranging from image capturing devices to daylight measurement devices as well as collecting and calibrating the colour spectrum in a space.

It was important to ensure that the equipment used for this study has been calibrated to ensure the measurement process was accurate. The equipment was calibrated in the lighting laboratory as it would not have any external environment affecting the results and are then compared to each other and to ensure that the measurements recorded are within $\pm 10\%$ of each other (Hayman 2003, 106). The calibration process is documented in *Appendix D: Equipment Calibration Process*.

Chapter 4: Pilot Study

The objective of this chapter was to document the pilot study for this study conducted primarily in the lighting laboratory at Victoria University of Wellington. The pilot study was conducted under an artificial sky. This allowed the pilot study to be conducted under an even lighting distribution and provided a more controllable environment when compared to the real sky. Under this controlled environment, measurement errors were minimised and the technology of using an Android device to capture the HDR photographs could be developed. If the pilot study was conducted under real skies, the light distribution cannot be controlled and various aspects of the external environment can create errors in the measurement processes.

Section 4.1 explores the experiments in the lighting laboratory including using a physically scaled model of a study room and generating a camera response curve. This leads to the exploration of daylight measurements and HDR photographs of the life-size study room for comparison in section 4.2, along with the measurement process for the pilot study. Section 4.3 documents the pilot study simulation process in Radiance and the development of the technique used for creating HDR skies, referred to in *Chapter 2.3.4: HDR Sky Models and Image-Based Lighting Techniques*. Lastly, section 4.4 documents the comparison process of real and simulated data.

4.1. The Lighting Laboratory

To begin, the study was taken down to the lighting laboratory in the School of Architecture and Design Campus at Victoria University of Wellington. The lighting laboratory measures 3500 mm by 3500 mm with a ceiling height of 2330 mm, illustrated in figure 4.01. It has rotating effulger panels as the walls which provide the user with two wall options; glossy white or mirrored, illustrated in figure 4.02. The effulger panels provide a mirror box sky distribution similar to the CIE overcast sky suitable for daylight analysis for a scale model (Matusiak and Arnesen 2005). Fluorescent tubes line the ceiling of the laboratory. There are four different colour tubes providing white, red, green and blue lighting which are able to recreate an artificial sky. The brightness of the “sky” can be controlled by a simple remote.

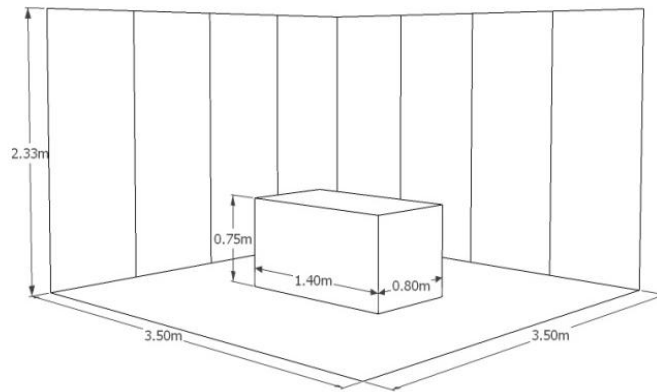


Figure 4.01: Dimensions of the lighting laboratory at Victoria University of Wellington



Figure 4.02: Rotating effulger panels with glossy white or mirrored options. For this research, only the mirrored panels were used.

The pilot study was conducted under the artificial sky to allow the experiments to be conducted under a controlled environment. Any issues or errors that arise under an artificial sky in the lighting laboratory can be easily fixed. This was used to ensure that once the monitoring process began in a commercial building the complications of the measurement process had been resolved and any further errors would be due to the on-site measurement process.

4.1.1. Camera Response Curve

In order to create an accurate HDR image for daylight measurements, a camera response curve must first be generated. An advantage of Photosphere was that it automatically calculates the camera response curve while fusing the LDR photographs. The camera response curve for the Nikon D200, illustrated in figure 4.03, was easily generated through Photosphere. Photosphere is an Apple operated software that can accurately create HDR images and generate camera response curve, unique for each image capturing device (Ward Larson, Anywhere Software).

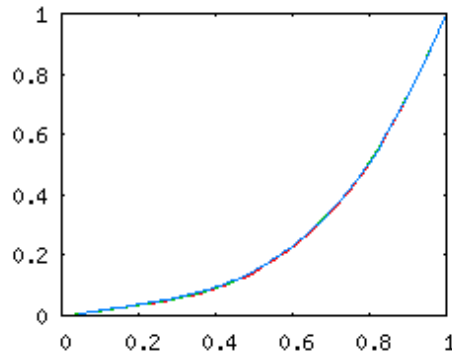


Figure 4.03 Camera response curve for Nikon D200

However, it was determined that a camera response curve was not as easy to generate with the Motorola Defy Smartphone camera. This appears to be because the images captured by the Smartphone using the built-in camera, have less data contained within their EXIF file, whereas using the HDR Camera application, the EXIF data were not written to the image. The basic camera application in the Smartphone does however permit the manual capture of a series of images with different exposure values, ranging from -3.00 to +3.00. Through numerous tests and experimentations, a camera response curve for the Motorola Defy Smartphone could not be generated. However, it was later discovered that a camera response curve could be generated using a Samsung Galaxy Tablet. The tests and experiments conducted are documented in *Appendix: G: Generating a Camera Response Curve*. This resulted in creating the HDR image by using the generic camera response curve available in Photosphere.

4.1.2. Physically Scaled Model

For the pilot study, a model of a study room at the School of Architecture and Design Campus was used. The model is a 1:20 scale of the actual room, and was placed in the mirror box artificial sky. The scale model is approximately 600 mm by 600 mm by 150 mm providing adequate space to insert a light meter or a Photometric Illuminance sensor (Jarvis and Donn 1997).

The model created by Dave Jarvis, (Jarvis and Donn 1997), was constructed out of 5 mm thick card/polystyrene sandwich board with cut-outs where the windows are located. The interior and exterior of the physical model was painted with various shades of grey so that the reflectances of the surfaces are as close as possible to the actual study room, illustrated in figure 4.04. The carpet sample of the actual study room was collected and used as the flooring.



Figure 4.04: Interior and exterior photographs of the physically scaled model used for the pilot study

The scale model was set up on a table, at 700 mm above floor level, in the centre of the artificial sky with white florescent tubes turned on and mirrored effulger panels for the walls. This provided the scaled model with overcast sky conditions.

The Nikon D200 camera was set up inside the physically scaled model at a door opening, facing the windows. The camera was set so that five images ranging in EV -2.0 to +2.0 with 1-step increments were captured automatically.

The illuminance distribution of the artificial sky was captured on a three by three grid to see how the artificial light was distributed in the scene. This measurement can be found in *Appendix E: Lighting Laboratory Illuminance Distribution*.

A light meter was placed on the desk next to the scaled model to capture the external illuminance. Five illuminance sensors were placed inside the scaled model. One was placed facing out the window so that the vertical illuminance produced by the artificial sky could be captured. Three illuminance sensors were spaced evenly about 100 mm from the window's edge and the last illuminance sensor was placed a further 100 mm away in the centre of the scaled model. This allowed for an even distribution of measurements in the scale model. Figure 4.05 illustrates the location of the sensors. The measurements were then recorded every minute for a period of one hour to ensure that the illuminance measurements were correct. A further step to calibrate the HDR image created under the artificial sky was to use a luminance meter to measure the luminance of the artificial sky from nine different points on the ceiling. The nine measurement points were marked with a red sticker dots so that each spot can have five measurements recorded and the average of those measurements were recorded.

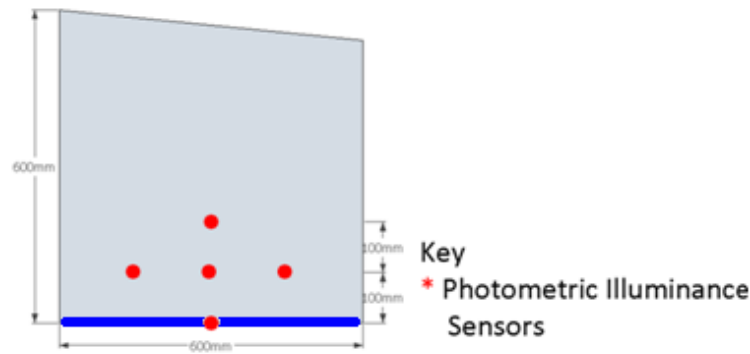


Figure 4.05: Plan view of the physically scaled model illustrating the location of the Photometric Illuminance sensors. The blue line at the bottom of the image is where the windows were located.

These measurements form the basis of the calibration of the HDR Image. Once these steps were completed, the photographs were fused into HDR images and the illuminance measurements recorded during the measurement process were used for calibration. This was done by using Photosphere and picking the same spot within the HDR image produce as the measurement point to ensure that the lighting data within the images were accurate. Next, the same process was repeated using the Android Smartphone. An example of the photographs captured using the HDR Camera application is illustrated in figure 4.06.



Figure 4.06: HDR photographs taken inside the physically scaled model using the Android Smartphone (From left to right: -1.50 EV, +0.0 EV, +1.5 EV and +3.0 EV)

4.2. The Study Room

To validate the measurements recorded in the lighting laboratory, and to ensure their accuracy, measurements were conducted in the actual study room that the scale model represented. The study room is located on the second floor at the School of Architecture and Design Campus with windows on the north-east elevation. The building itself was set back from the street with a relatively large tree obstructing the view from the left-hand side of the window. High rise buildings are located on the opposite side of the street (see figure 4.07). A photograph of the interior of the study room is illustrated in figure 4.08.

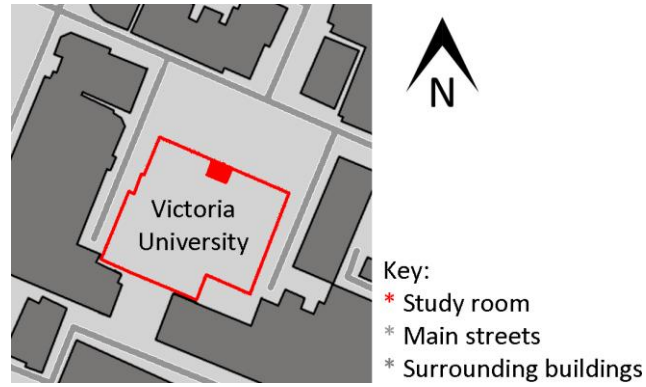


Figure 4.07: Site plan showing the location of the study room in relation to surrounding environment (Not to scale) (Image adapted from (Google 2012))



Figure 4.08: The study room used for validation of the daylight measurements recorded under the artificial sky HDR photographs of the sky and the study room were taken simultaneously as well as a vertical photograph of the sky through a window, illustrated in figure 4.09. This was undertaken as capturing the sky from the ground or roof level does not take into account the surrounding environment which can affect the daylight availability in the space including trees and surrounding buildings (Inanici 2010). The vertical photographs were captured by pressing the fisheye lens hard up against the inside of the window. This was able to account not only for the surroundings, but also the transmissivity of the glazing.

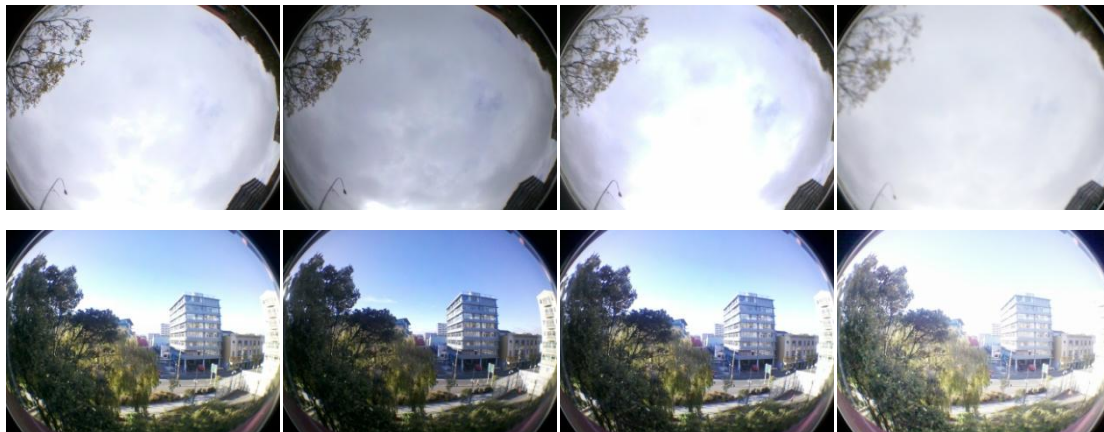


Figure 4.09: HDR photographs capturing the real horizontal (top) and vertical skies (bottom) for the pilot study (From left to right: -1.50 EV, +0.0 EV, +1.5 EV and +3.0 EV)

4.2.1. Measurement Process

Daylight measurements were collected in the study room between 12th April and 17th April 2012, for every 15 minute using Photometric Illuminance sensors with all artificial lighting switched off. It was also important to ensure that light measurements of the external illuminance were recorded at the same time as the internal illuminance measurement as this will ultimately determine the type of sky – i.e. sunny, overcast, etcetera. Therefore, one of the illuminance sensors was taped horizontally to the window. Another sensor was also placed on the window sill. These two sensors were used to measure the external illuminance value. The other three sensors were placed at desk level (720 mm above floor level) and approximately 1000 mm from the windows. The daylight measurement points can be seen in figure 4.10. A hand-held light meter was used to calibrate the results. The measurement results can be found in *Appendix F: Daylight Measurements using Photometric Illuminance Sensors in the Study Room*.

The glazing transmissivity was determined using the light meter by calculating the daylight ratio between the inside and outside illuminance. A light meter was pressed up against the sky while another light meter was held just outside the window. This step was repeated five times and the average measurement was used.

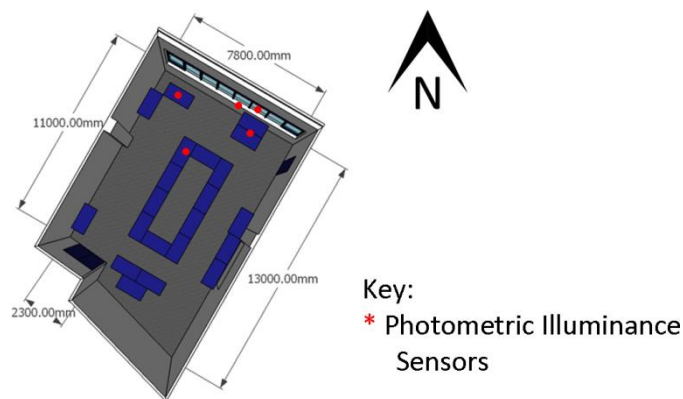


Figure 4.10: Location of the Photometric Illuminance sensors in the study room (Not to scale)

A floor plan, illustrated in figure 4.10, of the study room was drawn with the dimensions of the room measured using a laser distance meter. The location of the desks and window height were also noted on the floor plan. The ceiling height was measured at 3600 mm.

Interior and external HDR photographs of the study room were captured during the measurement period to capture the various skies. The Macbeth ColorChecker chart was inserted into each photograph facing the camera and the ColorMunki was used around the

room to capture all of the RGB and reflectance values in the room. They were saved as a .cxf file.

4.3. Simulation of Pilot Study

Throughout the background study outlined in *Section 2.6.3. Daylight Simulation Software*; it was determined that Radiance Lighting Simulation and Rendering System is the most suitable software to use in this research. To simulate the geometric form of the building, Google SketchUp 8 was used. The floor plan of the simulated study room is illustrated on the previous page in figure 4.10. All of the desks and major surfaces were included in the simulation as this will affect the daylight reflectivity.

The different components with different materiality were separated into individual layers. For example, the internal walls were on one layer, and the external wall was on a separate layer. This will reduce the amount of time required to assign the surface materials in the Ecotect™ Radiance Control Panel. This software was used to manage the Radiance files through the exportation process in Google SketchUp 8. The orientation and the distance between the ground level and the floor of the monitored premises needs to be double checked before exporting the simulated model to Radiance.

A ground plane needs to be simulated with a reflectance value of 0.2 (Mardaljevic 2000, 37). This reflectance value is the worst case scenario for daylight simulations. Cameras were placed at approximately the same location in the study room as the photographs that were previously captured. The simulated model was exported, via “layers” so that each component, for example walls, internal walls, was kept in its individual layers. This allows the materials to be easier to assign to the model in Radiance. The simulated model was exported to Radiance using the “su2rad” plug-in for Google SketchUp (su2rad n.d.).

The average material properties of each surface are illustrated in table 4.01, along with the RGB values to be entered into the `material.rad` file, where all the material information is contained, and the reflectance of each surface determined by using the *Colour Picker for Radiance Online Tool* (JALOXIA 2012).

Surface	R	G	B	RGB value for Radiance	Reflectance
Carpet	57	56	58	0.224, 0.220, 0.227	0.222
Desks	38	64	89	0.149, 0.251, 0.349	0.231
Chairs	88	94	115	0.345, 0.369, 0.451	0.368
Walls	232	229	225	0.910, 0.898, 0.882	0.895
Wall with windows	48	50	71	0.188, 0.196, 0.278	0.199
Window sill	129	128	128	0.506, 0.502, 0.502	0.503
Window frames	64	67	69	0.251, 0.263, 0.271	0.260

Table 4.01: Average surface colours in the study room captured using the ColorMunki

It is important to take into account the variation in material reflectivity. The maximum and minimum surface reflectance variations for the study room can be found in *Appendix H: Variation of Surface Colours in the Monitored Buildings*. These values were used to determine if there are any errors during the material surfaces measurement process.

4.3.1. Simulating an HDR Sky

For the pilot study, HDR images used as an environment map for the simulation included: the artificial sky from the lighting laboratory; a horizontal real overcast sky captured from the ground; and a vertical sky image also captured under an overcast day from the window of the monitored room. To map the “environment” into the scene, a script was written containing a mathematical formula in Notepad and was saved as a “.cal” file. The scripts were created following Paul Debevec’s image-based lighting tutorial. This file instructs Radiance “how to map the direction vectors in the world” (Debevec 2002, 5). Two different mathematical formulae were used for this research as both horizontal sky probe and a vertical sky probe were used and are required to be mapped differently. Both scripts can be found in *Appendix I: Radiance Sky Mapping Scripts*.

The next step was to replace the existing light source, the CIE sky, with an IBL environment, using the HDR sky image. The ground plane needs to have a “ground glow and source” added for the horizontal overcast sky image as with a 180° sky probe, as no ground source information was captured in these photographs (Cheney 2008, 44). The term “colorpict” indicates the file name of the light probe image and the mathematical formula for the direction map; “glow” indicates the material property of the light probe being “treated as an emissive glow” and “source” states the infinite sphere geometry mapped “with the emissive glow of the light probe” (Debevec 2002, 6). When the scene was simulated in Radiance, the

rays hitting the surfaces will contribute their illuminance as the “light specified for the corresponding direction in the light probe image” (Debevec 2002, 6).

4.4. Comparison Between Real and Simulated Data

After the environment map was added into the simulated model, the rendering process can then be commenced. A Radiance Picture, `.pic` was produced (Ward Larson, Radiance file formats). To compare the real and simulated data, HDRShop was used as it was able to do the comparison using a subtraction method.

In a recent study conducted by Coralie Cauwerts from Université Catholique de Louvain in Belgium, she determined four methods to compare the luminance distribution in the HDR images. These are:

- “Pixel to pixel comparison” – problems due to geometrical misalignment;
- Section to section pixel comparison – reduce the error due to geometrical misalignment and quick visual identification of regions with large relative errors;
- “Surface to surface comparison” – on an evenly spaced grid; and
- “Comparison in the visual field” – numerical value easier to compare.

(Cauwerts 2012, 14)

This research used all four methods to compare the real and simulated HDR images. Figure 4.11 illustrates the HDR image of the study room using the Motorola Defy Smartphone along with a false colour rendering of the scene. The simulated images produced from the Radiance simulation under horizontal and vertical skies are illustrated below, along with the false colour renderings and the sky images.

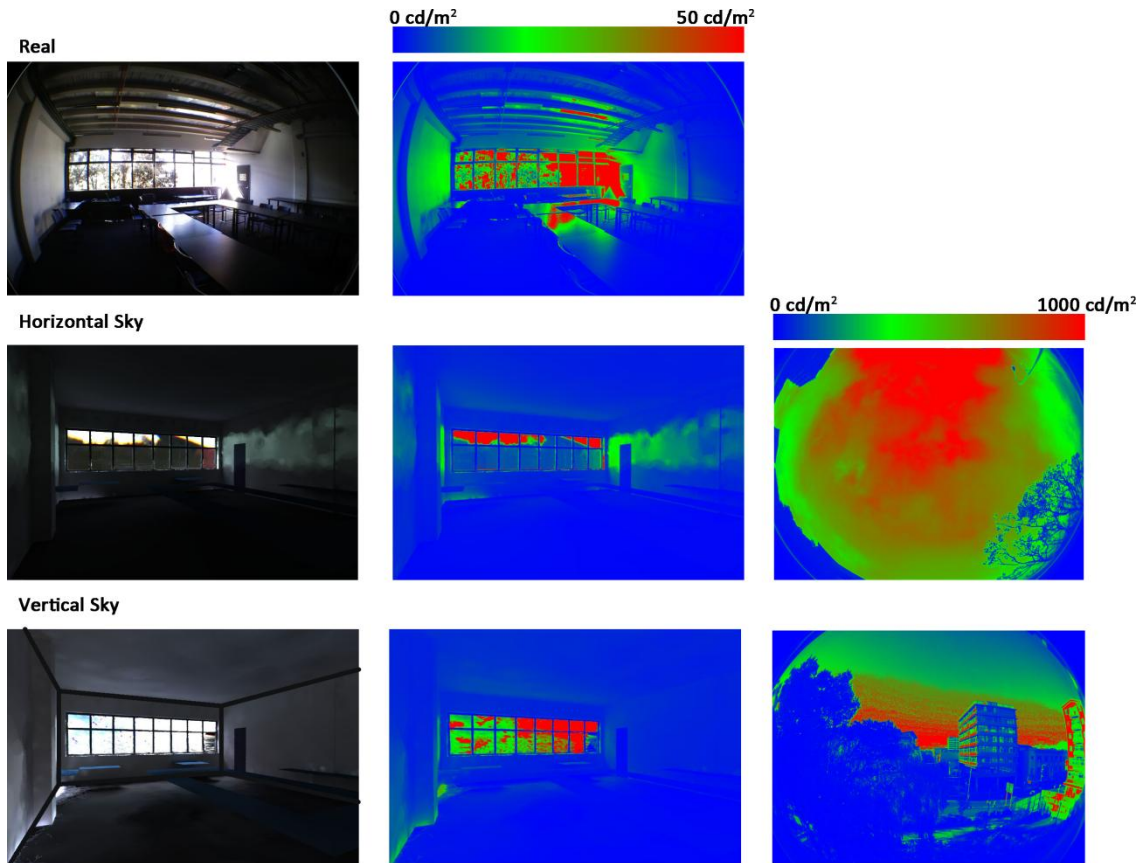


Figure 4.11: Comparison between the HDR image of study room, Radiance simulation with the real horizontal and vertical HDR skies

As illustrated in figure 4.11, the simulated resultant images produced from Radiance were not distorted with the fisheye lens effect. This results in complications when it comes to a pixel to pixel comparison between the real and simulated data as the geometrical forms do not align.

Figure 4.12 illustrates the results of a *pixel to pixel* comparison between the real and simulated measurements using HDRShop and RadDisplay. The blue pixels are where the two images compared contain the same luminance data. The red pixels illustrate where there was more than a 50 cd/m^2 difference. As illustrated in the two images below, the comparison between the two images have about a 50% correlation, however, there was quite a large area that contains more than 50 cd/m^2 difference.

Unfortunately, due to geometrical misalignments, these images may not portray the results clearly. The major issues in these resultant images are around the window areas. The next step was to enlarge the images and focus on the window corners for a closer study.

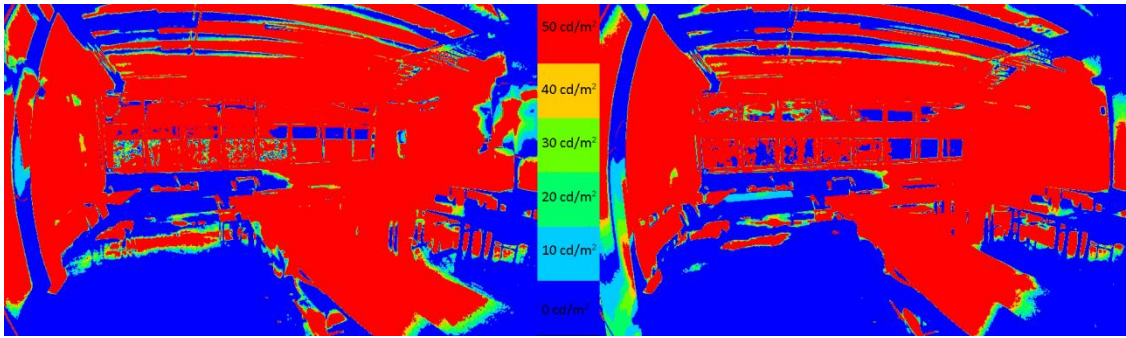


Figure 4.12: Pixel to pixel comparison between real and simulated luminance data using horizontal HDR sky (left) and vertical HDR sky (right) generated in HDRShop and RadDisplay

The next method was a *section to section* comparison. The sections selected for the comparison was the four corners around the window as these produced minimal geometrical distortion and from the resultant images in figure 4.12, this has the most luminance difference between real and simulated data.

Sections from the images produced by the simulated model with the horizontal and vertical sky mapped as the light source were compared to the real HDR image captured from the field. Figure 4.13 illustrates the eight resultant images produced by subtracting the simulated image from the real HDR image of the study room. The scale, on the left hand side of the image, illustrates the range of luminance measurement difference ranging from 0 cd/m^2 to 50 cd/m^2 .

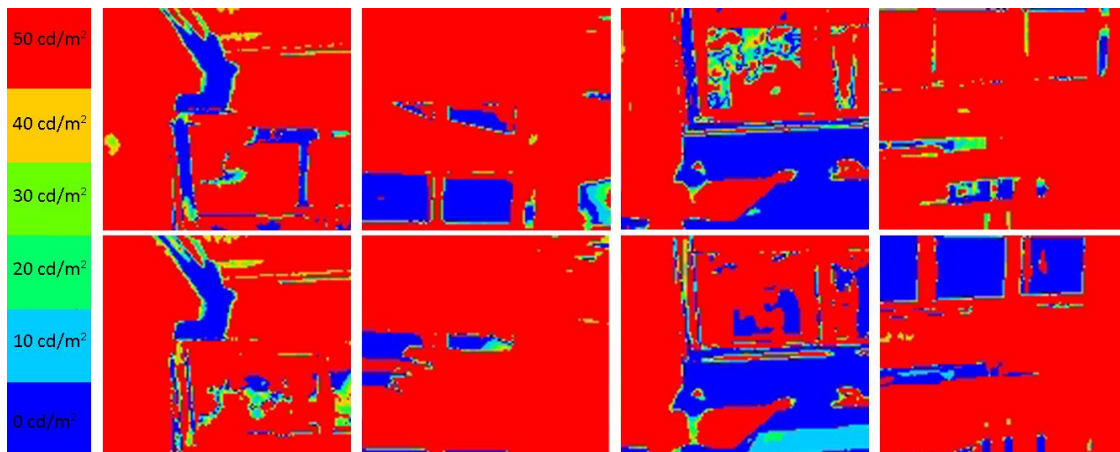


Figure 4.13: Resultant images produced from HDRShop and RadDisplay of the four sections selected in the study room using the horizontal sky (top) and vertical sky (bottom)

The top row of the image illustrated in figure 4.13 above, shows the image produced using the horizontal sky in the daylight simulation. The biggest correlation of the images produced was the third image in from the left as approximately half of the image contained the same luminance data. The section with the lowest correlation was the comparison shown in the last image. It has approximately 10% area with the same luminance data.

The daylight simulation using the vertical sky as a light source is illustrated in the bottom row. This shows similar results compared to the simulated model with the horizontal HDR sky.

There are more areas in the resultant images where the luminance data was 10 cd/m² to 20 cd/m² difference.

The next method used is the *surface to surface* comparison where the surface values were compared between the two images. An eight by four grid was placed over the images containing 28 light measurement points. The relative error percentage between real and simulated data was calculated and was illustrated in table 4.02 for the horizontal HDR sky.

56%	27%	53%	53%	55%	54%	55%
20%	82%	1%	2%	0%	8%	16%
29%	19%	6%	3%	41%	9%	33%
2%	13%	8%	31%	81%	79%	1%

Table 4.02: Relative error percentage between real and simulated data under the horizontal HDR sky

The yellow highlighted measurements were where the window glazing was located in the image. The mean relative error percentage under the horizontal sky simulation was calculated to be 30% with the largest relative error ranging from 0% to 82%. Both of these values were located within the window glazing area. Outside of the glazing area, the largest relative error of 81% was located at the bottom centre of the image, whereas the lowest relative error was at the bottom left and right corners.

In John Mardaljevic's Doctor of Philosophy thesis in 1999, a study was done on validating daylight simulations. If the relative error percentage of a scene is within $\pm 10\%$, the model is deemed to be "highly accurate" (Mardaljevic 2000, 31) and within $\pm 20\%$ the model is deemed to "provide very reasonable accuracy" (Borisuit, Scartezzini and Thanachareonkit 2010, 360). Of the 28 measurement points, 10 points (36%) were within $\pm 10\%$; and 13 points (46%) were within the $\pm 20\%$ margin.

Table 4.03 illustrates the relative error percentage between real and simulated data under the vertical HDR sky.

49%	27%	50%	47%	43%	48%	47%
22%	45%	73%	71%	71%	22%	45%
18%	23%	39%	9%	51%	27%	41%
43%	18%	42%	64%	75%	65%	24%

Table 4.03: Relative error percentage between real and simulated data under the vertical HDR sky

As mentioned above, the yellow highlighted data illustrates where the glazing area was located in the image. The mean relative error percentage between the two HDR images was 43% with the largest relative error of 75%, and 9% as the lowest. Out of the 28 measurement points, only 1 point (4%) was within $\pm 10\%$; and 3 points (11%) were within the $\pm 20\%$ margin.

Daylight simulation with the vertical HDR sky had a higher relative error margin when compared to the horizontal HDR sky for the pilot study.

The last method used was comparing the numerical values in the scene with the simulated data. Using the Minolta light meter, spot measurements were recorded in the study room. The average relative error percentage for the 5 illuminance points measured under the horizontal HDR sky was 11%. Whereas, the average relative error percentage for the 5 illuminance points under the vertical HDR sky was 9%.

4.5. Conclusion

The objective of this chapter was to outline the process taken for the pilot study for this research conducted in the lighting laboratory and the study room conducted at Victoria University of Wellington. This pilot study was used to help develop the methodology for this research so that errors can be minimised on site and ensure accuracy of this research study.

The study room was simulated in Radiance using IBL techniques to map an artificial sky, a horizontal sky and a vertical sky and to use these HDR skies as a light source (Debevec 2002). The resultant false colour images produced from Radiance were compared using HDRShop against the real HDR image of the study room. Four different comparison methods were used to determine how accurate a simulated model with HDR sky light source can be. The first two comparison methods were visually based whereas the final two methods depend on numerical factors.

The pixel by pixel comparison illustrated that the areas where the two images contain the same luminance data was mainly around the ground and worst around the walls and window areas. Whereas, when comparing window sections of the real and simulated images, the bottom left corner of the window had the highest correlation whereas the right hand side of the window had more than 50 cd/m² difference. The biggest issue in this comparison method was due to the geometrical misalignments of the two images.

When comparing the real and simulated images using the surface to surface method, on an eight by four grid, the relative error percentage was higher than the spot measurements comparison method. This was because it contained more measurement points in the image and some points had a higher relative error margin. Whereas when comparing only the spot measurements captured in the study room, with the simulated images, the relative error percentage was a lot lower. This was because it only focuses on a smaller aspect of the image itself, and does not represent the whole image.

Chapter 5: Methodology

The objective of this chapter was to develop a methodology that would be used in the three randomly selected buildings for this study. The methodology was developed in the pilot study outlined in *Chapter 4: Pilot Study*, and was further refined in this chapter. It begins with the process to capture the daylit scene in section 5.1 and continues on with the process of fusing the photographs to create the HDR image in section 5.2. Section 5.3 explored the simulation process that was followed for simulating the three buildings and continued on to the process for creating the HDR skies as the light source for the scene. Lastly, section 5.5 discusses the process used to compare the HDR image captured on site and the simulated image.

5.1. Measurement Process

Three buildings were randomly selected from the BEES strata five database. In each building, three to four photographs were captured using the HDR camera application on the Android Smartphone or Tablet and the built-in camera application, in at least three different rooms facing different orientations. However, this was not always possible as some of the spaces selected were empty in order to ensure privacy of the tenant companies. All internal HDR photography was captured facing towards the window to capture the daylight penetration in the room.

This study explores the daylight potential in commercial buildings using HDR photography as a daylight measurement tool, using both vertical and horizontal HDR skies. The horizontal HDR sky was captured on the ground level, as roof access was not available. The vertical HDR sky was captured from the room being tested by pressing the fisheye lens hard-up against the window glass. The Smartphone camera was placed on a stable surface with the lens facing towards the sky at approximately 1500 mm above ground level. Four different HDR skies were captured outside, from ground level, one from each orientation of the building as roof access was not available. The vertical skies were captured at eye level from each analysed room.

Since the monitoring processes in the commercial buildings were conducted during a typical workday, artificial lighting was used in most of the test areas. To subtract the artificial lighting information, lighting measurements were recorded at night using the HOBO data loggers from BRANZ. Through a simple subtraction method, the artificial lighting data was extracted from the HDR image, and the lighting measurements were compared with the HDR image and the data from the HOBO data logger to ensure that the measurements in the photograph and the light measurement equipment corresponds with each other and can be compared.

A hand-held light meter was also placed on desktops within the scene captured and a Macbeth ColorChart was also inserted into the scene. Five measurements were recorded off the light meters and the average was used. This will help calibrate the HDR images after fusing them in Photosphere.

Floor plans of each premise were collected from the company managers and three dimensions of the rooms were recorded using a laser distance meter and was later used scale the floor plans to the correct size for simulation. The ceiling height and window sizes were also measured on site. The surface RGB values were captured using the X-Rite ColorMunki device five times and the average were used as base models for this research. The reflectance was calculated using the *Colour Picker for Radiance Online Tool* (JALOX 2012).

5.2. Creating HDR image

To create a camera response curve and to fuse the photographs together to create an HDR image in Photosphere, an EXIF file was required for each photograph. At minimum, the data required is the exposure value. Unfortunately at this stage, an EXIF file could not be automatically created using the HDR Camera application used on the Android device. Therefore, an EXIF file was created by using a software called “ExifTool”. This is a “command-line” software where “all work must be completed by typing commands inside the “command prompt” window” (Hrastnik 2012). The software can be installed and used in two different methods:

1. Keeping the original downloaded file name `exiftool(-k).exe` and use the program through your desktop by dragging the image you want onto the Exiftool icon to view the EXIF file; or
2. Saving `exiftool(-k).exe` in `C:\Windows` and renaming the file to `exiftool.exe`. This will allow the user to use the command prompt window to view, edit or write EXIF files.

This study uses the command prompt option as there was more information on how to write the EXIF information than the other method. To create the EXIF file for an HDR photograph, the existing EXIF information was deleted and a new EXIF file was created by copying the EXIF file from another image captured using the built-in camera application on the same Android Smartphone. After that the “exposure compensation value” will also be added through ExifTool.

It was unknown what type of metadata information is required in order to create an accurate EXIF file and by looking through the EXIF file of an image taken by the built-in camera application, and the DSLR camera, the minimum metadata required could be determined.

It was later determined that the EXIF data required to create the camera response curve was available in the photographs captured using the built-in camera application in the Android device. Therefore, the EXIF data from these photographs will act as a basis for the new EXIF data required to be created for the photographs using the HDR Camera application. Firstly, the metadata in the EXIF file needs to be deleted in image “a” and copied from image “b”:

```
exiftool -all= -tagsfromfile b.jpg -exif:all a.jpg
```

Next, the correct exposure compensation values will need to be added. To decrease the exposure compensation value by 0.5:

```
exiftool -exposurecompensation+/-0.5 a.jpg
```

And to increase the exposure compensation value by 0.5:

```
exiftool -exposurecompensation+=0.5 a.jpg
```

After the EXIF file was created and the exposure compensation values are added, the image can then be fused in an HDR program. The software used for this research was Photosphere as it has previously been validated as one of the most accurate HDR programs available and it was one of the most commonly used HDR software (Bloch 2007) (Inanici 2010). Photosphere is a free software that is only available for use on the Apple operated system. It was developed by Greg Ward and it supports all HDRI formats, automatically calculates the camera response curve while fusing the photographs. The most prominent feature of Photosphere is that accurate luminance values can be obtained by just “picking the pixel value” where currently no other HDR software is available to do so (Bloch 2007).

“So for lighting designers and applications in the architectural field, Photosphere is the only option. It can also generate false coloured luminance maps, which is very useful for all you professional lighting analysts.”

(Bloch 2007)

As mentioned previously in *Chapter 4.1.1 Camera Response Curve*, a camera response curve could not be generated for the Motorola Defy Smartphone. Numerous experiments and tests were conducted using the Smartphone to try and determine why a camera response curve could not be generated. Through numerous tests and experimentations documented in *Appendix G: Generating a Camera Response Curve*, it was determined that the Motorola Defy

Smartphone provided an insufficient level of data within the JPEG image format required to generate this curve.

Therefore the HDR images were created using the generic camera response curve in Photosphere. The photographs may not be as accurate as using the specific camera response curve for a Smartphone, but the images were later calibrated using the luminance and illuminance measurements recorded during the image capturing process.

Another image capturing tool was introduced after the second building was monitored to determine whether it was possible to create a camera response curve for an inexpensive Android device. The device used was the Samsung Galaxy Note Tablet. A camera response curve could be created from Photosphere. This curve is illustrated in figure 5.01. After the photographs were fused, the resultant HDR image can be saved as a “Radiance RGBE” format with an `.hdr` file extension. When saving the file, it was important to ensure that there are no spaces in the file name.

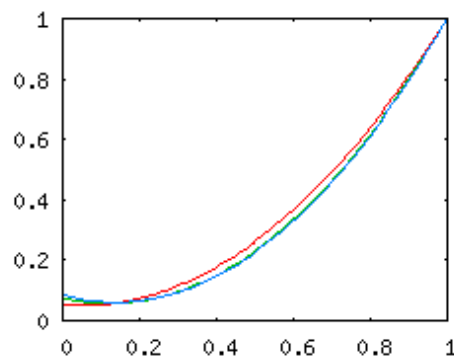


Figure 5.01: Camera response curve for the Samsung Galaxy tablet

5.3. Simulation

The simulation process was outlined in *Chapter 4.4 Simulation of Pilot Study*. The geometric form of the building was simulated in Google SketchUp 8 (Google SketchUp) and exported to Radiance via the `su2rad` plug-in (`su2rad`). The files were edited and rendered using the Ecotect™ Radiance Control Panel (U.S Department of Energy 2011).

Each component containing a different surface material colour was created on a new layer so that the materials could easily be assigned in Radiance. The buildings were orientated based on the site plans drawn in *Chapter 6: The Buildings* and the surrounding environment i.e. buildings were not modelled as this information should be provided by the HDR sky images. The floors were raised to the approximate height above ground level.

A circular ground plane was simulated with a reflectance value of 0.2 and cameras were placed at approximately the same location in the monitored room as the photographs captured (Mardaljevic 2000, 37). The simulated model was exported, via layers, to Radiance using the “su2rad” plug-in.

The average material properties of each surface was used in the base model simulations with the RGB values to be entered into the .mat file and the reflectance of each surface determined by using the *Colour Picker for Radiance Online Tool* (JALOX 2012).

5.3.1. Potential Simulation Errors and Variations in Simulation

No matter how precise the modelling process is, there will always be possible errors and variation in the results (Post and Koutamanis 2005). The question is how accurate and reliable can a daylight simulation be? There can be minor mistakes that affect the results or there may be assumptions made where the data for that aspect of simulation was unavailable. Mistakes conducted during the measurement processes can lead onto simulation errors. Therefore it was important to explore the possible variations in a daylight simulation especially in materiality.

The first variations that were explored are window sizes as this will affect the amount of daylight penetration into the monitored rooms. Even though the window dimensions were measured on site, there may still be a slight variation due to accuracy. Therefore the window sizes were changed by $\pm 10\%$ to determine how this will affect the daylight conditions of that room.

The next variations that were explored are the window transmissivity value of the glazing materials. Manufacturers’ information regarding window glazing was unavailable as it was not noted down in the floor plans provided; therefore the window transmissivity was measured on site using the Minolta light meter. However, all the buildings monitored were multi-storey, with no openable windows. This meant that a time delay may occur when measuring the outside illuminance to determine the transmissivity of the glazing. During this period, the climatic conditions may change. Since each building has at least five transmissivity values calculated the first base model used the average of the five values recorded. Later a variation was simulated using the highest and the lowest transmissivity values and when required the tint of the glazing will also be varied.

The last variation that was explored was the surface RGB values. This was an important aspect to explore as the surfaces reflectivity will affect the amount of light reflecting off of the surfaces in the room. The X-Rite ColorMunki recorded five surface RGB values of each material

in a scene where the average value was used in the base model and the variation consisted of using the highest and lowest RGB values measured.

5.4. Creating HDR Skies

The HDR skies captured on site were used as an environment map as a light source for the simulated model instead of using a CIE sky (Cheney 2008). Two models were simulated at this stage; one for a vertical sky and the other for the horizontal sky. A vertical image capturing the external environment through the window provides the simulation with light sources that capture any trees and buildings that can obstruct daylight penetration into the room, plus the ground reflections affecting that façade; however, a horizontal sky view captured from the ground or roof can provide information of the surrounding environment above the level that it was captured from. Both methods are used in this research for the HDR sky simulation and comparisons were made. Unfortunately, roof access was not available in the buildings selected, therefore only the ground level horizontal sky was captured.

After the geometric model was simulated in Google SketchUp 8 and exported into Radiance, the material properties were altered in the `material.rad` file. The next step was to map the horizontal and vertical HDR sky into the simulated model. This is done by altering the Radiance files created through the exportation process and adding a script specific to the type of sky used so that Radiance will know how to map the environment map into the scene. Both scripts can be found in *Appendix I: Radiance Sky Mapping Scripts*. The steps for this process can be found in *Chapter 4.3.1: Simulating an HDR Sky*

5.5. Comparison of Real and Simulated Measurements

Before the comparisons between real and simulated data can be completed, it was important to subtract any artificial lighting in the room from the HDR image created. The artificial lighting information was gathered from the HOBO data loggers during night time. The four methods used for comparing the luminance values in *Chapter 4.4: Comparison Between Real and Simulated Data* was used for comparison between HDR images of the three buildings. These were a pixel to pixel comparison; section to section pixel comparison; surface to surface comparison; and comparison in the visual field (Cauwerts 2012, 14).

The software used to compare the real and simulated data was HDRShop. It was important to ensure that the two images compared have the same picture resolution and have the same image size.

For HDRShop, two images were loaded using the “Calculate tool”. Each image was selected under either “Image A” or “Image B” and the “Operation” used for this process were “Image A – Image B”. “New Image” was then selected under “Destination Image” so that the image can be saved and the results could be analysed.

It does not matter which image was “A” or “B” as it provides a resultant image where both images have the same pixel value at the same spot, that section was replaced with black pixels. The image was later opened in RadDisplay to provide a false colour rendering of the resultant image on a 0 cd/m² to 50 cd/m² scale. For this research, the simulated image was subtracted from the real HDR image. An example from the pilot study of this process is illustrated in figure 5.02.

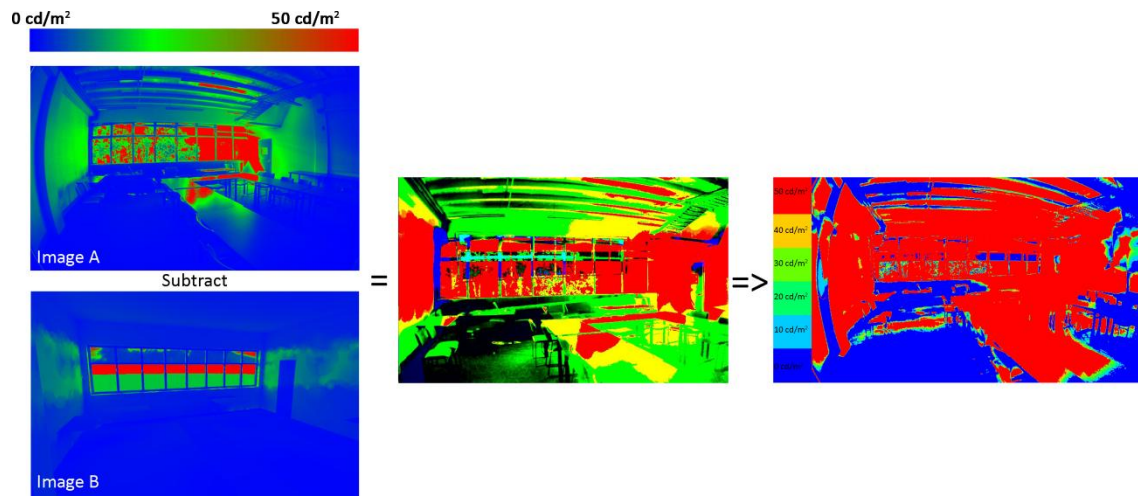


Figure 5.02: An example from the pilot study illustrating the pixel to pixel comparison study process.

The other two comparison methods: surface to surface comparison and visual based comparison used the actual illuminance and luminance data to calculate the relative error percentages of each real and simulated comparison.

5.6. Conclusion

The objective of this chapter was to develop a methodology for this study following the pilot study outlined in *Chapter 4: Pilot Study*. This chapter further developed this method and took into account the possible errors in both measurement and simulation processes in order to minimise this. The next step was to take this methodology and testing it out in the first two buildings. The methodology may then be developed further in the final building if required. This will ensure that the accuracy of the measurement process was at its maximum.

Following the methodology developed, the three randomly selected buildings will determine whether the overall aim of this research can be achieved.

Chapter 6: The Buildings

The objective of this chapter was to discuss the three randomly selected strata five buildings from the BEES study. All three buildings were located in the Auckland region and were monitored for a period of one day for this research in addition to the BEES study. The first two buildings monitored were done on the first day of the BEES monitoring period, whereas the last building was revisited almost a year later.

Each room was captured using a Smartphone camera, for the first two monitored buildings and a Tablet for the last, every 30 minutes to capture any changes in the interior scene and the sky. HDR photographs of at least three orientations of the premises were captured and empty office areas or empty desks areas in open plan offices were selected due to confidentiality and privacy reasons. Otherwise meeting rooms and lunchrooms were selected as these are the two other spaces that were commonly used.

6.1. Building 1

The first building was a four storied building, with two basement levels underneath. Construction for this building began in 2000, while a refurbishment was undertaken in 2010 due to windows leaking water. The building was orientated north-west and was set back from the main street with two almost identical buildings on the north-west and south-west elevation. The site plan for this building is illustrated in figure 6.01.

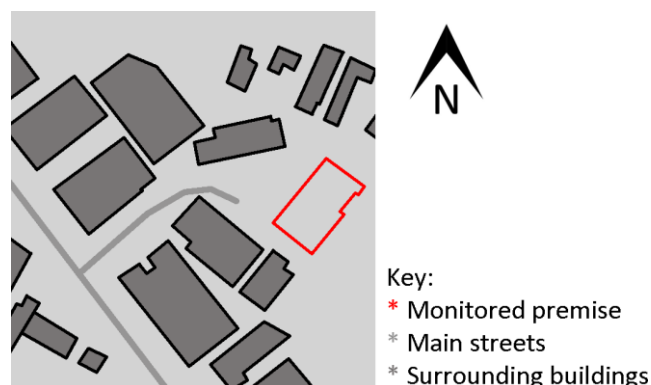


Figure 6.01: Site plan of Building 1 (Not to scale) (image adapted from (Google 2012))

The premise monitored for the purposes of this study was located on the second floor and occupies the whole floor. The floor comprises of open plan offices mainly in the centre of the building with individual offices on the perimeter of the floor, illustrated in figure 6.02.

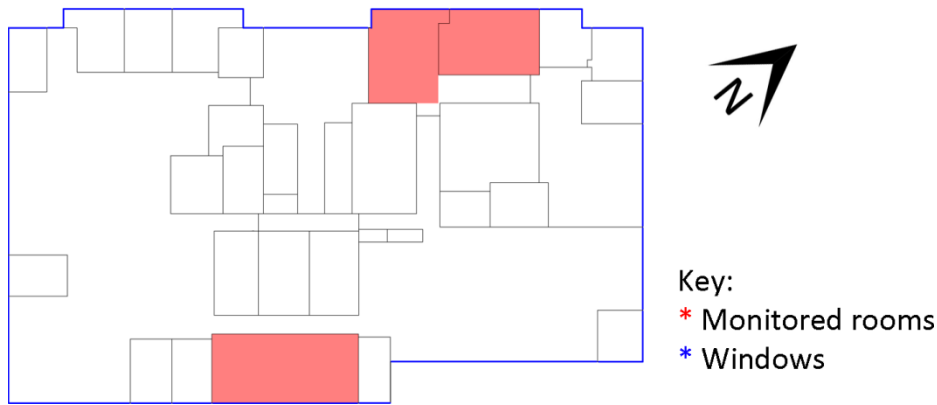


Figure 6.02: Floor plan illustrating level 2 in Building 1 (Not to scale)

The rooms selected to be monitored included the lunchroom computer area – facing south-east; the waiting room – facing north-west; and the large meeting room – facing north-west as well. These areas are highlighted in red on the floor plan illustrated in figure 6.02. The average surface RGB values and reflectance values in all three rooms are shown in table 6.01.

Surface	R	G	B	RGB value for Radiance	Reflectance
Wall/ceiling	237	231	221	0.929, 0.906, 0.867	0.910
Carpet	56	51	49	0.220, 0.200, 0.192	0.205
Window frame	158	159	157	0.620, 0.624, 0.616	0.622
Lunchroom table	151	153	150	0.592, 0.600, 0.588	0.596
Lunchroom bench	179	180	177	0.702, 0.706, 0.694	0.704
Lunchroom coffee table	45	29	23	0.177, 0.114, 0.090	0.128
Sofa	130	46	53	0.510, 0.180, 0.208	0.266
Waiting room table	138	102	67	0.541, 0.400, 0.263	0.430
Meeting room table	101	63	33	0.396, 0.217, 0.129	0.262
Meeting room chair	83	75	69	0.325, 0.294, 0.271	0.301

Table 6.01: The average surface RGB and reflectance values for Building 1

6.2. Building 2

The second building monitored was a four storied building constructed in 2001. The premise monitored was located on the third floor and occupies the whole floor. The building was orientated north-east with multi-level buildings surrounding all elevations. The site plan for Building 2 is illustrated in figure 6.03.

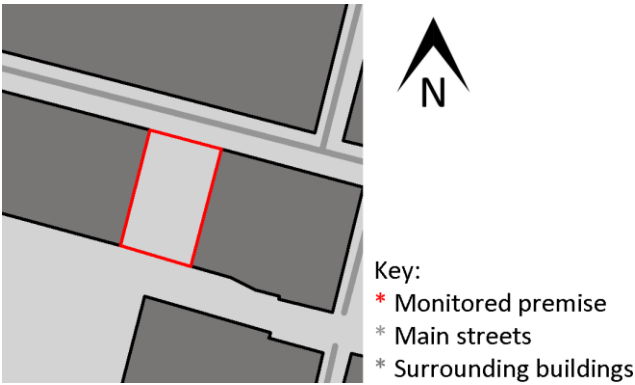


Figure 6.03: Site plan of Building 2 (Not to scale) (image adapted from (Google 2012))

The premise monitored occupies the whole of level three. It comprises of open plan offices surrounding the perimeter of the building, with meeting rooms positioned around the core of the building. Figure 6.04 illustrates the layout of the floor.

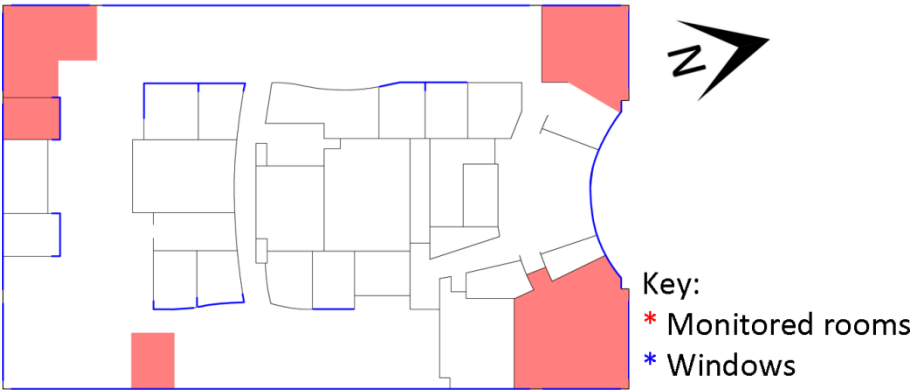


Figure 6.04: Floor plan illustrating level 3 in Building 2 (Not to scale)

The monitored rooms that were selected, in red above, include a meeting room – facing south; an empty open plan office corner with windows both on the west and south elevations; a desk space in an open plan office area – facing east; the lunchroom with windows on both the north and west elevations; and a large meeting room with windows on both the north and east elevations. The average surface RGB values and reflectance values in all five rooms are shown in table 6.02.

Surface	R	G	B	RGB value for Radiance	Reflectance
Carpet	69	68	66	0.271, 0.267, 0.259	0.270
Wall/ceiling	226	218	208	0.886, 0.855, 0.816	0.860
Window frame	169	171	169	0.663, 0.671, 0.663	0.668
Chair	54	54	55	0.212, 0.212, 0.216	0.212
Lunchroom - sofa	132	57	69	0.518, 0.224, 0.271	0.301
Lunchroom – table	233	235	230	0.914, 0.922, 0.902	0.919
Lunchroom -bench	235	236	231	0.922, 0.925, 0.906	0.923
Meeting room – table	211	171	128	0.827, 0.671, 0.502	0.701
Open plan office – table	208	173	134	0.816, 0.678, 0.525	0.706
Open plan office – dividers	156	155	148	0.612, 0.608, 0.580	0.607
Open plan office – cabinet	90	94	97	0.353, 0.369, 0.380	0.365
Meeting room (small) – table	214	175	132	0.839, 0.686, 0.518	0.714
Meeting room (small) – wall	71	71	100	0.278, 0.278, 0.392	0.286

Table 6.02: The average surface RGB and reflectance values for Building 2

6.3. Building 3

The final premise monitored for the purpose of this research was located in a seventeen floor commercial office building. The building was orientated north-east with multi-storey buildings surrounding the monitored building. The site plan for this building is illustrated in figure 6.05.

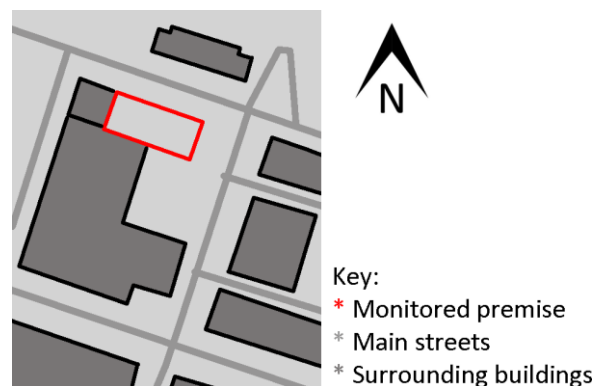


Figure 6.05: Site plan of building 3 (Not to scale) (image adapted from (Google 2012))

The premises monitored for this study are located on the eleventh floor of this building and occupy the whole floor. The floor comprises of open plan offices mainly on the north-west elevation with meeting rooms on the north-east elevation, illustrated in figure 6.06.

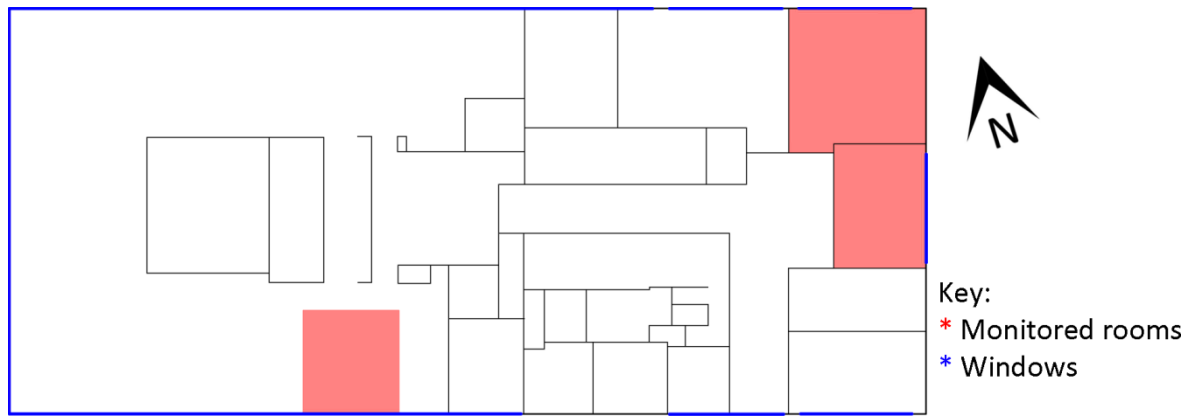


Figure 6.06: Floor plan illustrating level 11 in building 3 (Not to scale)

The monitored rooms, in red above, include two meeting rooms – one facing north-west, and the other facing north-east; and an empty section in the open plan office facing south-west. The average surface RGB values and reflectance values in all three rooms are shown in table 6.03.

Surface	R	G	B	RGB value for Radiance	Reflectance
Table	194	154	108	0.761, 0.604, 0.424	0.634
Cabinet	210	187	149	0.824, 0.733, 0.584	0.747
Chair	27	61	96	0.106, 0.239, 0.376	0.214
Carpet	80	80	81	0.314, 0.314, 0.318	0.314
Dividers	167	173	174	0.655, 0.678, 0.682	0.672
Window ledge	196	171	121	0.769, 0.671, 0.475	0.684
Window frame	160	164	166	0.627, 0.643, 0.651	0.639
Column/ wall/ceiling	227	223	218	0.890, 0.875, 0.855	0.878
Meeting room table	234	237	238	0.918, 0.929, 0.933	0.926
Meeting room chair	48	50	52	0.188, 0.196, 0.204	0.194
Meeting room wall	102	145	156	0.400, 0.569, 0.612	0.527

Table 6.03: The average surface RGB and reflectance values for Building 3

6.4. Conclusion

The objective of this chapter was to outline the three buildings selected from the BEES strata five database, for this research and to describe the monitored rooms. All three buildings were located in the Auckland region, all of which are multi-levelled commercial office buildings. All buildings were monitored using the measurement processes outlined in *Chapter 5: Methodology*. All of the equipment used was the same as described in *Chapter 3: Equipment*,

building 3 being the exception where an Android Tablet was used instead of the Smartphone due to problems involving the camera response curve.

In *Chapter 7: Results* the daylight simulation results using both horizontal and vertical HDR skies as a light source for each of the three buildings was documented.

Chapter 7: Results

The objective of this chapter is to report the results and the comparison between real and simulated data for the three buildings monitored. HDRShop and RadDisplay were used for this comparison study, using four different comparison methods mentioned in *Chapter 4.4: Comparison Between Real and Simulated Data*. They were; pixel to pixel comparison; section to section pixel comparison; surface to surface comparison; and visual field comparison. The outcome from this comparison study, determined the adequacy of Smartphone based High Dynamic Range (HDR) photography as a tool for daylight analysis.

At least three rooms were monitored in each building each facing a different orientation. *Appendix K: Results* contains the images illustrating the HDR image of the scene, the simulated scene under both horizontal and vertical skies as well as the false colour renderings of the scene with false colour rendering of the sky used.

The variation tests outlined in *Chapter 5.3.1: Potential Simulation Errors and Variations* provided the simulated model with a 5% to 10% variation in luminance data. When the images with variations were compared to the real HDR image, they provided similar results with $\pm 5\%$ difference.

7.1. Pixel to Pixel Comparison

Due to the geometric misalignment between the real and simulated image, pixel to pixel comparison was the most inaccurate method out of the four comparison methods. The misalignment of the geometric forms makes the comparison between two images almost impossible and inaccurate.

The images were converted to false colour renderings in Radiance using the same luminance scale. The images were opened in HDRShop and using the “calculate” function, the real HDR images were selected under “Image A”, where the simulated image was selected under “Image B”. The operation used was “Image A – Image B” and a new image was produced. The image was saved as a Radiance image and was opened in RadDisplay.

In RadDisplay, a luminance scale ranging from 0 cd/m^2 (blue pixels) to 50 cd/m^2 (red pixels) was created and an additional false colour rendering image was generated. The blue pixels in these images show where the two images compared contain the same luminance data, whereas the red pixels illustrate where the luminance data difference between the two images was greater than 50 cd/m^2 .

7.1.1. Building 1

The rooms monitored in Building 1 were the waiting area – facing north-west; the lunchroom computer area – facing south-east; and the large meeting room – facing north-west as well. Figures 7.01, 7.02 and 7.03 illustrates the comparison between the real and simulated HDR images under both the horizontal and vertical skies for Building 1. The resultant images were generated using HDRShop and RadDisplay.

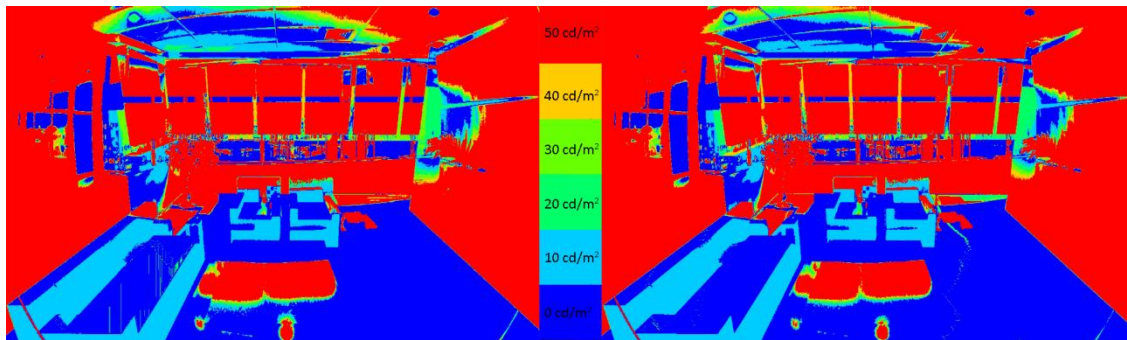


Figure 7.01: Pixel to pixel comparison between real and simulated luminance data of the waiting area using horizontal (left) and vertical (right) HDR sky generated in HDRShop and RadDisplay

Figure 7.01 illustrates the pixel by pixel comparison for the waiting area. The walls and window areas have the largest luminance difference whereas the floor area had the highest correlation values under both skies.

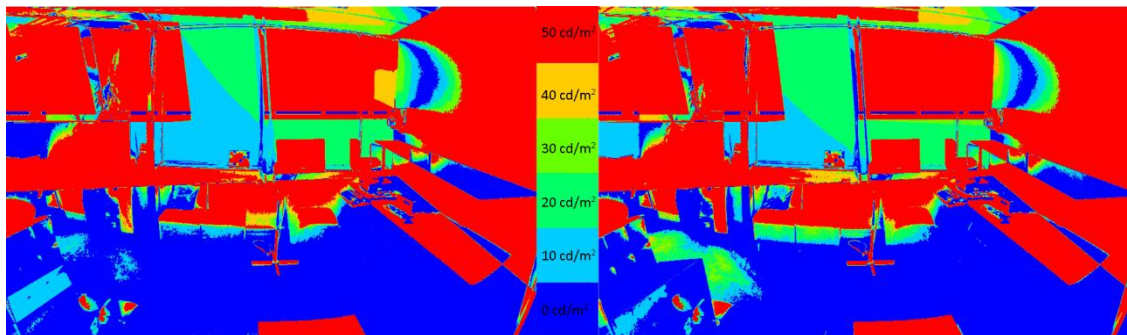


Figure 7.02: Pixel to pixel comparison between real and simulated luminance data of the lunchroom using horizontal (left) and vertical (right) HDR sky generated in HDRShop and RadDisplay

Figure 7.02 illustrates the pixel by pixel comparison for the lunchroom. The walls and window areas have the largest luminance difference except for the wall of which the window was located. It only had a 10-20 cd/m^2 difference. The floor area had the highest correlation, illustrated by the blue pixels, under both skies.

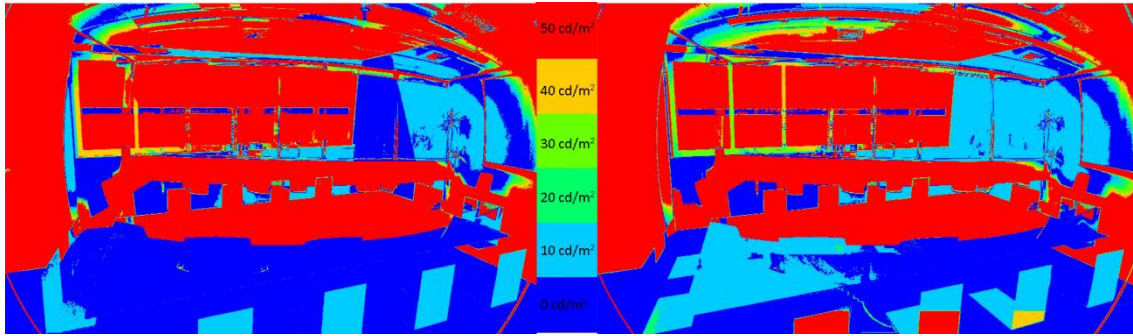


Figure 7.03: Pixel to pixel comparison between real and simulated luminance data of the meeting room using horizontal (left) and vertical (right) HDR sky generated in HDRShop and RadDisplay

Figure 7.03 illustrates the pixel by pixel comparison for the meeting room. The window areas had the largest luminance difference whereas the floor area and the right-hand side wall had the highest correlation values under both skies.

7.1.2. Building 2

Five rooms were monitored in Building 2. These included a lunchroom with windows on both the north and west elevations; a large meeting room with windows on both the north and east elevations; a small meeting room – facing south; a corner open plan office with windows both on the west and south elevations; and a desk area in an open plan office – facing east, illustrated in figures 7.04 to 7.08 respectively.

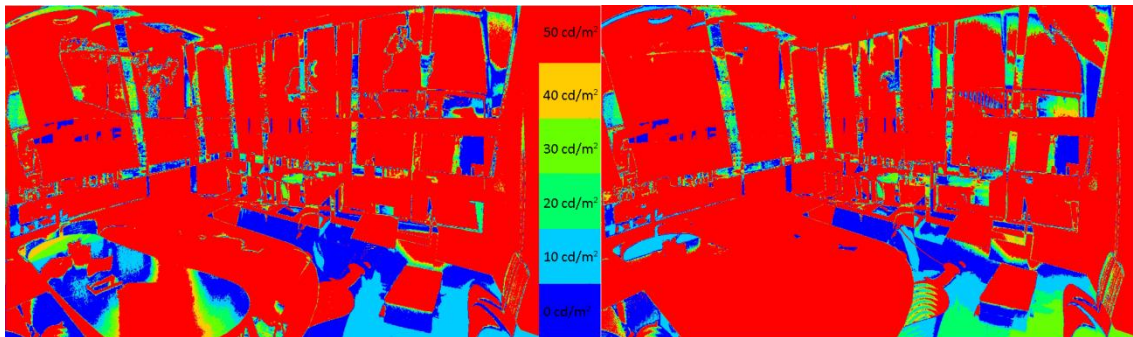


Figure 7.04: Pixel to pixel comparison between real and simulated luminance data of the lunchroom using horizontal (left) and vertical (right) HDR sky generated in HDRShop and RadDisplay

Figure 7.04 illustrates the pixel by pixel comparison for the lunchroom. There were very limited correlations between the two images. This could be because the day the building was monitored was a sunny day. The walls and window areas have the largest luminance difference whereas the floor area had the highest correlation values under both skies.

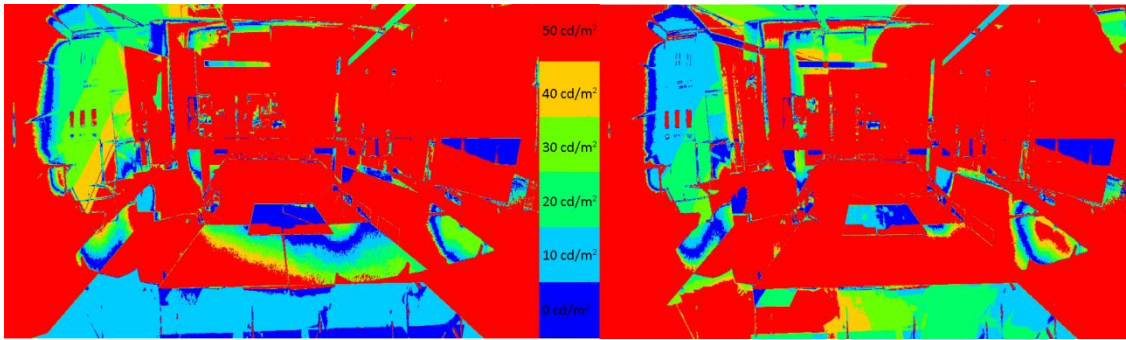


Figure 7.05: Pixel to pixel comparison between real and simulated luminance data of the large meeting room using horizontal (left) and vertical (right) HDR sky generated in HDRShop and RadDisplay

Figure 7.05 illustrates the pixel by pixel comparison for the large meeting room. The walls and window areas have the largest luminance difference whereas the floor area had the highest correlation values under both skies.

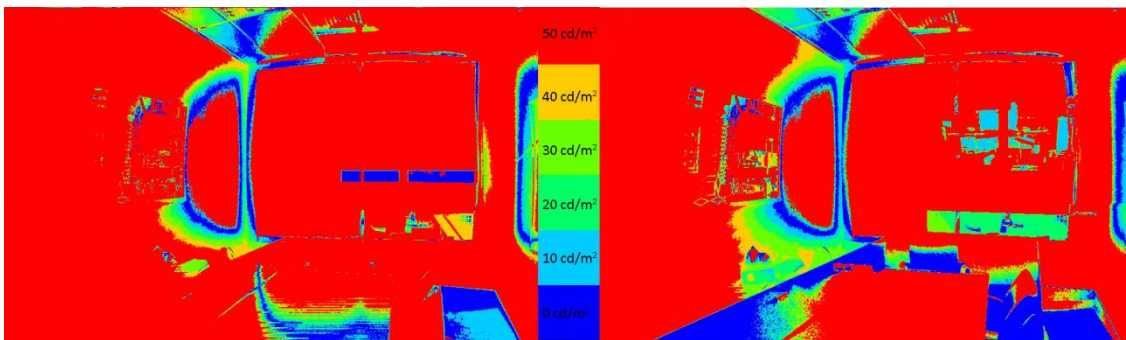


Figure 7.06: Pixel to pixel comparison between real and simulated luminance data of the small meeting room using horizontal (left) and vertical (right) HDR sky generated in HDRShop and RadDisplay

Figure 7.06 illustrates the pixel by pixel comparison for the small meeting room. The floor area has the highest correlation between the real and simulated images for both the horizontal and vertical skies. The image simulated with the vertical sky, on the right, as the light source provided a higher correlation when compared to the image simulated by the horizontal sky, on the left.

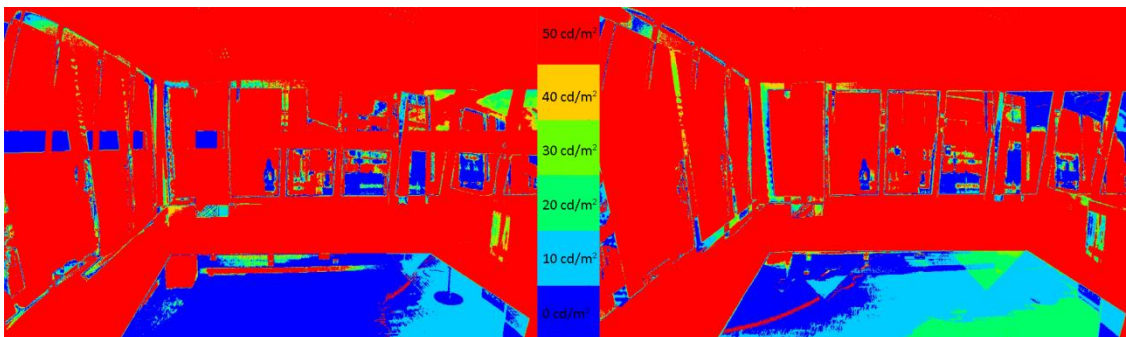


Figure 7.07: Pixel to pixel comparison between real and simulated luminance data of the corner open plan office using horizontal (left) and vertical (right) HDR sky generated in HDRShop and RadDisplay

Figure 7.07 illustrates the pixel by pixel comparison for the corner open plan office. The floor area had the highest correlation in the images simulated under the horizontal and vertical

skies. The image produced using the horizontal sky, on the left, provided a higher correlation when compared to the vertical sky, on the right.

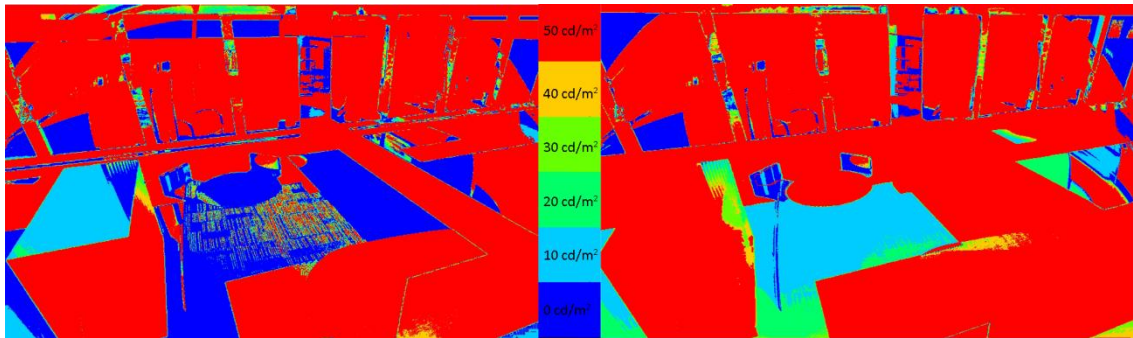


Figure 7.08: Pixel to pixel comparison between real and simulated luminance data of the open plan office using horizontal (left) and vertical (right) HDR sky generated in HDRShop and RadDisplay

Figure 7.08 illustrates the pixel by pixel comparison for the open plan office. The window areas had the largest luminance difference whereas the floor area had the highest correlation values under both skies. This scene had the highest correlation value compared to all of the rooms that were monitored.

7.1.3. Building 3

Three rooms were monitored for the final building. There were two meeting rooms – one large and one small – one facing north-west, and the other facing north-east; and a desk area in an open plan office facing south-west.

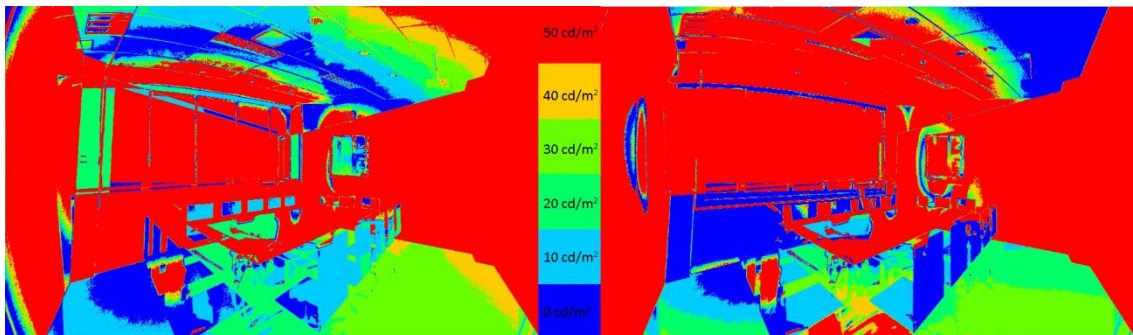


Figure 7.09: Pixel to pixel comparison between real and simulated luminance data of the large meeting room using horizontal (left) and vertical (right) HDR sky generated in HDRShop and RadDisplay

Figure 7.09 illustrates the pixel by pixel comparison for the large meeting room. The walls and window areas have the highest luminance difference whereas the floor area had the highest correlation values under both skies. Under the vertical sky the wall in which the window was located had a higher correlation value as well as the ceiling area when it was further away from the windows.

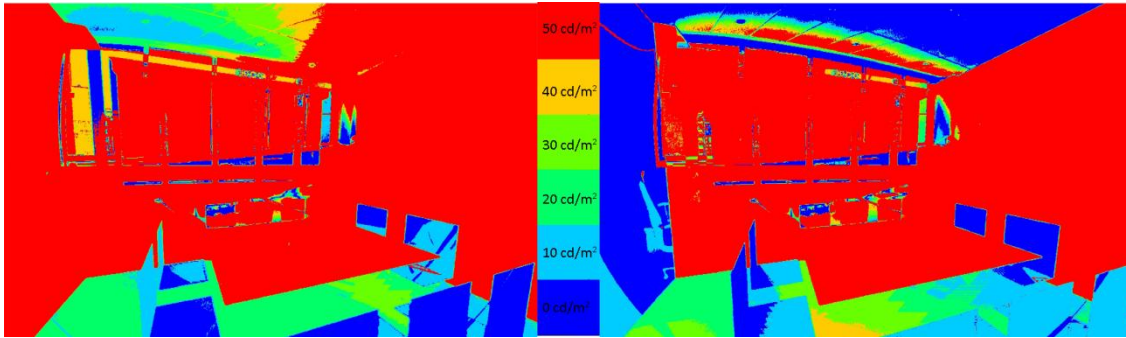


Figure 7.10: Pixel to pixel comparison between real and simulated luminance data of the small meeting room using horizontal (left) and vertical (right) HDR sky generated in HDRShop and RadDisplay

Figure 7.10 illustrates the pixel by pixel comparison for the smaller meeting room. The walls and window areas had the largest luminance difference under the horizontal sky and had a very low correlation area. Under the vertical sky, the ceiling and the left-hand side wall had a high correlation area whereas the window and the right-hand side wall had the largest difference.

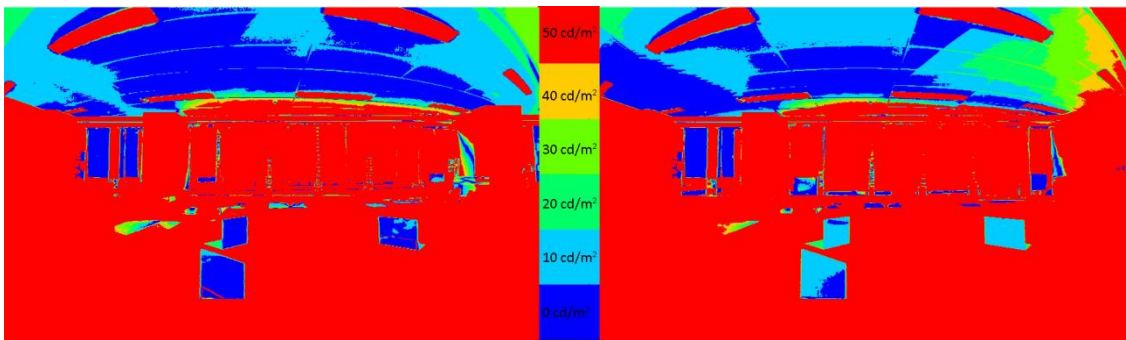


Figure 7.11: Pixel to pixel comparison between real and simulated luminance data of the open plan office using horizontal (left) and vertical (right) HDR sky generated in HDRShop and RadDisplay

Figure 7.11 illustrates the pixel by pixel comparison for the open plan office area. Majority of the scene had a high luminance difference whereas the ceiling area had the highest correlation values under both skies. The large area of difference could be due to the fact that artificial lighting was turned on and this was the only room in the whole research that included artificial light in the comparison.

7.2. Section to Section Pixel Comparison

This comparison method focuses on specific sections within an image where the geometric forms within the two images align. This allows a closer inspection of the comparison and provides a more focused analysis. The sections for this comparison method chosen were the desk corners and window areas as this had the least deformation due to the fisheye lens used in field. This section illustrates a section comparison from each scene from the three monitored buildings.

7.2.1. Building 1

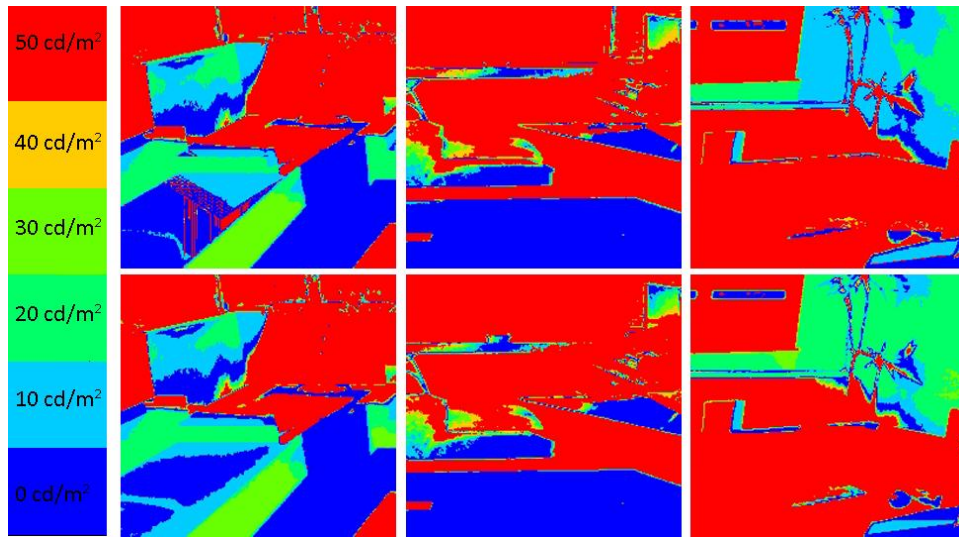


Figure 7.12: Comparison between sections of real and simulated images using horizontal (top) and vertical (bottom) HDR sky. From left to right; waiting room, lunchroom and meeting room.

For Building 1, a section from the waiting area, lunchroom and meeting room were selected, illustrated in figure 7.12. Both the horizontal and vertical skies provided similar results, with the meeting room the exception as illustrated in the image on the right, where the horizontal sky simulation had a larger area where the difference between the real and simulated luminance data was between 10 cd/m^2 to 20 cd/m^2 . The area selected for the waiting area and the lunchroom contained approximately 50% correlation, where the difference in luminance data is 0 cd/m^2 .

7.2.2. Building 2

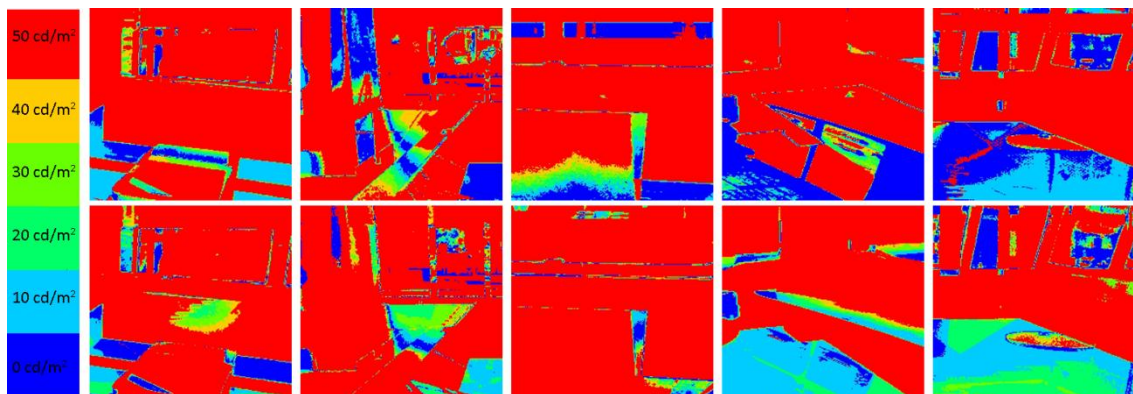


Figure 7.13: Comparison between sections of real and simulated images using horizontal (top) and vertical (bottom) HDR sky. From left to right; lunchroom, large meeting room, small meeting room, corner open plan office and an open plan office.

For Building 2 an area from the lunchroom, large meeting room, small meeting room, a corner open plan office and an open plan office were selected, illustrated in figure 7.13. The open plan office simulated with the horizontal HDR sky had the highest correlation, whereas, the

small meeting room simulated under the vertical sky model had the least correlation between the real and simulated luminance data.

7.2.3. Building 3

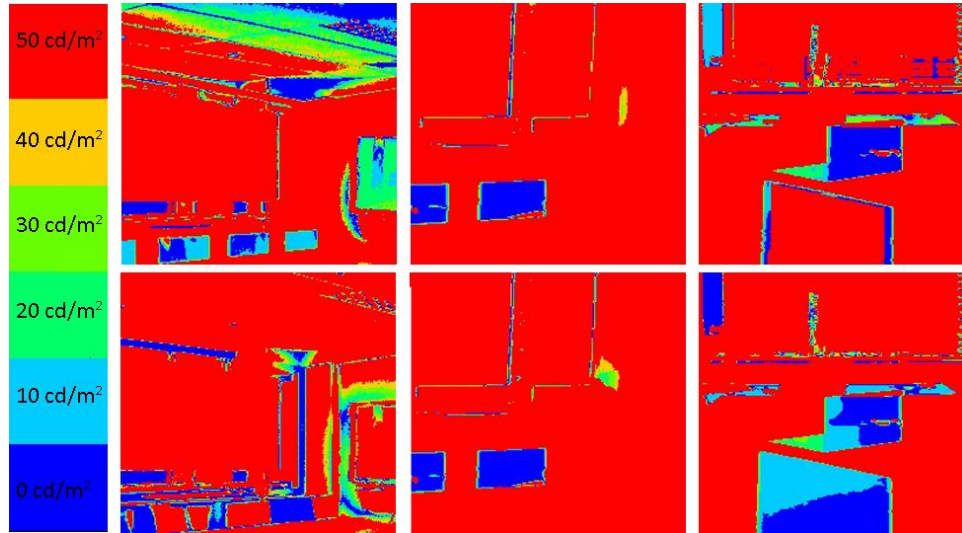


Figure 7.14: Comparison between sections of real and simulated images using horizontal (top) and vertical (bottom) HDR sky. From left to right; large meeting room, small meeting room and open plan office.

The final building monitored, Building 3 consisted of a large meeting room, a small meeting room and an open plan office, illustrated in figure 7.14. The ceiling of the large meeting room simulated under the horizontal sky had the highest correlation between the real and simulated images. However, the small meeting room contained the least correlation between the two images.

7.3. Surface to Surface Comparison

The surface to surface comparison method used an evenly spaced grid over the real and simulated images and calculates the relative error percentages under the horizontal and vertical HDR skies. If the error is within $\pm 10\%$ then the simulation is highly accurate (Mardaljevic 2000, 31). An evenly spaced seven by four grid was placed over the image to determine the relative error percentage between the real and simulated data.

7.3.1. Building 1

52%	41%	51%	47%	7%	14%	28%	52%	41%	51%	57%	49%	17%	22%
23%	44%	60%	29%	66%	46%	29%	23%	43%	9%	67%	65%	41%	33%
50%	7%	49%	13%	46%	2%	60%	40%	8%	54%	32%	31%	21%	57%
54%	63%	79%	58%	50%	50%	73%	61%	63%	79%	61%	58%	63%	71%

Table 7.01: Relative error percentage for the waiting area under the horizontal (left) and vertical (right) HDR skies

Table 7.01 illustrates the first room that was monitored in Building 1, was the waiting area. Under the horizontal sky, the mean relative error percentage was 42%. The maximum relative error percentage was 79%, whereas the minimum relative error percentage was 2%. Of the 28 measurement points, only 3 points (11%) were within $\pm 10\%$; and 5 points (18%) were within the $\pm 20\%$ margin of error.

For the vertical sky, the mean relative error percentage was 45% with relative error percentages ranging from 8% to 79%. Of the 28 measurement points, only 2 points (7%) were within a $\pm 10\%$ margin of error; while 3 points (11%) were within the $\pm 20\%$ margin of error.

7%	60%	41%	15%	56%	8%	65%	32%	72%	43%	9%	42%	7%	65%
18%	26%	39%	45%	45%	16%	55%	22%	23%	40%	46%	46%	17%	55%
53%	49%	53%	51%	44%	73%	20%	53%	51%	56%	55%	46%	73%	8%
57%	17%	58%	50%	59%	34%	74%	47%	31%	48%	44%	53%	43%	74%

Table 7.02: Relative error percentage for the lunchroom under the horizontal (left) and vertical (right) HDR skies

Table 7.02 illustrates the relative error percentages between the real and simulated data under both the horizontal and vertical HDR skies for the lunchroom. Under the horizontal sky, the mean relative error percentage was 42%. The largest relative error percentage was 73%, with 7% as the lowest relative error percentage. Of the 28 measurement points, only 2 points (7%) were within a $\pm 10\%$ margin of error; while 7 points (25%) were within the $\pm 20\%$ margin of error.

For the vertical sky, the mean relative error percentage was 43%. The percentages range from 7% to 73%. Of the 28 measurement points, only 3 points (11%) were within a $\pm 10\%$ margin of error; while 4 points (14%) were within the $\pm 20\%$ margin of error.

51%	11%	36%	4%	19%	32%	37%	29%	29%	54%	4%	19%	34%	35%
13%	56%	72%	4%	27%	31%	20%	2%	41%	60%	4%	35%	36%	24%
50%	54%	7%	27%	40%	50%	26%	41%	49%	14%	27%	30%	52%	19%
68%	74%	69%	60%	70%	72%	71%	61%	80%	78%	67%	60%	65%	74%

Table 7.03: Relative error percentage for the meeting room under the horizontal (left) and vertical (right) HDR skies

Table 7.03 illustrates the relative error percentages for the meeting room. Under the horizontal sky, the mean relative error percentage was 41%. The largest relative error percentage was 72%, whereas the lowest relative error percentage was 4%. Of the 28 measurement points, only 3 points (11%) were within a $\pm 10\%$ margin of error; while 5 points (18%) were within the $\pm 20\%$ margin of error.

For the vertical sky, the mean relative error percentage was 40% with a maximum relative error percentage of 80% and 2% was the lowest relative error percentage in the image. Of the

28 measurement points, only 3 points (11%) were within a $\pm 10\%$ margin of error; while 6 points (21%) were within the $\pm 20\%$ margin of error.

7.3.2. Building 2

67%	8%	34%	42%	11%	22%	22%	23%	6%	39%	26%	7%	9%	23%
57%	42%	13%	34%	47%	49%	16%	57%	42%	15%	34%	56%	50%	11%
42%	28%	39%	4%	11%	6%	2%	40%	31%	43%	9%	12%	24%	5%
40%	13%	27%	12%	38%	35%	40%	22%	10%	54%	45%	30%	19%	36%

Table 7.04: Relative error percentage for the lunchroom under the horizontal (left) and vertical (right) HDR skies

Table 7.04 illustrates the relative error percentages for the first monitored room in Building 2. The mean relative error for the lunchroom was 29% under the horizontal sky simulation. The maximum relative error percentage was 57%, whereas the lowest relative error percentage was 2%. Of the 28 measurement points, 4 points (14%) were within a $\pm 10\%$ margin of error; while 10 points (36%) were within the $\pm 20\%$ margin of error.

For the vertical sky, the mean relative error percentage was 28% with a maximum relative error percentage of 56% and 5% was the lowest relative error percentage in the image. Of the 28 measurement points, 6 points (21%) were within a $\pm 10\%$ margin of error; while 10 points (36%) were within the $\pm 20\%$ margin of error.

17%	36%	41%	45%	58%	29%	32%	30%	30%	27%	45%	22%	33%	36%
1%	33%	14%	29%	14%	54%	26%	21%	22%	31%	16%	36%	55%	1%
28%	45%	15%	34%	42%	59%	6%	37%	39%	22%	29%	17%	61%	7%
64%	22%	14%	13%	6%	19%	63%	58%	13%	38%	34%	27%	0%	63%

Table 7.05: Relative error percentage for the large meeting room under the horizontal (left) and vertical (right) HDR skies

Table 7.05 illustrates the relative error percentages for the large meeting room in Building 2. The mean relative error was 31% under the horizontal sky simulation. The maximum relative error percentage was 64%, whereas the lowest relative error percentage was 1%. Of the 28 measurement points, only 3 points (11%) were within a $\pm 10\%$ margin of error; while 10 points (36%) were within the $\pm 20\%$ margin of error.

For the vertical sky, the mean relative error percentage was 30% with a maximum relative error percentage of 63% and 0% was the lowest relative error percentage in the image. Of the 28 measurement points, only 3 points (11%) were within a $\pm 10\%$ margin of error; while 6 points (21%) were within the $\pm 20\%$ margin of error.

84%	76%	49%	50%	60%	11%	19%	84%	75%	47%	47%	60%	43%	18%
83%	50%	6%	51%	42%	10%	17%	83%	49%	10%	48%	51%	56%	20%
83%	71%	7%	51%	49%	47%	19%	83%	70%	12%	48%	44%	39%	26%
84%	79%	69%	64%	55%	31%	5%	84%	76%	67%	22%	3%	33%	2%

Table 7.06: Relative error percentage for the small meeting room under the horizontal (left) and vertical (right) HDR skies

Table 7.06 illustrates the relative error percentages for the small meeting room. The mean relative error was 47% under the horizontal sky simulation. The maximum relative error percentage was 84%, whereas the lowest relative error percentage was 5%. Of the 28 measurement points, only 4 points (14%) were within a $\pm 10\%$ margin of error; while 8 points (29%) were within the $\pm 20\%$ margin of error.

For the vertical sky, the mean relative error percentage was 46% with a maximum relative error percentage of 84% and 2% was the lowest relative error percentage in the image. Of the 28 measurement points, only 3 points (11%) were within a $\pm 10\%$ margin of error; while 6 points (21%) were within the $\pm 20\%$ margin of error.

17%	36%	41%	45%	58%	29%	32%	30%	30%	27%	45%	22%	33%	36%
1%	33%	14%	29%	14%	54%	26%	21%	22%	31%	16%	36%	55%	1%
28%	45%	15%	34%	42%	59%	6%	37%	39%	22%	29%	17%	61%	7%
64%	22%	14%	13%	6%	19%	63%	58%	13%	38%	34%	27%	0%	63%

Table 7.07: Relative error percentage for the corner open plan office under the horizontal (left) and vertical (right) HDR skies

Table 7.07 illustrates the relative error percentages for the corner open plan office. Under the horizontal sky, the mean relative error percentage was 33%. The relative error percentage ranges between 0% and 81%. Of the 28 measurement points, 8 points (29%) were within a $\pm 10\%$ margin of error; while 12 points (43%) were within the $\pm 20\%$ margin of error.

For the vertical sky, the mean relative error percentage was 21% with relative error percentage ranging between 0% and 91%. Of the 28 measurement points, 12 points (43%) were within a $\pm 10\%$ margin of error; while 16 points (57%) were within the $\pm 20\%$ margin of error.

57%	43%	47%	58%	70%	13%	76%	7%	28%	9%	41%	12%	35%	6%
56%	81%	77%	62%	10%	47%	22%	37%	15%	16%	41%	32%	6%	22%
79%	39%	71%	18%	43%	80%	80%	16%	32%	12%	64%	50%	6%	73%
87%	87%	12%	10%	56%	58%	19%	2%	2%	71%	72%	47%	46%	7%

Table 7.08: Relative error percentage for the open plan office under the horizontal (left) and vertical (right) HDR skies

Table 7.08 illustrates the relative error percentages for the last room monitored in Building 2. Under the horizontal sky, the mean relative error percentage was 52% for the open plan

office. The relative error percentage ranges between 10% and 87%. Of the 28 measurement points, only 2 points (7%) were within a $\pm 10\%$ margin of error; while 5 points (18%) were within the $\pm 20\%$ margin of error.

For the vertical sky, the mean relative error percentage was 29% with relative error percentage ranging between 2% and 73%. Of the 28 measurement points, 8 points (43%) were within a $\pm 10\%$ margin of error; while 13 points (21%) were within the $\pm 20\%$ margin of error.

7.3.3. Building 3

53%	15%	19%	7%	20%	82%	65%	38%	56%	58%	51%	36%	63%	70%
68%	52%	57%	35%	37%	8%	59%	10%	33%	38%	54%	18%	23%	65%
72%	69%	55%	36%	14%	2%	59%	1%	39%	23%	33%	30%	11%	61%
56%	65%	23%	14%	84%	78%	72%	37%	22%	24%	14%	59%	75%	73%

Table 7.09: Relative error percentage for the large meeting room under the horizontal (left) and vertical (right) HDR skies

Table 7.09 illustrates the relative error percentages for the first room monitored in Building 3. Under the horizontal sky, the mean relative error percentage was 45% for the large meeting room. The relative error percentage ranges between 2% and 72%. Of the 28 measurement points, only 3 points (11%) were within a $\pm 10\%$ margin of error; while 8 points (28%) were within the $\pm 20\%$ margin of error.

For the vertical sky, the mean relative error percentage was 40% with relative error percentage ranging between 1% and 75%. Of the 28 measurement points, only 2 points (7%) were within a $\pm 10\%$ margin of error; while 5 points (18%) were within the $\pm 20\%$ margin of error.

67%	59%	42%	70%	44%	50%	51%	67%	59%	42%	70%	44%	50%	51%
70%	57%	73%	56%	5%	80%	60%	70%	61%	73%	55%	2%	80%	60%
78%	81%	82%	75%	22%	62%	34%	78%	81%	84%	75%	22%	62%	34%
68%	78%	88%	22%	84%	74%	79%	70%	78%	88%	22%	84%	74%	79%

Table 7.10: Relative error percentage for the small meeting room under the horizontal (left) and vertical (right) HDR skies

Table 7.10 illustrates the relative error percentages for the small meeting room. Under the horizontal sky, the mean relative error percentage was 61% for the large meeting room. The relative error percentage ranges between 5% and 88%. Of the 28 measurement points, only 1 point (4%) was within the $\pm 10\%$ and $\pm 20\%$ margin of error.

For the vertical sky, the mean relative error percentage was 61% with relative error percentage ranging between 2% and 88%. Of the 28 measurement points, only 1 point (4%) was within the $\pm 10\%$ and $\pm 20\%$ margin of error.

51%	35%	25%	22%	19%	27%	47%	40%	39%	31%	22%	29%	37%	54%
57%	45%	42%	29%	1%	35%	20%	53%	70%	50%	37%	35%	19%	8%
1%	18%	72%	39%	16%	14%	18%	14%	9%	70%	36%	43%	39%	6%
80%	3%	79%	67%	48%	63%	82%	80%	6%	71%	66%	27%	65%	73%

Table 7.11: Relative error percentage for the open plan office under the horizontal (left) and vertical (right) HDR skies

Table 7.11 illustrates the last room monitored in building 3. Under the horizontal sky, the mean relative error percentage was 38% for the open plan office. The relative error percentage ranges between 1% and 82%. Of the 28 measurement points, only 2 points (7%) were within a $\pm 10\%$ margin of error; while 9 points (32%) were within the $\pm 20\%$ margin of error.

For the vertical sky, the mean relative error percentage was 40% with relative error percentage ranging between 6% and 80%. Of the 28 measurement points, 4 points (14%) were within a $\pm 10\%$ margin of error; while 6 points (21%) were within the $\pm 20\%$ margin of error.

7.4. Visual Field Comparison

This comparison method uses the spot illuminance measurements recorded in the monitored buildings and compared to the simulated images. The illuminance measurements were recorded on table tops, at approximately 750 mm above floor level. This was because it provided a flat surface and this is the typical height in which daylight measurements are recorded (Hayman 2003). The relative error percentage was calculated for each spot measurement and the mean relative error percentage was calculated for the monitored space.

7.4.1. Building 1

Under the horizontal sky simulation, the mean relative error percentage for the small meeting room was 11% with the largest percentage value being 15% and 9% as the lowest. The lunchroom had a mean relative error percentage of 7% with relative error percentage ranging from 1% to 12%. 7% was the mean relative value for the large meeting room with percentage values ranging from 3% to 9%. One of the open plan offices had a mean relative error of 10% while the other was 12% ranging from 6% to 17%.

For the vertical sky simulation, 11% was the mean relative error for the meeting room where the largest relative error percentage was 13% and the lowest was 8%. The lunchroom had a mean relative error of 9% with values ranging from 1% to 22%. The large meeting room had a mean relative value of 9% with 17% as the highest and 2% as the lowest percentage. The two open plan offices had mean relative errors of 11%, ranging from 8% to 13%.

Most of the mean relative errors fell within the $\pm 10\%$ margin stated in Mardaljevic's study meaning the model is "highly accurate" under this comparison method (Mardaljevic 2000, 31).

7.4.2. Building 2

Under the horizontal sky, the mean relative error percentage for the meeting room was 12% with 22% as the highest and 4% as the lowest percentage error. For the lunchroom, the mean relative error was 11% with 24% as the highest while the lowest percentage error was less than 1%. 12% was the mean relative error for the waiting area with the largest percentage being 24% and 4% as the lowest.

For the daylight simulation under a vertical sky, the mean relative error for the meeting room was 12% with 16% as the highest and 4% as the lowest percentage area. 13% was the mean relative error for the lunch room where 24% was the highest percentage error and 6% was the lowest. Lastly, 12% was the mean relative error for the waiting area, where the highest error percentage was 24% and the lowest was 5%.

Most of the mean relative errors fell within the $\pm 10\%$ margin stated in Mardaljevic's study meaning the model is "highly accurate" under this comparison method (Mardaljevic 2000, 31).

7.4.3. Building 3

For the office area, the mean relative error percentage on desk level under the horizontal sky simulation was 5%. The highest relative error percentage was 8% while the lowest percentage was 2%. The mean relative error percentage for the large meeting room was 6% with the largest relative error being 8%. The lowest percentage was 4%. For the small meeting room, the mean relative error percentage was 1% as all the relative error percentage for that scene was less than 1%.

Under the vertical sky simulation, the mean relative error percentage for the office area was 7%. The largest relative error percentage was 8% with the lowest percentage at 7%. The large meeting room was 11%. The largest relative error percentage was 13% where the lowest percentage was 9%. For the small meeting room, the mean relative error was 10% with 13% as the largest and 8% as the lowest relative error percentage.

This means that comparing the simulated with the field measurements, the simulated daylight model, falls mainly in the "highly accurate" category according to Mardaljevic's study (Mardaljevic 2000, 31).

7.5 Conclusion

This chapter explored the simulation results for the three buildings monitored selected from the BEES strata five database. It used four different methods to compare the real and simulated luminance data in both the HDR images captured and the images created through simulations. Two of the comparison methods were visual while the other two were numerical.

The first comparison method used was pixel by pixel comparison. This only provided limited results due to geometrical misalignments in the two images. This misalignment is mostly due to the scene being captured with a fisheye lens causing distortion in the HDR images produced.

The next comparison method used was a section to section pixel comparison where sections within the images are selected for a closer comparison. This allows the selection to be aligned more as only sections of the images were required to be aligned instead of the whole image. However, this method only provides a comparison between the two sections selected and does not provide the daylight distribution within the scene as a whole.

A numerical comparison method was used next where an evenly spaced seven by eight grid was placed over the images so that the relative error percentage between the real and simulated image can be calculated. The relative error percentages for the three monitored buildings, ranges between 20% to 45%, where a $\pm 10\%$ margin of error represents that the simulation is highly accurate (Mardaljevic 2000).

The last comparison method used was a visual field comparison where the illuminance values in the scene were measured during the monitored day and compared to the simulated image. The illuminance measurements were recorded by placing the light meter on the desktop within the scene. This provided the highest correlation between the measurements recorded in the scene and the illuminance data calculated from the simulated image.

Chapter 8: Conclusions

The objective of this research was to determine the adequacy of Smartphone based High Dynamic Range (HDR) photography as a tool for daylight analysis in New Zealand's commercial building stock. This study was conducted with an Android Smartphone and later, with an Android Tablet, employing the use of a \$50 USD magnetic fisheye lens. The overall aim of this research was to evaluate whether an inexpensive programmable data acquisition system could provide meaningful and useful data.

The research questions developed for this research were:

- Can capturing HDR images using (an Android) Smartphone be an adequate tool in determining the potential of daylight analysis?
- Can a suitable comparison technique be developed to compare the real and simulated luminance data?
- How accurate could using HDR photography as a daylight measurement tool be for daylight analysis?
- How can this measurement process be implemented into further research?

One of the main issues during the image capturing process for this research was that the internal and external HDR images of the building cannot be captured simultaneously. To capture both internal and external HDR images simultaneously, two researchers are required at the same site with two Smartphone cameras. Another way to overcome this issue is to design a software for the Smartphone camera that will automatically capture images at the same time set up on a tripod. This will also mean that roof access needs to be available so that the equipment would not be tampered with during the study period. However, two researchers are still required to be at the site as luminance and illuminance measurements are required to be recorded when the images were captured so that they can be calibrated in Photosphere.

A literature review was completed at the beginning of the research to document the background to this research. The literature review showed that the main inaccuracy in daylight simulation models was due to the simulated sky. Typically, a CIE or a Perez sky model would be used in daylight simulations, but this is only a generic sky model and does not provide accurate sky conditions of the specific time and location. This is when image-based lighting can be introduced in daylight simulations. It uses a calibrated HDR sky image, and uses it as a light source by mapping the image as an environment map in a software like Radiance

Lighting Simulation and Rendering System. This provides the daylight simulation with the real sky conditions with a more precise sky model for the specific time and location.

8.1 HDR Photography Using an Android Operated Device

In previous studies when HDR photography is used as a tool for daylight analysis, HDR images are usually captured using an expensive DSLR camera with a fisheye lens so that the daylight performance of the whole room can be captured quickly and easily (Inanici 2010) (Cheney 2008).

This research utilises an Android operated device to capture HDR photography in a daylight room. It began with a cheap Motorola Defy Smartphone and the HDR Camera application available for free from Google Play where four low dynamic range (LDR) images could be captured using a single button (Google Play). The number of photographs captured depends on the type of Smartphone used. However, through experimentations and tests, complications arose when it came to generating a camera response curve in both Photosphere and WebHDR (JALOX 2011) so that the HDR image produced could provide accurate daylight data. It was determined that a camera response curve could not be generated for the Motorola Defy Smartphone.

Due to the fact that a camera response curve could not be generated for the Motorola Defy Smartphone, it was decided that another Android operated device would be used to determine if it provided with the same outcome. Therefore, the Samsung Galaxy Note Tablet was used for the final monitored building as a camera response curve could be generated in Photosphere.

There are a few HDR programs that could be used to fuse HDR images and a comparison between them had been conducted. However, for this research it was decided that Photosphere will be used as it has been used in previous studies when determining the accuracy of HDR images as a daylight analysis tool (Inanici 2010) and has been validated. The disadvantage of using this software was that it is only available on the Apple operated platform.

This concludes that not all Smartphone's can provide the information required to generate a camera response curve and it was not determined exactly why this is. Although, through experimentations and tests, in both the lighting laboratory and in the first two monitored buildings, it was determined that it had nothing to do with the EXIF data, but the data embedded within the JPEG image itself.

8.2 Comparison of Real and Simulated Measurements

Four methods were used to compare the real and simulated measurements. They were pixel to pixel comparison, section to section pixel comparison, surface to surface comparison and visual field comparison. The first two methods were a visual analysis, whereas the last two methods were mathematical. Some of these methods provided a higher correlation factor between the two images than the others whereas some of these methods did not.

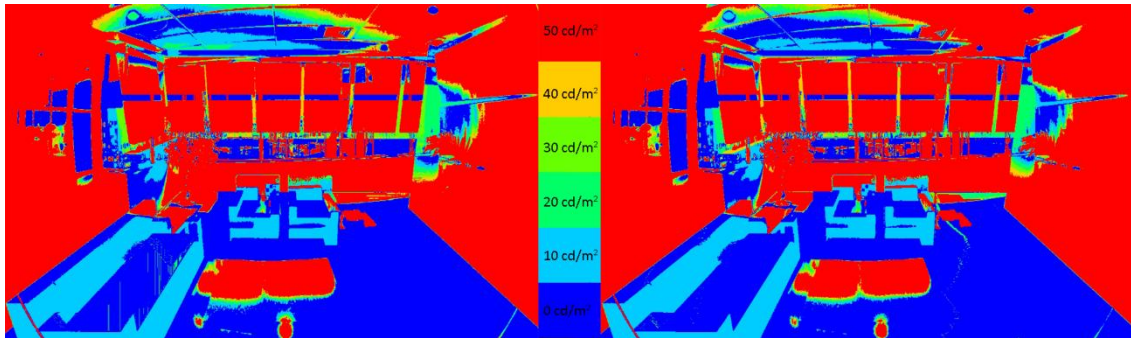


Figure 8.01: An example from Building 1 waiting area illustrating the pixel to pixel comparison between the real and simulated images under a horizontal (left) and vertical (right) HDR sky simulations

The pixel to pixel comparison, example of this illustrated in figure 8.01, where the real and simulated HDR images were compared as it was, had a large error margin due to the geometrical misalignment between the two images. Most of the images compared at a pixel level had only a 50% correlation between simulated and measured images.

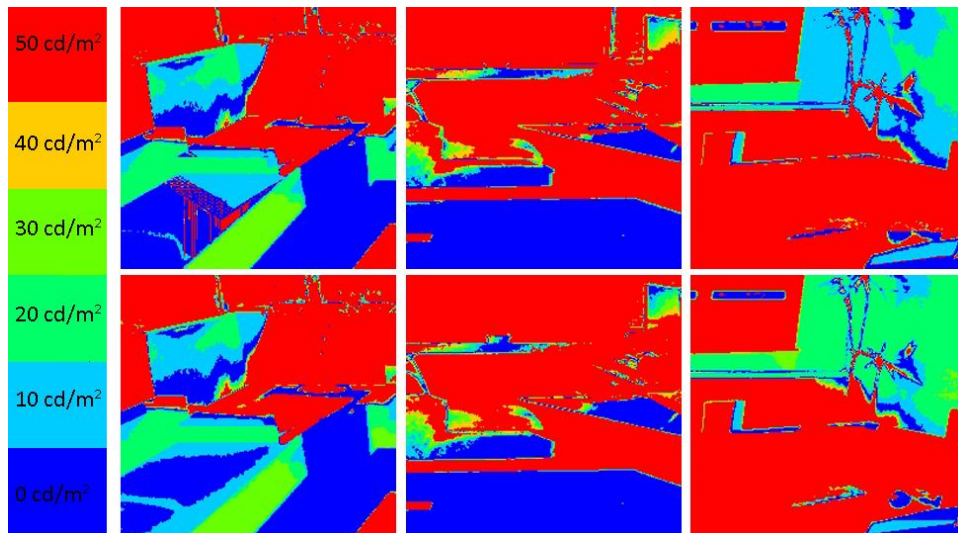


Figure 8.02: An example from Building 1 illustrating the section to section pixel comparison between the real and simulated images under a horizontal (top) and vertical (bottom) HDR sky simulations

The section to section pixel comparison, an example illustrated in figure 8.02, where a section of the real and simulated images were compared, had a similar result as the pixel to pixel comparison. Only some of the images compared had a high correlation whereas other images compared did not.

The surface to surface comparison and the visual field comparison provided this research with the best results. The surface to surface comparison used an evenly spaced seven by four grid placed over both the HDR image and the simulated images. This comparison method had a mean relative error of between 30% and 45% for all the buildings monitored. According to John Mardaljevic's study where if the relative errors fell within the $\pm 10\%$, the simulated model is deemed highly accurate (Mardaljevic 2000, 31).

However, using the visual field comparison where the illuminance measurements were recorded in the monitored buildings on desktops, most of the scenes studied had a mean relative error percentage of around $\pm 10\%$, never exceeding $\pm 20\%$. This means that when comparing the simulated data with the in-field measurements with a hand-held light meter provided accurate illuminance values in the scene.

The last building, was the only building monitored with artificial lighting turned on in the open plan office area as it was not possible to turn the artificial lights off. This scene provided the least correlation in all of the comparison methods used for this research. Therefore, further study is required for comparing an image between a scene with artificial lighting and a simulated image.

8.3 Accuracy of HDR Imagery as a Tool for Daylight Analysis

This research proves that it was possible to capture HDR photography using an Android Smartphone. However, when visually comparing the real and simulated images, about 60% of the images have the same luminance data. Whereas, through numerical comparison methods when simulating the buildings under a real HDR vertical and/or horizontal sky, this provides a "highly accurate" simulated model with a $\pm 10\%$ mean relative percentage error margin (Mardaljevic 2000).

This research concludes that while it was possible to capture HDR images using a Smartphone, there is a 60% correlation between real and simulated images using the pixel to pixel comparison methods. When comparing the simulated model with HDR skies as a light source, it provided a reliable daylight simulated model. Therefore, with more development with HDR photography using an Android Smartphone, along with more analysis and further research, this daylight measurement tool can become more accurate and provide a "highly accurate" simulation model.

8.4 Future work

“High dynamic range photography has taken off in the last couple of years [...] Even the iPhone is doing HDR – a true sign that this art form is hitting the mainstream.”

(Concepcion 2011, xii)

This is only the beginning for Smartphone cameras. As the technology develops, more measurements can be captured using one device. Currently there is a light meter and a sound level meter available for free on the Google Play Store (formerly Android Market) and with additional calibrated accessories, a Smartphone can start replacing the numerous number of equipment required to measure the environment of a space, with just one device.

This research could also help further analyse the data already collected by the Building Energy End-use Study team from BRANZ. With the light measurements collected from the monitored buildings, and extracting the hourly lighting data, along with additional LDR photographs of each premise, the measured illuminance can be analysed. The photographs can be calibrated and through the process developed in this research, the buildings can be simulated using a weather file created for that specific time period. The resultant daylight simulation can then provide results different range of daylight calculation, for example glare.

Bibliography

Bellia, L., A. Cesarano, G.F. Iuliano, and G. Spada. "HDR luminance mapping analysis system for visual comfort evaluation." *International Instrumentation and Measurement Technology Conference*. Singapore, 2009. 957 - 961.

Bloch, C. *The HDRI Handbook*. Canada: Rocky Nook Inc., 2007.

Bodart, M., A. Deneyer, A. De Herde, and P. Wouters. "A guide for building daylight scale models." *Architectural Science Review* 50, no. 1 (2007): 31-36.

Borisuit, A., J.L. Scartezzini, and A. Thanachareonkit. "Visual discomfort and glare rating assessment of integrated daylighting and electric lighting systems using HDR imaging techniques." *Architectural Science Review*, 2010: 359-373.

Cadik, M., M. Wimmer, L. Neumann, and A. Artusi. "Evaluation of HDR tone mapping methods using essential perceptual attributes." *Computer and Graphics* 32 (2008): 330-349.

Cai, H., and T. M. Chung. "Improving the quality of high dynamic range images." *Lighting Research Technology*, 2010: 1-16.

Cambridge in Colour. *High dynamic range photography*.

<http://www.cambridgeincolour.com/tutorials/high-dynamic-range.htm> (accessed March 05, 2012).

Carr, P., and R. Correll. *HDR photography: Photo workshop*. Indianapolis, Indiana: Wiley Publishing, Inc., 2009.

Carrier, K., and M. S. Ubbelohde. "The role of daylighting in LEED certification: A comparative evaluation of documentation methods." *Proceedings of the 2005 Solar World Conference*. Orlando, FL, 2005.

Cauwerts, C. "Potential of image-based lighting (IBL) pictures for subjective lighting quality evaluations - A comparison with real world luminances and physically based renderings (PBR)." *11th International Radiance Workshop*. Copenhagen, 2012.

Cheney, K. C. "Image based rendering: using high dynamic range photography to light architectural scenes." Master of Science in Architecture, University of Washington, 2008.

Chung, T.M., and R.T.H. Ng. "Variation of calibration factor over time for high dynamic range photography in a single daylit interior scene." *Journal of Light and Visual Environment* 34, no. 2 (2010): 87-93.

Concepcion, R. *The HDR book: Unlocking the pros' hottest post-processing techniques*. USA: Peachpit Press, 2011.

Debevec, P. "Image-based lighting." *IEEE Computer Graphics and Applications*, March/April 2002: 26 - 34.

Doyle, S., and C. Reinhart. *High dynamic range imaging and glare analysis - i. Definitions*. Harvard Graduate School of Design. Cambridge, July 15, 2010.

eCubed Building Workshop Limited. *Passive solar design guidance*. Wellington: Ministry for the Environment, 2008.

Google. *Google Maps*. 2012. <https://maps.google.co.nz/maps?hl=en&tab=wl> (accessed May 26, 2012).

Google Play. *HDR Camera*. 2012.
<https://play.google.com/store/apps/details?id=com.almalence.hdr&hl=en> (accessed April 26, 2012).

Google SketchUp. *What's new in SketchUp 8*. <http://www.sketchup.com/product/newin8.html> (accessed March 20, 2012).

Greenup, P., J.M. Bell, and I. Moore. "The importance of interior daylight distribution in buildings on overall energy performance." *Renewable Energy*, 2001: 45-52.

Groat, L., and D. Wang. *Architectural research methods*. New York: Wiley, 2001.

Hagner International UK Limited. "Hagner Universal Photometer Models S1 and S2 - Description and instruction manual." Sweden, 1974.

Hayman, S. "Daylight measurement error." *Lighting Research Technology* 35, no. 2 (2003): 101-110.

Heim, D., and E. Szczepanska. "Daylight distribution in a building space: A comparison of real conditions and theoretical sky models." *Proceedings of Building Simulation 2011: 12th Conference of International Building Performance Simulation Association*. Sydney, 2011. 2718-2723.

Hrastnik, B. *ExifToolGUI for Windows v5.xx*. May 2012. <http://u88.n24.queensu.ca/~bogdan/> (accessed July 23, 2012).

Inanici, M. "Evaluation of high dynamic range image based sky models in lighting simulation." *Journal of the Illuminating Engineering Society (IES)*, 2010: 69-84.

International Energy Agency. *Daylight in buildings: A source book on daylighting systems and components*. Report of the IEA SHC Task 21/ECBCS, Berkeley, CA: Lawrence Berkeley National Laboratory, 2000.

Isaacs, N., et al. *Building Energy End-Use Study (BEES): Years 1 and 2*. Wellington: BRANZ, 2009.

Jacobs, A. "High dynamic range imaging and its application in building research." *Advances in Building Energy Research* 1 (2007): 177-202.

JALOX. *Colour picker for Radiance*. 2012.

http://www.jaloxa.eu/resources/radiance/colour_picker/index.shtml (accessed May 05, 2012).

JALOX. *WebHDR*. April 16, 2011. <http://www.jaloxa.eu/webhdr/> (accessed May 05, 2012).

Jarvis, D., and M. Donn. "Comparison of computer and model simulations of a daylit interior with reality." *Fifth International IBPSA Conference/Building Simulation*. Czech Republic, 1997. Vol III-9.

Kim, M.H., and J. Kautz. "Characterisation for high dynamic range imaging." *Computer Graphics Forum (Proc. EUROGRAPHICS)* 27, no. 2 (2008): 691-697.

Kittler, R. "Daylight prediction and assessment: Theory and design practice." *Architectural Science Review* 50, no. 2 (June 2007): 94-99.

Konica Minolta. "Minolta Illuminance Meter T-1H."

<http://www.pages.uoregon.edu/~fbaker/~f/tools/~finstruction%2520manuals/~f/Minolta%2520Illuminance%2520Meter.pdf> (accessed June 05, 2012).

Konis, K. "HDR imaging in the field." *10th Annual International Radiance Workshop*. 2011.

Kumaragurubaran, V. "High dynamic range imaging processing toolkit for lighting simulations and analysis." Masters Thesis, University of Washington, 2012.

LI COR Environmental Division. "Light measurement." *LI COR environment*. February 14, 2012. <http://www.licor.com/env/pdf/light/210.pdf> (accessed April 21, 2012).

Li, D.H.W., and E.K.W. Tsang. "An analysis of daylighting performance for office buildings in Hong Kong." *Building and Environment*, 2008: 1446–1458.

Li, D.H.W., G.H.W. Cheung, K.L. Cheung, and J.C. Lam. "Simple method for determining daylight illuminance in a heavily obstructed environment." *Building and Environment*, May 2009: 1074-1080.

- Mardaljevic, J. "Daylight simulation: Validation, sky models and daylight coefficients." PhD Thesis, De Monfort University, 2000.
- Mardaljevic, J. "Parallax errors in sky simulator domes." *Joint IEA 31 - CIE 3.33 Meeting*. Ottawa, 2002.
- Mardaljevic, J., B. Painter, and M. Andersen. "Transmission illuminance proxy HDR imaging: A new technique to quantify luminous flux." *Lighting Research Technology* 41 (2009): 27-49.
- Matusiak, B., and H. Arnesen. "The limits of the mirror box concept as an overcast sky simulator." *Lighting Research and Technology* 37, no. 4 (2005): 313-328.
- McCann, J.J., and A. Rizzi. *The art and science of HDR imaging*. United Kingdom: John Wiley & Sons, Ltd., 2012.
- McCollough, F. *Complete guide to high dynamic range: Digital photography*. New York: Lark Books, 2008.
- Nabil, A., and J. Mardaljevic. "Useful daylight illuminance: A new paradigm for assessing daylight in buildings." *Lighting Research and Technologies*, July 2004: 41 - 59.
- Ng, R.T.H., and T.M. Chung. "On the calibration of high dynamic range photography for luminance measurements in indoor daylight scenes." *Architectural Science Review* 54 (2011): 39-49.
- Nightingale, D. *Practical HDR: A complete guide to creating High Dynamic Range images with your digital SLR*. United Kingdom: The Ilex Press Limited, 2009.
- Nikon. *AF DX Fisheye-Nikkor 10.5mm f/2.8G ED*. 2012.
http://imaging.nikon.com/lineup/lens/specialpurpose/fisheye/af_dx_fisheye105mmf_28g_ed/index.htm (accessed May 20, 2012).
- Osborne, J., and M. Donn. "Defining parameters for a quality daylight simulation validation dataset." *International Building Performance Simulation Association 2011*. Sydney, 2011. 1481-1488.
- Otis, T., and C. Reinhart. *A design sequence for diffuse daylighting - 'Daylighting rules of thumb'*. Harvard Graduate School of Design. Cambridge, March 16, 2009.
- Perez, R., P. Ineichen, R. Seals, J. Michalsky, and R. Stewart. "Modelling daylight availability and irradiance components from direct and global irradiance." *Solar Energy* 44, no. 5 (1990): 271-289.

Photography Mad. *Fisheye lenses*. <http://www.photographymad.com/pages/view/fisheye-lenses> (accessed May 5, 2012).

Post, A.M.J., and A. Koutamanis. "Between past and future: Daylight simulation and analysis for today." *International Conference On Adaptable Building Structures*. Eindhoven, The Netherlands, 2006. 329-333.

Post, J., and A. Koutamanis. "Simulation for daylighting in the real world: The art and science of usability." *Digital design: The quest for new paradigms*. Lisbon: 23 eCAADe Conference Proceedings, 2005. 407-414.

Reinhart, C., and P.-F. Breton. "Experimental validation of 'Autodesk 3ds Max Design 2009' and Daysim 3.0." *Building Simulation*, 2009: 1514-1521.

Reinhart, C., M. Landry, and P.F. Breton. *Daylight simulation in 3ds Max Design 2009 – Getting started*. USA, November 27, 2008.

Reinhart, Christoph F., and Jan Wienold. "The daylighting dashboard - a simulation-based design analysis for daylit spaces." *Building and Environment* 46 (2011): 386-396.

Rogers, Z. "Overview of daylight simulation tools." *The Daylight Site*. 2007. <http://www.thedaylightsite.com> (accessed June 5, 2012).

Santa Clara, M. "Digital photography, a tool for lighting research: High-resolution sampling luminance maps with digital photographic technologies applied to diffuseness descriptors." *PLEA2009 - 26th Conference on Passive and Low Energy Architecture*. Quebec City, 2009.

Solemnia Environmental Tools to Empower Design. *DIVA for Rhino*. 2012. <http://www.diva-for-rhino.com/> (accessed May 23, 2012).

Stumpfel, J. "HDR lighting capture of the sky and sun." Master of Science Thesis, California Institute of Technology, Pasadena, California, 2004.

Stumpfel, J., A. Jones, A. Wenger, C. Tchou, T. Hawkins, and P. Debevec. "Direct HDR capture of the sun and sky." *AFRIGRAPH '04 Proceedings of the 3rd International Conference on Computer Graphics, Virtual Reality, Visualisation and Interaction*. Africa: ACM New York, 2004. 145-149.

su2rad. *Radiance exporter and other Ruby scripts for Google SketchUp*. <http://code.google.com/p/su2rad/> (accessed April 20, 2012).

- U.S Department of Energy. *Building energy software tools directory*. January 09, 2011.
http://apps1.eere.energy.gov/buildings/tools_directory/alpha_list.cfm (accessed April 18, 2012).
- USC Institute for Creative Technologies. *HDRShop*. 2012. <http://www.hdrshop.com> (accessed May 23, 2012).
- Van Den Wymelenberg, K., and M. Inanici. "A study of luminance distribution patterns and occupant preference in daylit offices." *PLEA2009 - 26th Conference on Passive and Low Energy Architecture*. Quebec City, Canada, 2009.
- Veitch, J.A. "Research matters: HDR making strides." *Lighting Design and Application* 39, no. 10 (October 2009): 18-21.
- Ward Larson, G. *Anywhere Software*. <http://www.anywhere.com/> (accessed May 13, 2012).
- Ward Larson, G. "Radiance file formats."
<http://www.radsite.lbl.gov/radiance/refer/filefmts.pdf> (accessed April 20, 2012).
- Wittkopf, S.K. "A method to construct virtual sky domes for use in standard CAD-based light simulation software." *Architectural Science Review* 47 (September 2004): 275-286.

Appendix

Appendix A: HDR Software

This section summarises the possible HDR programs that could be used for this research. The software required for this research needs to be able to fuse the photographs captured and generate an HDR image along with the possibility of calculating a camera response curve. A comparison between real and simulated HDR images is required for the analytical section of this research, therefore an HDR software will need to be selected to do this as well.

A1. hdrscope

Developed by Viswanathan Kumaragurubaran in collaboration with Mehlika Inanici at the University of Washington, hdrscope was developed as a partial fulfilment for a Master of Science in Architecture, Design Computing. It was developed because there was a lack of “user friendly tool that can process and analyse HDR photographs and simulation results from Radiance” (Kumaragurubaran 2012, 2). It allows the user to connect their Canon DSLR camera directly to the laptop and set up parameters to capture a scene with various exposure values.

This software also allows the user to conduct a comparison study between two images by using the “Image Operations” tool. The difference between pixel values can be calculated between two images. This way with the two images mapping all the luminance values for a whole scene can be compared if the two images are geometrically align.

A2. HDRShop

Developed in 1997, HDRShop was created by a group at the University of Southern California, led by Paul Debevec. HDRShop was created specifically following the principles of image-based lighting (IBL). HDRShop 1 was freely available for academics and non-commercial use; however, it costs approximately US\$400 to buy HDRShop 3.

The main disadvantage of HDRShop is that the software does not read EXIF data, requiring the user to manually insert f-stop information so that the software will know the exposure information for that image in order to fuse the photographs. Also the software does not provide an image align function. Therefore if there is movement in between photographs, this will not be the correct software to be used.

However, this software does allow the user to compare two images. It allows the user to resize the image and crop to a desired size instead of having to do this in a different software.

A3. Photomatix

One of the most popular programs amongst photographers, Photomatix was developed by Geraldine Joffre in 2003. Unlike other programs that were developed in a “science lab”, Photomatix was developed through “photographic practice”. It merges three photographs into a single HDR image (Bloch 2007, 77).

The software’s main focus is in creating HDR images and later tone mapping them, and not in the accuracy of the light measurements in the images.

A4. Photosphere

Photosphere has been validated to be one of the most accurate HDR software available and one of the most commonly used. Photosphere is a free program that is only available on the Apple operated system. It was developed by Greg Ward and it supports all HDR formats. The most predominant feature of Photosphere is that accurate luminance values can be obtained by just “picking the pixel value” where currently no HDR software is available to do so (Bloch 2007, 76).

Photosphere consists of a thumbnail browser supporting all HDR image formats. Assembling an HDR image by fusing multiple exposures is “both easy to use and highly accurate”. It is the only software that users can “obtain accurate luminance measurements from [...] by picking the pixel values” (Bloch 2007, 77).

“So for lighting designers and applications in the architectural field, Photosphere is the only option. It can also generate false coloured luminance maps, which is very useful for all you professional lighting analysts.”

(Bloch 2007, 77)

Real-world luminance (cd/m^2) can be determined in an HDR image produced in Photosphere. It is able to do so because the image produced contains the “absolute EV of the original exposures and aligns the numerical values of the HDR image to it” (Bloch 2007, 128). If luminance measurements are recorded in the scene, the HDR image can be calibrated in Photosphere.

Appendix B: Daylight Simulation Software

This section summarises the possible daylight simulation software that could be used in this research.

B1. Autodesk 3ds Max Design

One of the newer programs that can produce a “physically accurate” daylight simulation is Autodesk 3ds Max Design (Reinhart, Landry and Breton 2008). 3ds Max Design is a “mental ray rendering engine” that can produce “physically accurate” daylight simulation models (Reinhart, Landry and Breton 2008). The renderings from this program “should be accurate”, but it is important that the render settings are set at “high” and that the “lights and materials were previously defined in a physically correct way” (Reinhart, Landry and Breton 2008). Additionally, it is the better “geometric modelling” software (Post and Koutamanis 2005, 408) and can “predict interior lighting conditions, under the overcast and clear CIE sky as well as the Perez sky”. This software requires the user to be familiar with “basic concepts of 3ds Max” with accurate results (Reinhart, Landry and Breton 2008). It is discovered that results from 3ds Max Design are accurate and “sufficient for typical daylighting design” (Reinhart and Breton 2009).

3ds Max Design is able to light a scene with an HDRI source. However, this method has only been used to create visually appealing images, and it is unknown how accurate the lighting information is as no validation studies have been conducted at this stage.

B2. Daysim

Developed at Harvard University, Daysim is a free radiance daylight simulation program available to all users. However, it is recommended that the user should have some previous experience with Radiance “as it uses the same input files” (U.S Department of Energy 2011). It uses the Perez sky model to “predict hourly or sub-hourly” daylight penetration into the building (Reinhart and Breton 2009).

B3. Diva

DIVA is a plug-in for Grasshopper and Rhinoceros developed originally by Harvard University. DIVA stands for Design Iterate Validate Adapt. Currently, the plug-in is distributed by Solemma LLC, Diva is a “highly optimised daylighting and energy modelling plug-in” (Solemma Environmental Tools to Empower Design 2012). The environmental performance of a building can be simulated accurately.

B4. Radiance Lighting Simulation and Rendering System

One of the most commonly used lighting simulation program is Radiance Lighting Simulation and Rendering System. Initially developed by Greg Ward at Lawrence Berkeley National Laboratory, Radiance provides “reliable lighting calculations” (Post and Koutamanis 2006). It is a physically-based rendering program that has been validated for daylight analysis “with physically-based modelling of material and sky conditions” (Cheney 2008, 10). It contains a collection of fifty plus script-based programs requiring text files instead of using visualisation to simulate the building.

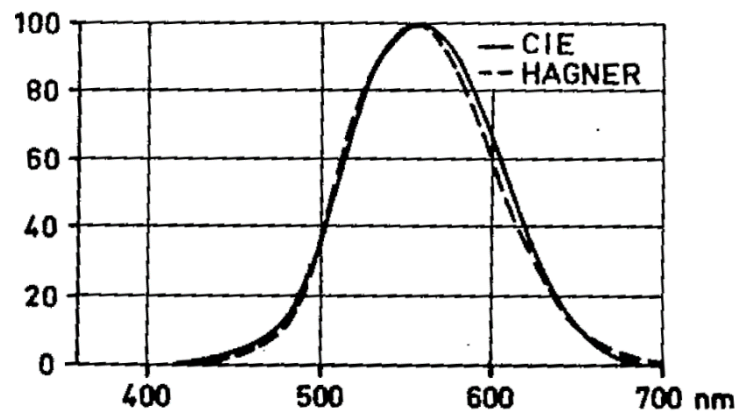
The software “reliability” and simulation method has “been proven by several validation studies” (Post and Koutamanis 2006). This software simulates and can visualise lighting “in and around the architectural environment”. Using a range of sky conditions “internal illuminance” can be predicted to a “high level of accuracy” (Li, Cheung, et al. 2009).

Radiance can “measure room illuminance levels, detect possible sources of glare and indicate visual comfort levels both qualitatively and quantitatively” (Greenup, Bell and Moore 2001). This way, designers will have general knowledge of what works and what does not. However, Radiance users have had trouble in creating “geometric modelling, texturing and surface smoothing capabilities” (Post and Koutamanis 2006). Therefore, Google SketchUp 8 was used to simulate the geometric form of the building so that it can be visually viewed and then exported by layers to Radiance for further editing. According to the U.S. Department of Energy, Radiance requires a “high level of computer literacy”, with at least “four days training” as the minimum recommended training time (U.S Department of Energy 2011).

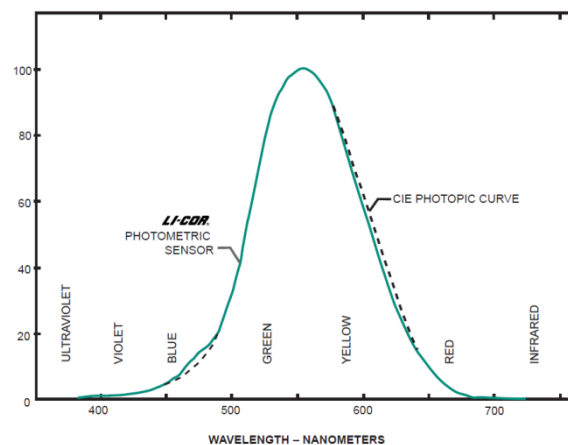
Appendix C: Equipment

This section contains the spectral response curve for the light meters compared to the CIE standard observer curve collected from manufacturers.

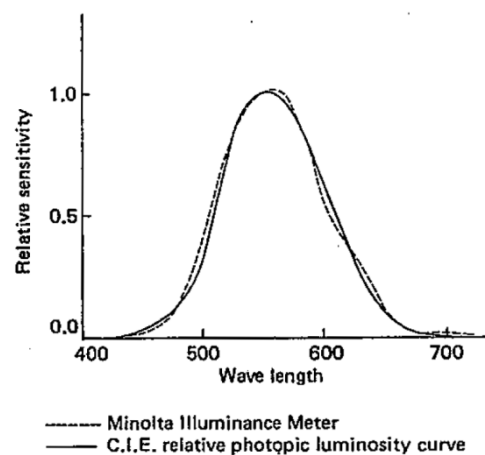
Hagner Universal Photometer (Hagner International UK Limited 1974)



Photometric Illuminance sensors (LI COR Environmental Division 2012)



Minolta Illuminance Meter T-1H (Konica Minolta)

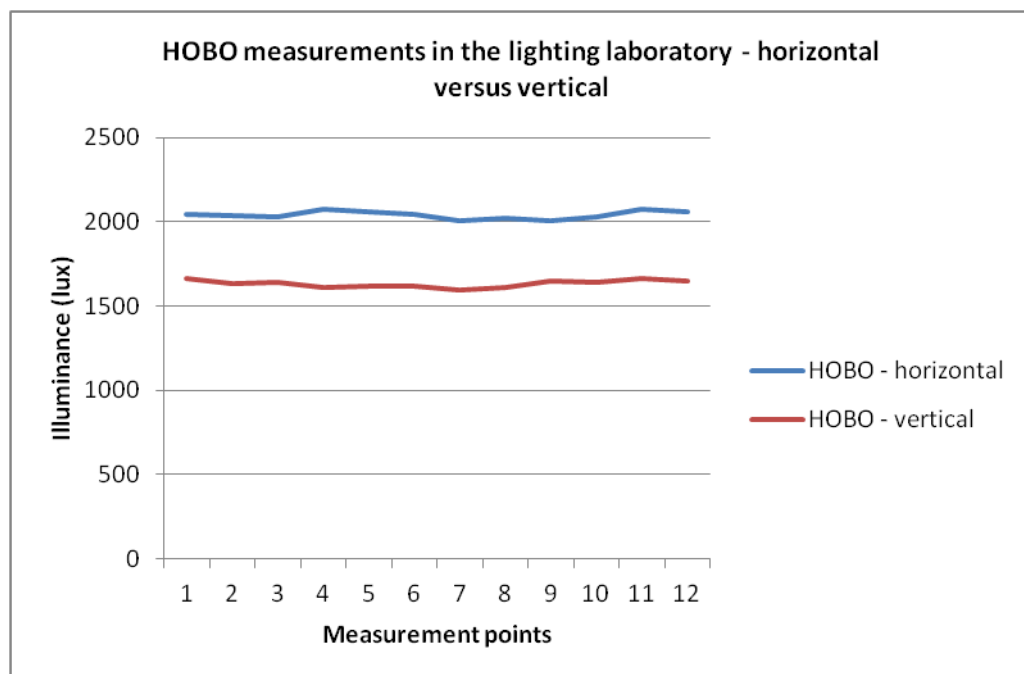


Appendix D: Equipment Calibration Process

This section explains the calibration process conducted in the lighting laboratory for all the daylight measurement devices. It was important to calibrate all the equipment used in this research to ensure that the daylight measurements taken on site are as accurate as possible. The luminance meter was calibrated by pointing it towards a white card and spot measurements were recorded.

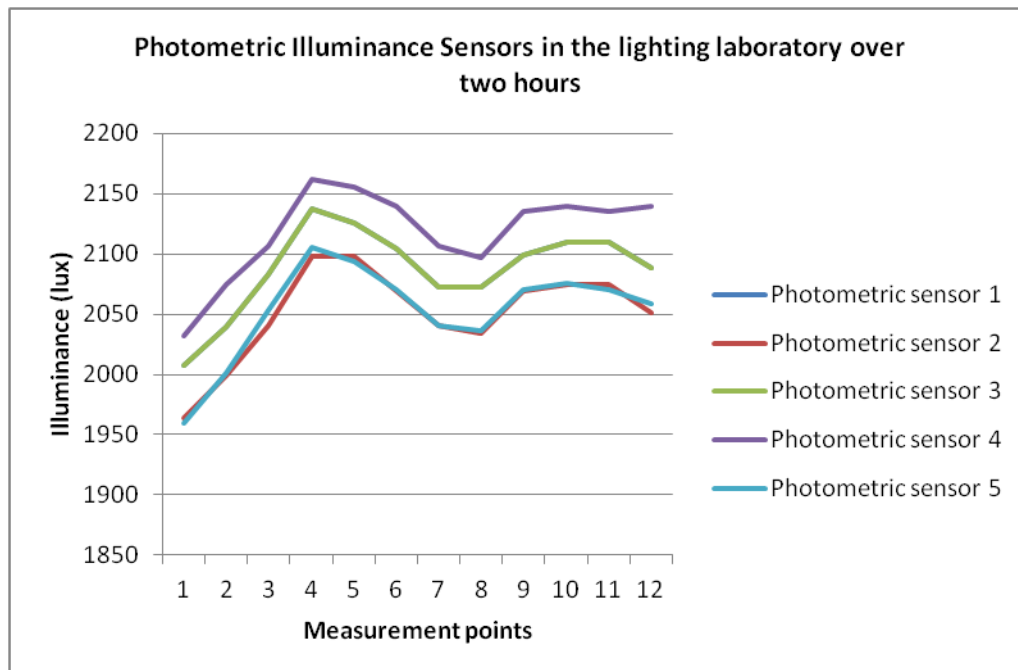
All the illuminance meters have been factory calibrated in the past couple of years. Therefore, for this study they will all be set up in the lighting laboratory under the artificial sky to calibrate them against each other and determine if there are any correction factors that needs to be applied to the equipment. All lighting equipment's were set so that illuminance measurements were recorded every ten minutes for two hours. All the light meters are within $\pm 10\%$ of each other therefore they do not need to be sent back for further calibration (Hayman 2003).

The two HOBO U-12 Data loggers from BRANZ were used. One was placed on the desk vertically and the other horizontally. The graph below illustrates illuminance comparison. This was because in the buildings monitored, some of the HOBO's were placed in vertically against the walls as empty desktops were not always available.

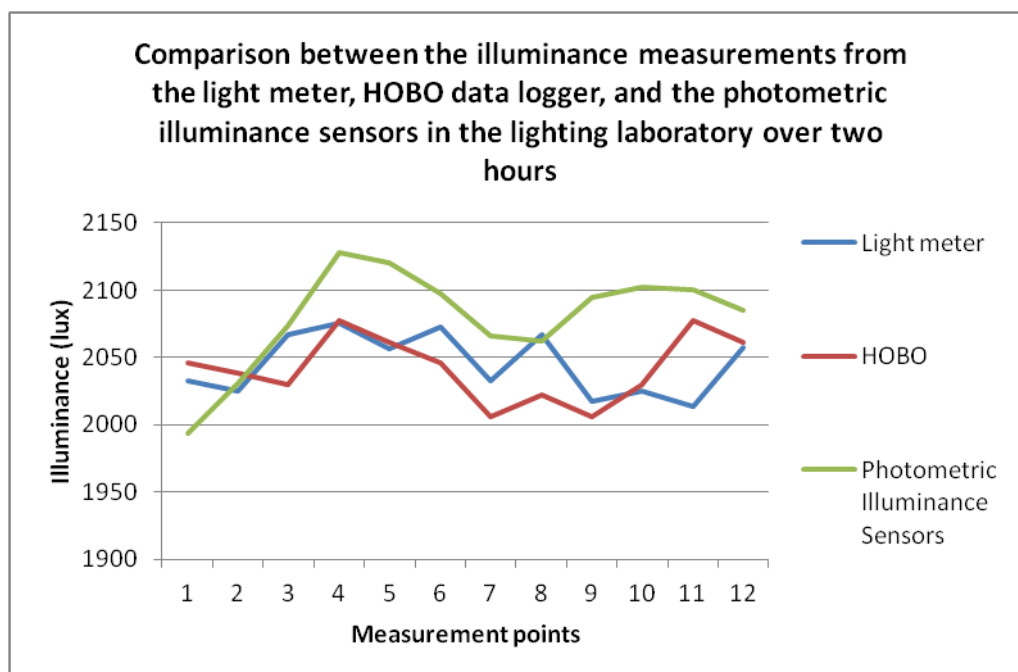


Two Minolta hand-held were placed side by side on the desktop, and the measurements were recorded manually during the two hours. Lastly, five Photometric Illuminance Sensors connected to a laptop, were taped next to each other on the desktop. The correction factors

that were recorded for these during the factory calibration were included in the final measurements.

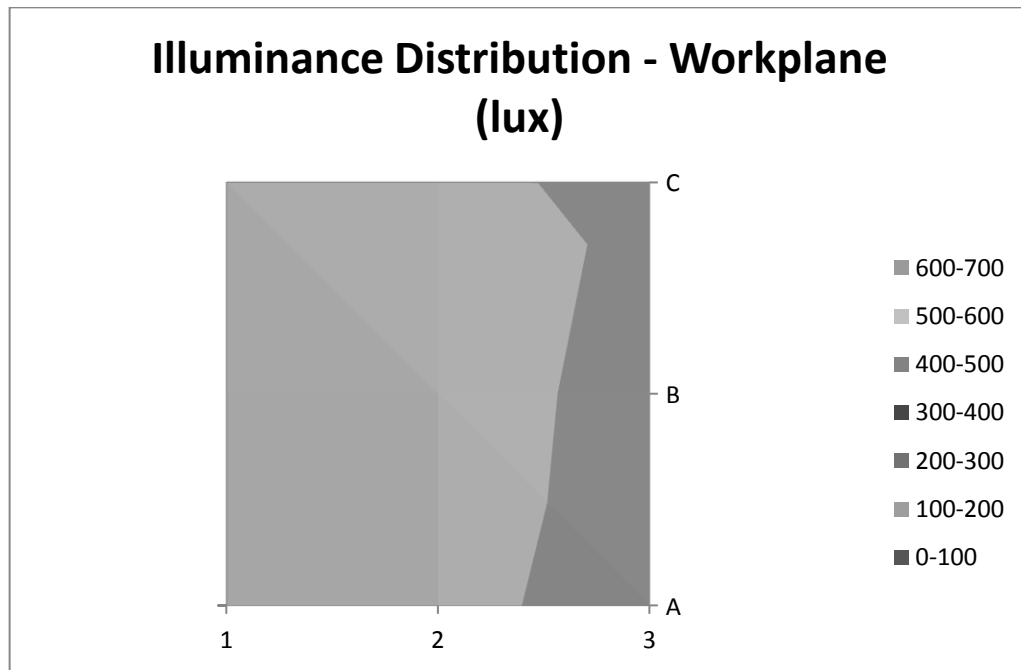


The results from the calibration for the light meter, the HOBO data logger and the Photometric Illuminance Sensors are illustrated in the line graph below.

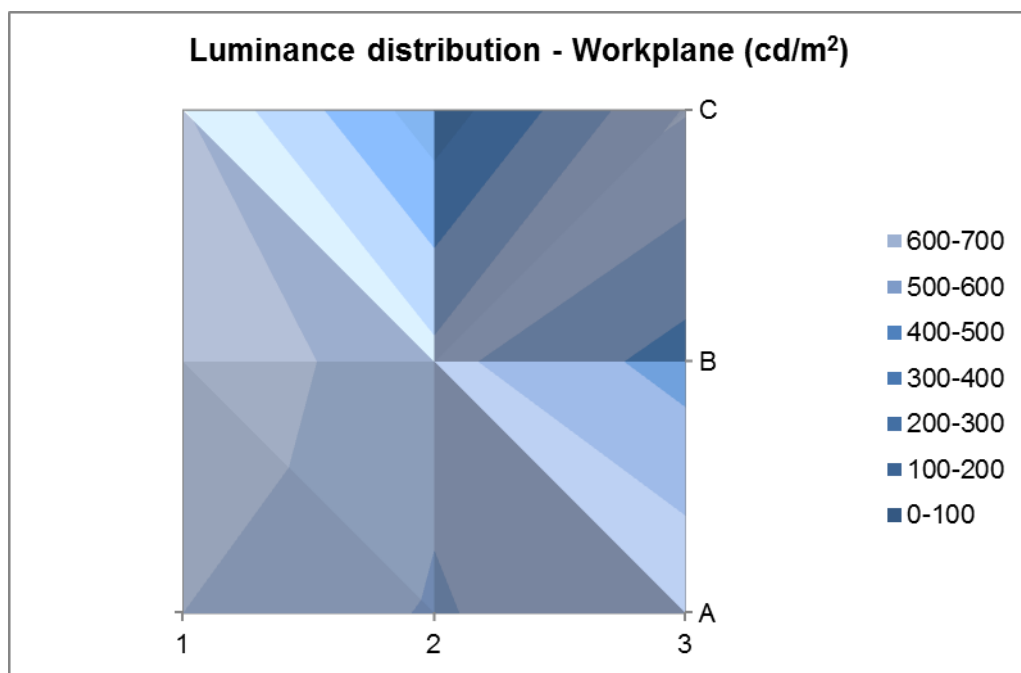


Appendix E: Lighting Laboratory Measurements

This section shows the lighting distribution in the lighting laboratory. The average illuminance distribution of the five measurements recorded at 800 mm above floor level on a three by three grid under a white light is illustrated below:

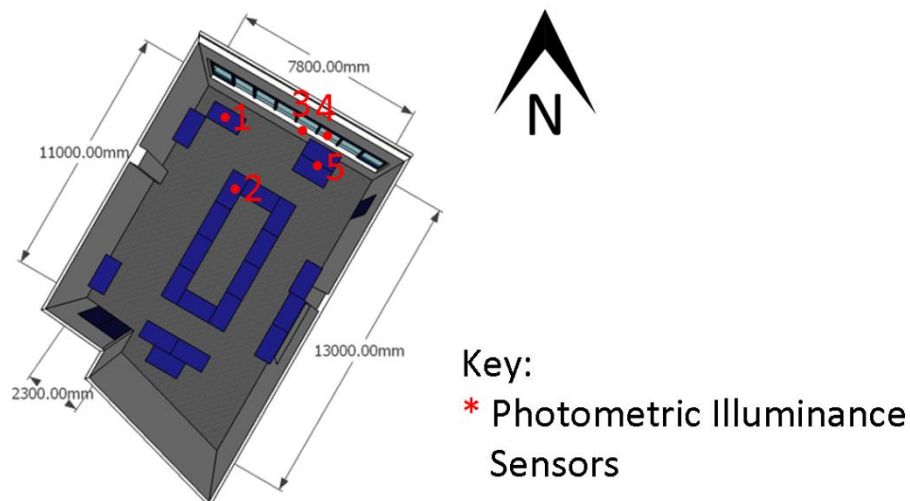


Luminance distribution of the ceiling of the lighting laboratory on a three by three grid under a white light is illustrated below:

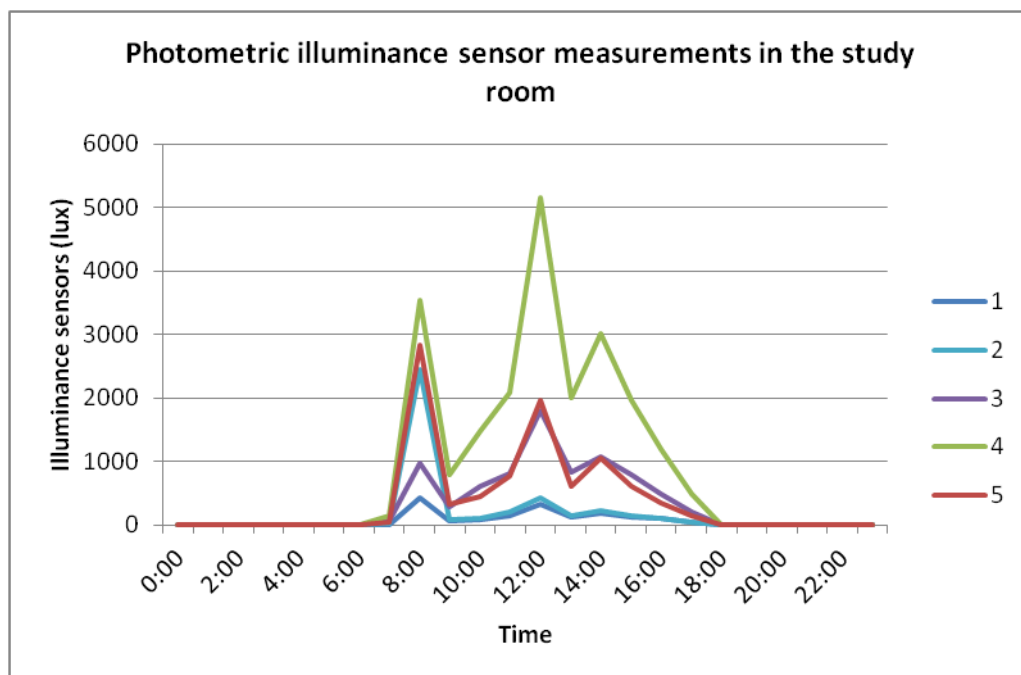


Appendix F: Daylight Measurements Using Photometric Illuminance Sensors in the Study Room

This section illustrates the results from the five photometric illuminance sensors in the study room from the 12th April to the 17th April 2012. The data loggers are set to record the illuminance measurements every five minutes. The location of the photometric illuminance sensors are shown in red.



The graph below illustrates the illuminance measurement recorded on the hour for 24 hours on an overcast day. The numbers on the right hand side legend represents the photometric illuminance sensors illustrated on the floor plan above.



Appendix G: Generating a Camera Response Curve

This section documents the experimentation and tests conducted to generate the camera response curve. The camera response curves for the devices used in this research were generated using an HDR software called Photosphere (Ward Larson, Anywhere Software). Each capturing device has its own camera response curve so it is important to generate one for each of the image capturing device used to ensure that the lighting data within the HDR image is accurate.

The EXIF data was the first explored and edited as the photographs captured using the HDR Camera application does not provide the images with EXIF data so the file will need to be created and added into the image. This mainly includes the exposure value and white balance information. The EXIF data can be edited through ExifTool.

Images within the lighting laboratory of a simple box were captured using both the Nikon D200 camera and the Motorola Defy Smartphone camera. Both the built-in camera and the HDR Camera application were used in the Smartphone. A camera response curve was easily generated for the Nikon camera.

Photographs captured using the built-in camera application provides the EXIF data including the exposure values. Therefore, the EXIF data for these photographs does not need to be altered. Unfortunately, the error message “cannot solve response function” appears when trying to generate a camera response curve.

The EXIF data from the Nikon camera was copied over to the Motorola Defy to determine if the EXIF data from Nikon camera is adequate in generating a camera response curve. However, when trying to generate the camera response the same error message appears. All the EXIF data from both devices generated were printed out and were compared against each other to ensure that none of the data required were missed.

The next step was to copy the EXIF data generated by the Smartphone using the built-in camera application was copied to the Nikon camera, with the camera model name changed. Using this method, the Nikon image with the Smartphone EXIF data, a camera response curve was able to be generated.

This meant that the cause of not being able to generate the camera response curve was due to the JPEG format itself, and not due to the EXIF data.

The photographs were opened in Photoshop to determine whether the JPEG format can be altered if the images were saved under both low and maximum qualities. However, after this

method, the same error message appeared when trying to generate the camera response curve.

It was then determined to experiment with another Android device available to see if a camera response curve could be created from Android devices. A Samsung Galaxy Note Tablet was used for the final monitored building as a camera response curve could be generated.

It was concluded that through the experimentations and tests that the camera response curve could not be generated for the Motorola Defy due to the JPEG format itself and not with the EXIF data.

Appendix H: Variation of Surface Colours in the Pilot Study

This section show the variations used in the daylight simulations for the study room.

Surface	R	G	B	RGB value for Radiance	Reflectance
Carpet	45	46	47	0.176, 0.180, 0.184	0.179
	74	72	75	0.291, 0.282, 0.294	0.255
Desks	36	62	88	0.141, 0.243, 0.345	0.223
	39	64	90	0.153, 0.251, 0.353	0.231
Chairs	87	92	115	0.341, 0.361, 0.451	0.362
	89	95	115	0.349, 0.373, 0.451	0.372
Walls/ceiling	228	225	221	0.894, 0.882, 0.866	0.884
	234	232	227	0.918, 0.910, 0.890	0.911
Wall with windows	47	49	71	0.184, 0.192, 0.278	0.195
	49	51	72	0.192, 0.200, 0.282	0.203
Window sill	126	125	124	0.494, 0.490, 0.486	0.491
	132	131	131	0.518, 0.514, 0.514	0.515
Window frames	63	66	68	0.247, 0.259, 0.266	0.256
	65	68	70	0.255, 0.266, 0.275	0.264

Appendix I: Radiance Sky Mapping Scripts

This section documents the Radiance scripts used to map the HDR image as the light source for both the horizontal and vertical skies. It is important to ensure that all file names do not contain spaces.

probe.rad

```
#IBR probe

Void colorpict hdr_radiance_image
7 red green blue [hdrskyfilename.hdr] [skymapfilename.cal] u v
0
0

hdr_radiance_image glow light probe
0
0
4 1 1 1 0

#

#ground (for use with 180 fisheye probes)

void glow ground_glow
0
0
4
    1 1 1 0

ground_glow source ground
0
0
4
    0 0 -1 180

#
```

For a 180 degree HDR horizontal probe

horizontal sky map.cal

```
u = .5 - Dx/hyp_rt * probe_dir;  
v = .5 + Dy/hyp_rt * probe_dir;  
  
hyp_rt = sqrt(Dx*Dx + Dy*Dy);  
probe_dir = acos(Dz) / PI;
```

For a 180 degree HDR vertical probe

If the HDR image of the surrounding environment and sky is a 180 degree vertical fisheye (i.e. from the window) instead of the sky, then each orientation has its own script.

For **North** facing images:

vertical sky map north.cal

```
u = .5 + Dx/hyp_rt * probe_dir;  
v = .5 + Dz/hyp_rt * probe_dir;  
  
hyp_rt = sqrt(Dx*Dx + Dz*Dz);  
probe_dir = acos(Dy) / PI;
```

For **East** facing images:

vertical sky map east.cal

```
u = .5 - Dy/hyp_rt * probe_dir;  
v = .5 + Dz/hyp_rt * probe_dir;  
  
hyp_rt = sqrt(Dy*Dy + Dz*Dz);  
probe_dir = acos(Dx) / PI;
```

For **South** facing images:

vertical sky map south.cal

```
u = .5 - Dx/hyp_rt * probe_dir;  
v = .5 + Dz/hyp_rt * probe_dir;
```

```
hyp_rt = sqrt(Dx*Dx + Dz*Dz);  
probe_dir = acos(-Dy) / PI;
```

For **West** facing images:

vertical sky map west.cal

```
u = .5 + Dy/hyp_rt * probe_dir;  
v = .5 + Dz/hyp_rt * probe_dir;
```

```
hyp_rt = sqrt(Dy*Dy + Dz*Dz);  
probe_dir = acos(-Dx) / PI;
```


Appendix J: Surface Reflectances in the Monitored Buildings

This section documents the lowest and highest RGB values measured using the ColorMunki in the three monitored buildings, as well as their locations.

Building 1

Surface	R	G	B	RGB value for Radiance	Reflectance
Wall/ceiling	225	218	205	0.882, 0.855, 0.804	0.859
	247	242	232	0.969, 0.949, 0.910	0.952
Carpet	52	48	46	0.204, 0.188, 0.180	0.193
	62	57	54	0.243, 0.224, 0.212	0.228
Window frame	157	157	155	0.616, 0.616, 0.608	0.615
	159	160	158	0.624, 0.627, 0.620	0.626
Lunchroom - table	148	150	147	0.580, 0.588, 0.576	0.585
	152	155	152	0.596, 0.608, 0.596	0.604
Lunchroom – bench	152	155	152	0.596, 0.608, 0.596	0.604
	192	196	189	0.753, 0.769, 0.741	0.763
Lunchroom – coffee table	40	24	19	0.127, 0.094, 0.075	0.102
	52	35	26	0.204, 0.137, 0.102	0.153
Sofa	122	46	52	0.478, 0.180, 0.204	0.261
	132	50	57	0.518, 0.196, 0.224	0.283
Waiting room table	125	92	60	0.490, 0.361, 0.235	0.388
	147	114	81	0.576, 0.447, 0.318	0.473
Meeting room – table	99	60	30	0.388, 0.235, 0.118	0.268
	104	63	35	0.408, 0.247, 0.137	0.300
Meeting room – chair	82	74	68	0.322, 0.290, 0.266	0.297
	84	76	70	0.329, 0.298, 0.275	0.305

Building 2

Surface	R	G	B	RGB value for Radiance	Reflectance
Carpet	61	61	60	0.239, 0.239, 0.235	0.239
	83	80	77	0.325, 0.314, 0.302	0.316
Wall/Ceiling	224	216	207	0.878, 0.847, 0.812	0.853
	229	222	212	0.898, 0.871, 0.831	0.876
Window frame	169	170	168	0.663, 0.666, 0.659	0.665
	170	172	171	0.666, 0.675, 0.671	0.672
Chair	52	52	53	0.204, 0.204, 0.208	0.204
	57	57	58	0.224, 0.224, 0.227	0.224
Lunchroom - sofa	71	26	30	0.278, 0.102, 0.118	0.150
	158	72	55	0.620, 0.282, 0.216	0.367
Lunchroom – table	230	233	228	0.902, 0.914, 0.894	0.910
	235	236	231	0.922, 0.925, 0.906	0.923
Lunchroom - bench	234	235	231	0.918, 0.922, 0.906	0.920
	235	236	232	0.922, 0.925, 0.910	0.923
Meeting room – table	210	170	127	0.824, 0.666, 0.498	0.697
	213	172	128	0.835, 0.675, 0.502	0.706
Open plan office – table	211	176	140	0.827, 0.690, 0.549	0.716
	214	179	142	0.839, 0.702, 0.557	0.729
Open plan office – Dividers	153	153	149	0.600, 0.600, 0.584	0.599
	160	156	143	0.627, 0.612, 0.561	0.612
Open plan office – cabinet	88	92	95	0.345, 0.361, 0.373	0.357
	91	95	99	0.357, 0.373, 0.399	0.371
Meeting room (small) – table	212	173	131	0.831, 0.678, 0.514	0.708
	216	177	134	0.847, 0.694, 0.525	0.722
Meeting room (small) – wall	71	71	100	0.278, 0.278, 0.392	0.285
	72	72	101	0.282, 0.282, 0.396	0.289

Building 3

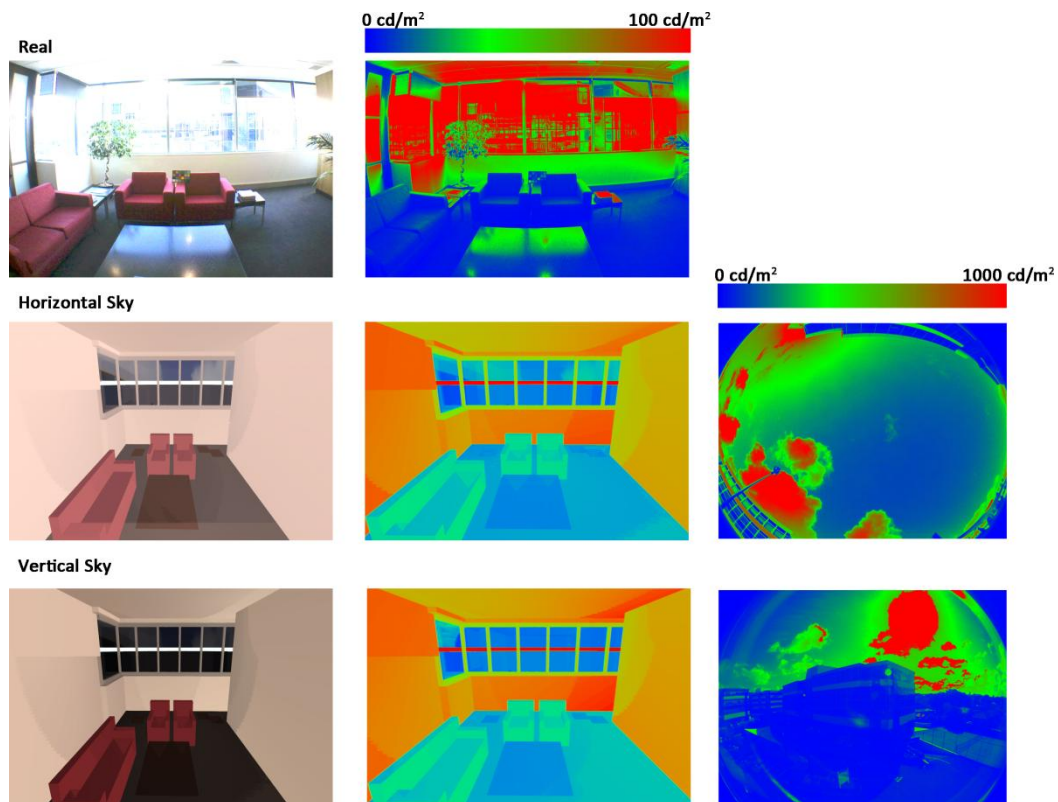
Surface	R	G	B	RGB value for Radiance	Reflectance
Table	193	151	106	0.757, 0.592, 0.416	0.624
	195	157	111	0.764, 0.616, 0.435	0.643
Cabinet	205	178	138	0.804, 0.698, 0.541	0.716
	214	192	155	0.839, 0.753, 0.608	0.767
Chair	25	62	98	0.098, 0.243, 0.384	0.212
	29	62	96	0.114, 0.243, 0.376	0.219
Carpet	74	74	75	0.290, 0.290, 0.294	0.290
	90	81	92	0.353, 0.318, 0.361	0.330
Dividers	147	152	154	0.576, 0.596, 0.604	0.591
	186	189	191	0.729, 0.741, 0.749	0.738
Window ledge	195	168	121	0.765, 0.659, 0.475	0.675
	199	173	125	0.780, 0.678, 0.490	0.693
Window frame	160	163	165	0.627, 0.639, 0.647	0.636
	161	165	167	0.631, 0.647, 0.647	0.643
Column/ wall/ceiling	219	215	210	0.859, 0.843, 0.824	0.846
	231	229	223	0.906, 0.898, 0.875	0.906
Meeting room table	233	236	237	0.914, 0.925, 0.929	0.922
	235	238	239	0.921, 0.933, 0.937	0.930
Meeting room chair	43	44	46	0.169, 0.173, 0.180	0.172
	52	54	56	0.165, 0.212, 0.220	0.200
Meeting room wall	79	112	121	0.310, 0.439, 0.475	0.407
	113	162	173	0.443, 0.635, 0.678	0.587

Appendix K: Results

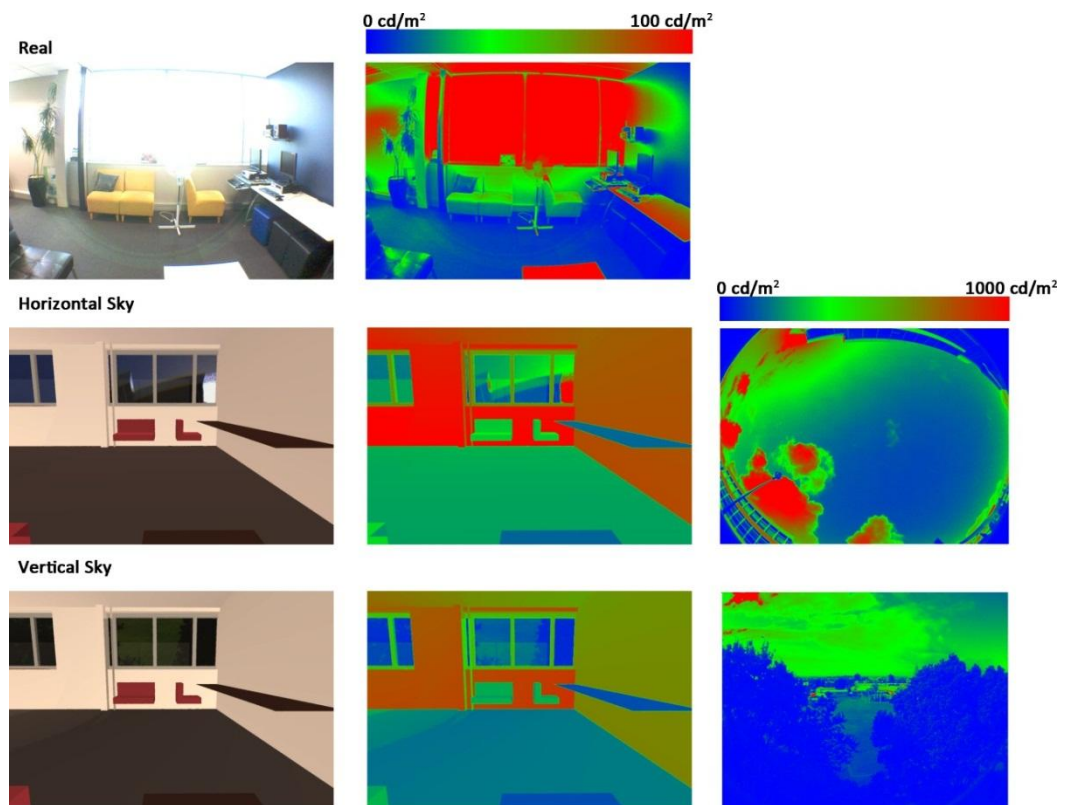
This section illustrates the HDR image captured from the three monitored buildings in Auckland, and daylight simulations under both the horizontal sky vertical sky along with their false colour renderings.

Building 1:

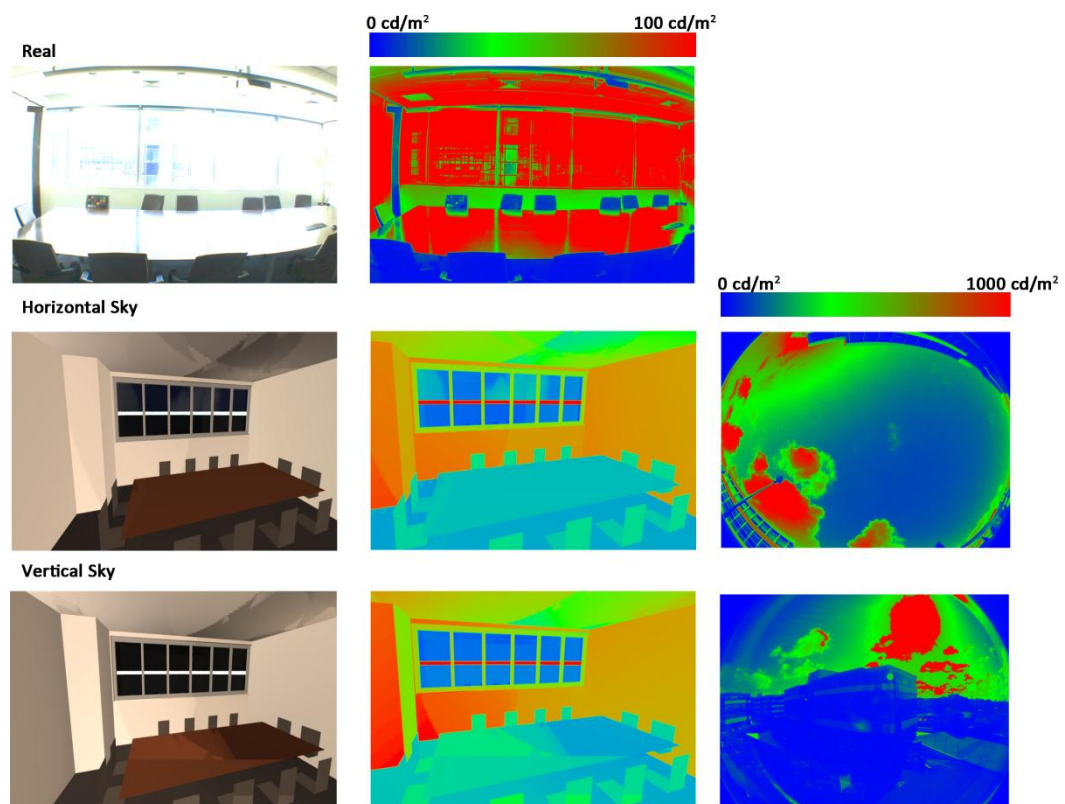
Waiting room



Lunchroom

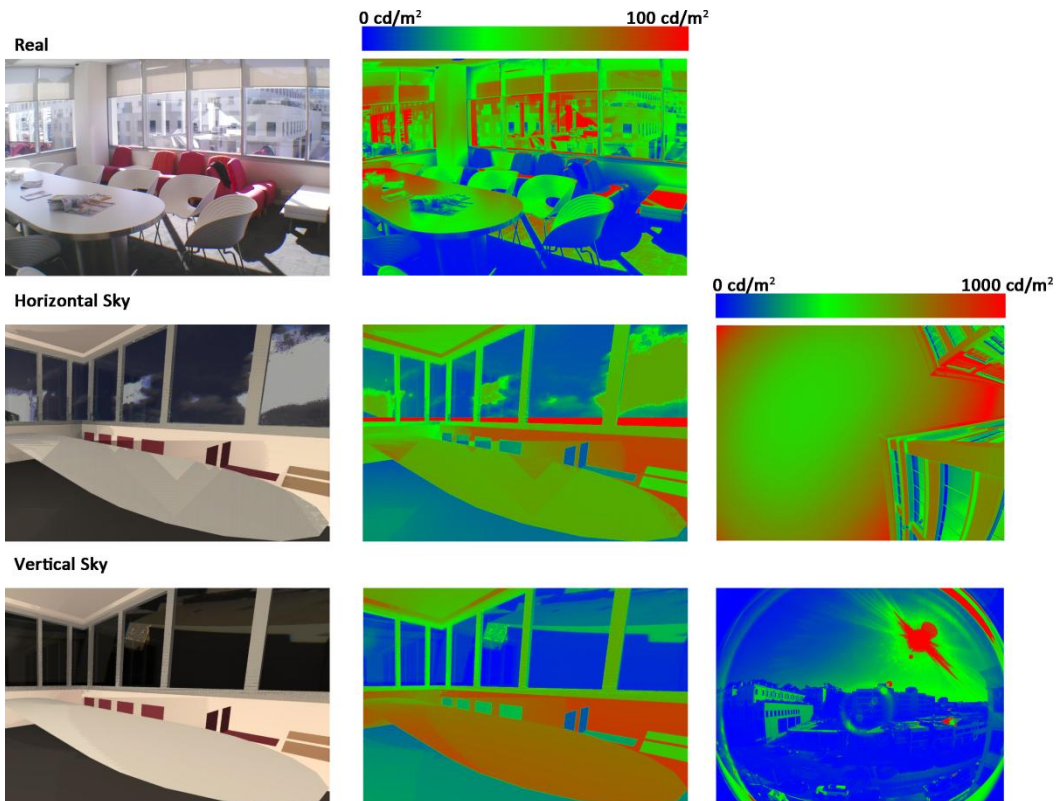


Meeting Room

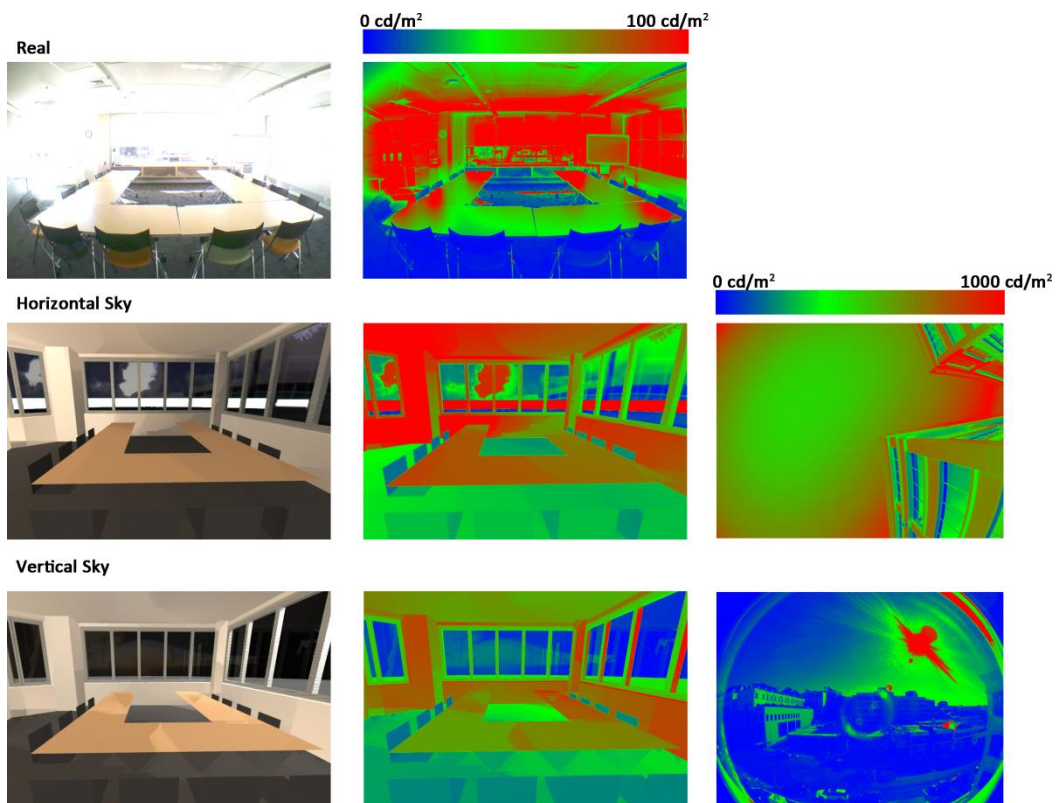


Building 2:

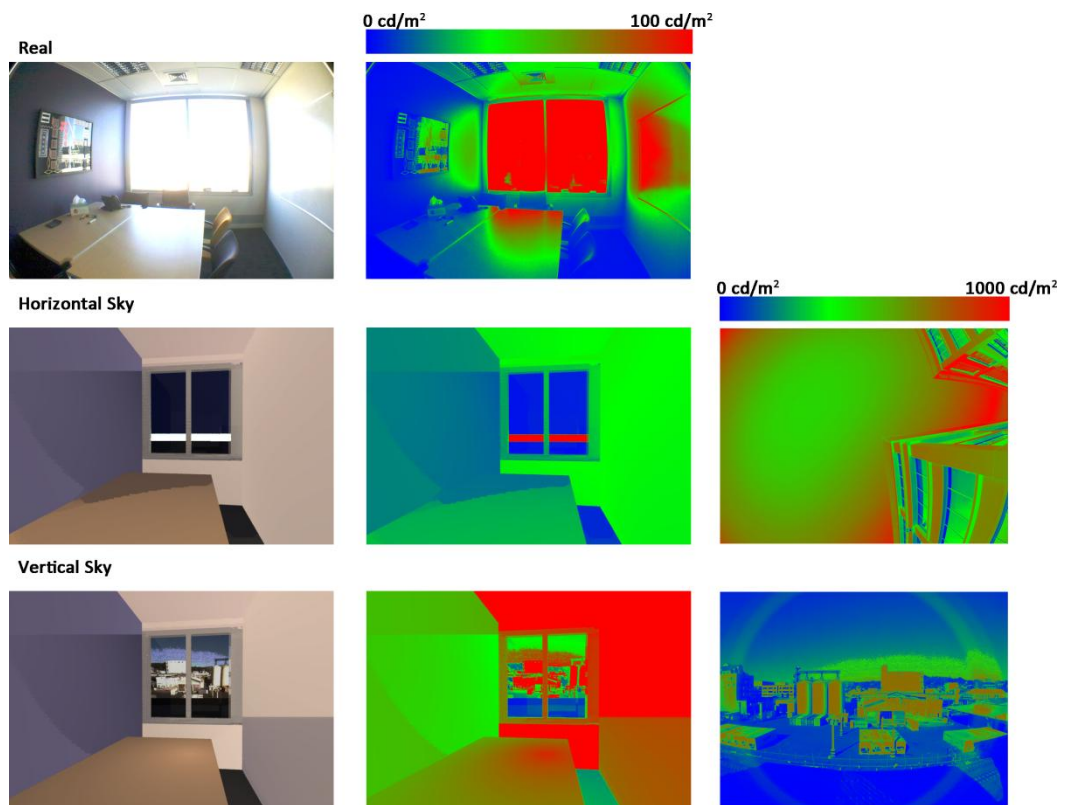
Lunchroom



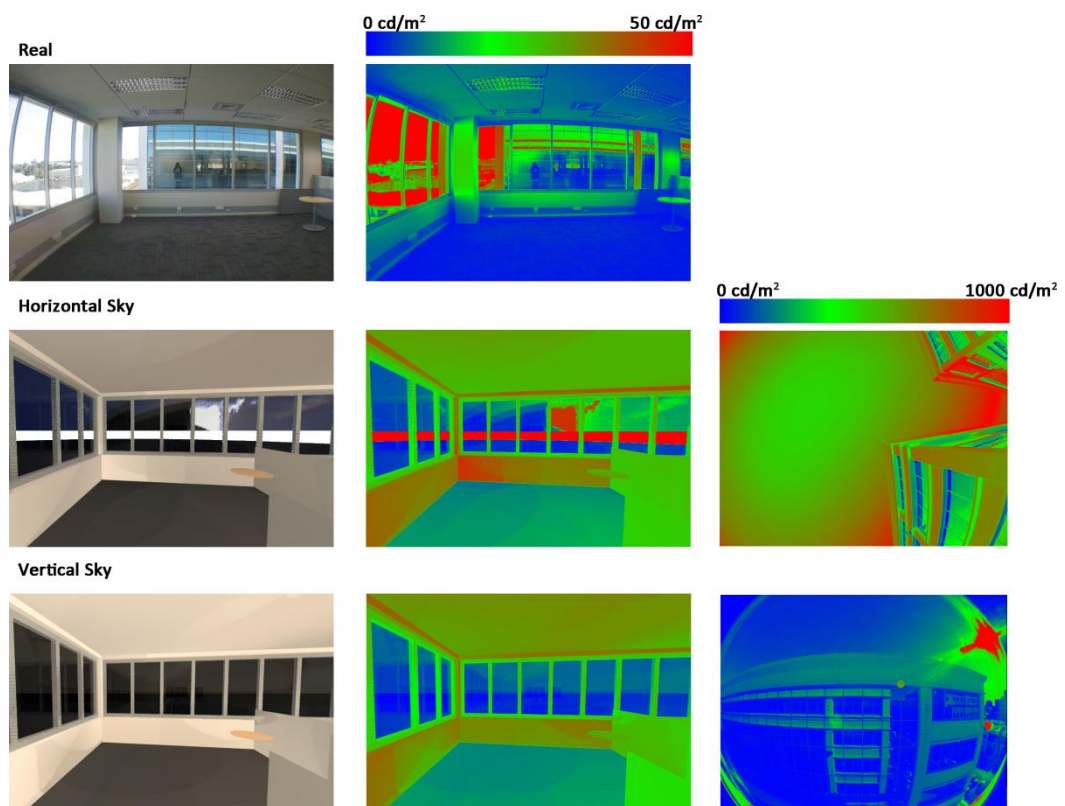
Large meeting room



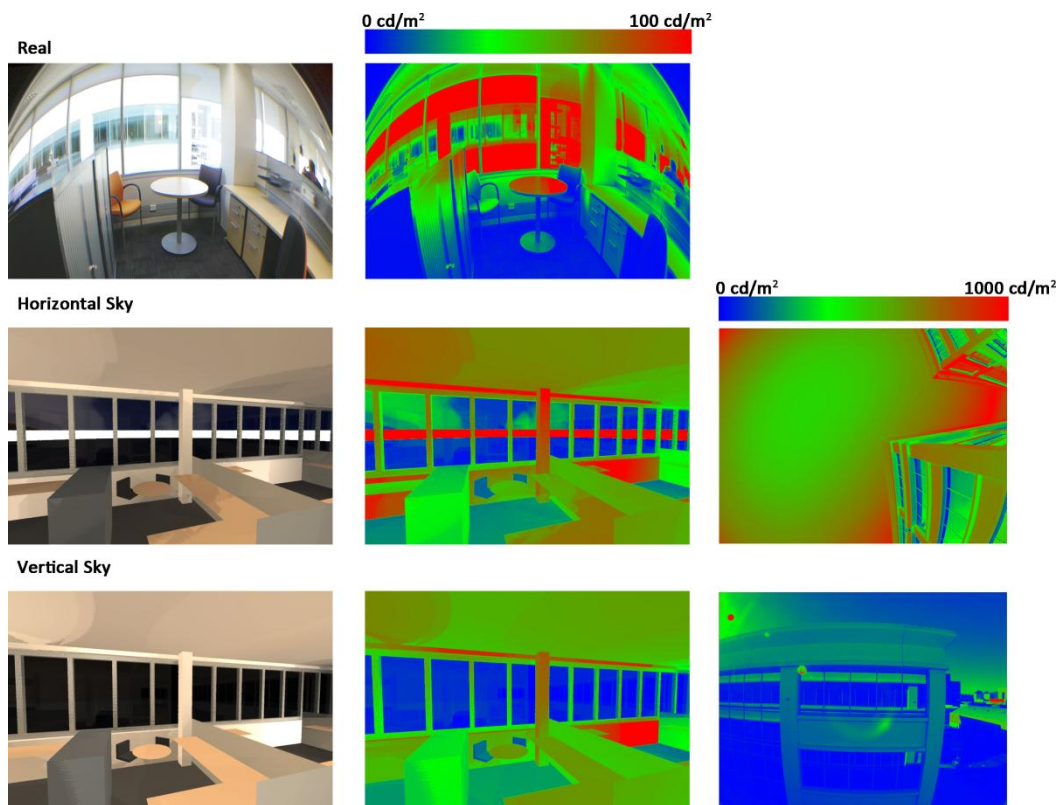
Small meeting room



Corner open plan office

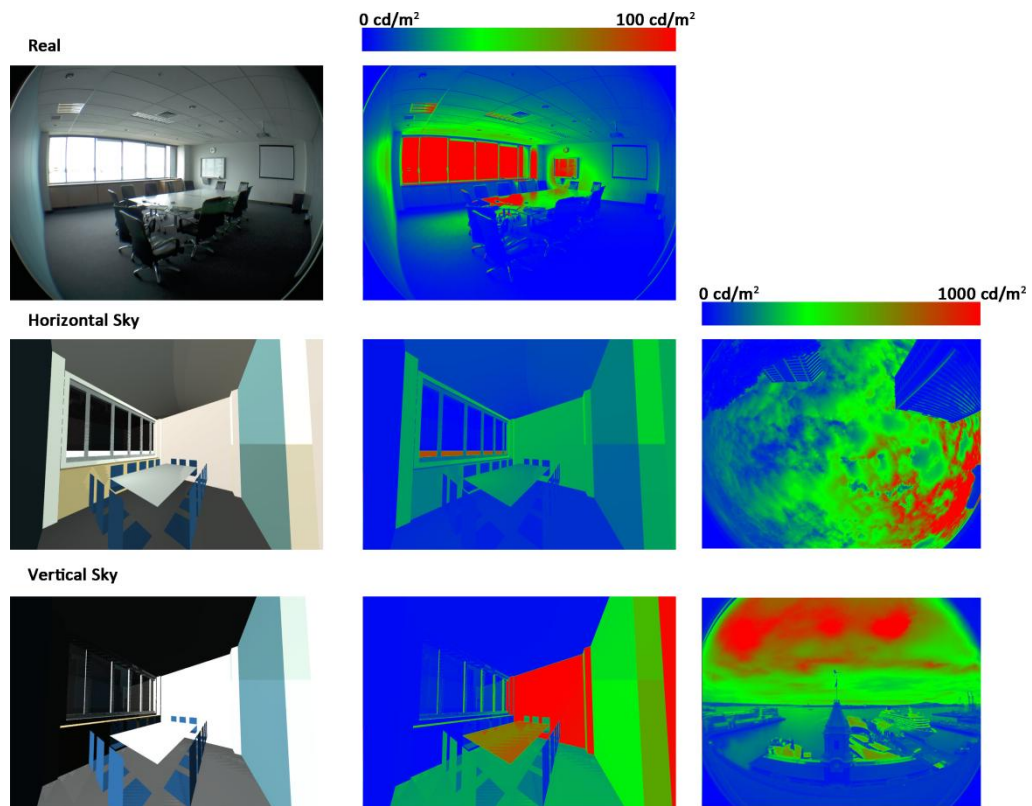


Open plan office

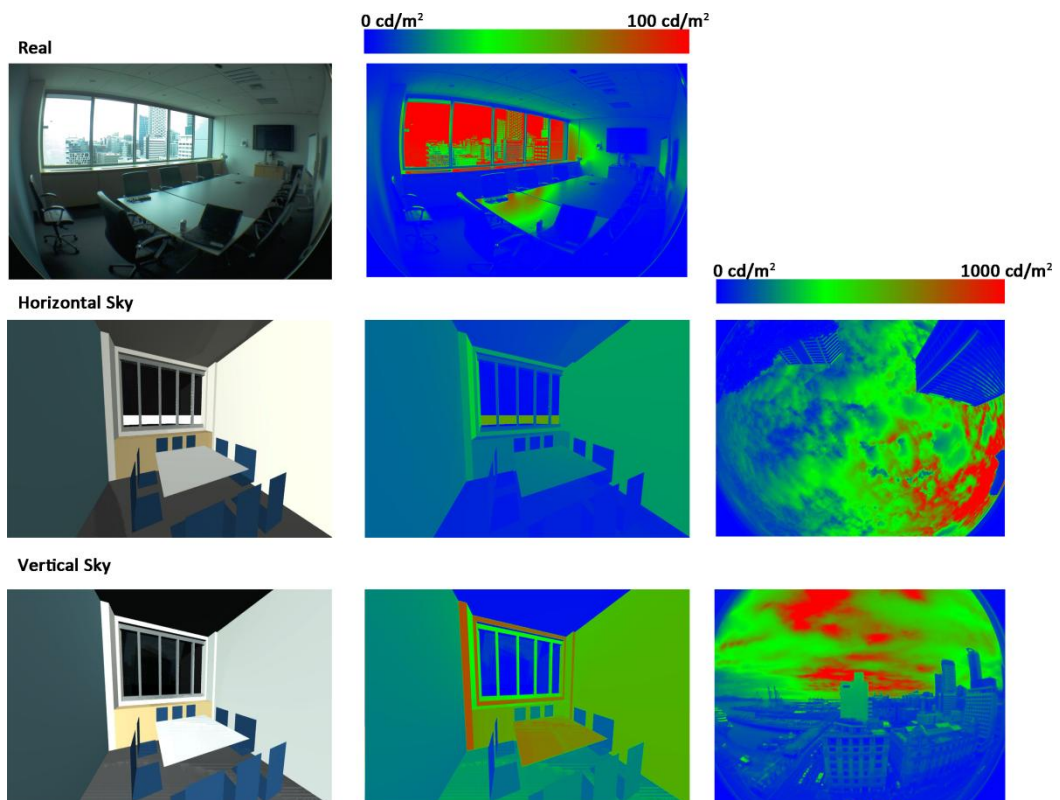


Building 3:

Large meeting room



Small meeting room



Office

